

RESERVOIR CHARACTERISTICS
IN UINTA BASIN GAS WELLS

FINAL REPORT

for the period

1 September 1978 - 31 January 1980

C. R. Boardman
C. F. Knutson

C. K. GeoEnergy Corporation
5030 Paradise Road, Suite A103
Las Vegas, Nevada 89119

Prepared for the
U. S. Department of Energy
Nevada Operations Office
Under Contract #DE-AC08-78ET11399

INTRODUCTION	1
NEAR RADIAL-FLOW WELL ANALYSIS	1
Production Data	1
Well Completion Data	2
Calculated Reservoir Rock Characteristics	2
Comparison of Reservoir Rock Characteristics with Type of Flow Exhibited	2
RELATIVE CONTRIBUTION TO FLOW OF INDIVIDUAL SANDS	3
INFERENCES FROM PRESSURE BUILDUPS IN SEVEN TIGHT WASATCH GAS WELLS IN THE UINTA BASIN	4
Introduction	4
Geology of the Wasatch Formation in the Uinta Basin	5
Geometry of Reservoir Beds	5
Basic Well Data	6
Reservoir Sand Characteristics	6
Sandstone Fraction	6
Initial Pressure and Temperature	6
Net Sand Thickness, Porosity, and Water Saturation	7
Gas Gravity	7
Reservoir Volumes Based on Log Data and Outcrop Geometry	7
Reservoir Flow Regimes	8
Permeability	8
Flow Periods Utilized in Pressure Buildup Analysis	9
Pressure Buildup Data	10
Determination of Pressures at Depth of Reservoir	10
Horner Plots	11
Agarwal-Carter-Pollock Plots	12
Reservoir Boundaries	13
Apparant Overall Reservoir Permeability (Radial Basis)	13
Reservoir Matrix Permeability Approximations	13
Gas Filled Reservoir Void Volumes	14
Reservoir Interconnection	16
Fracture Conductivity	16
Effective Fracture Half Lengths	16
SUMMARY AND CONCLUSIONS	18
ACKNOWLEDGEMENTS	20
REFERENCES	21
NOMENCLATURE	22
TABLES	24
FIGURES	54

LIST OF TABLES

<u>Table Number</u>		<u>Page Number</u>
1	Production Data-Near Radial Flow Uinta Basin Gas Wells	24
2	Well Completion Data-Near Radial Flow Uinta Basin Gas Wells	25
3	Some Reservoir Rock Characteristics-Near Radial Flow Wells	26
4	Apparent Clay Fraction-Producing Gross Sands	28
5	Gas Production Statistics - 7 Uinta Basin Wasatch Wells	29
6	Well Casing and Tubing Specifications	30
7	Perforation Depths	31
8	Frac Job Details	32
9	Fractional Sandstone Content in Production Interval	33
10	Initial Reservoir Pressures and Temperatures at Average Depth of Perforations	34
11	Completed Reservoir Sand Properties Calculated from Log Data	35
12	Reservoir Gross Sand Geometries Estimated From Rock Outcrop Studies	37
13	Reservoir Gas-Filled Void Volumes Based on Log Values of Net Sand Thickness, Porosity, and Water Saturation and Geometry Determined from Outcrops.	39
14	Flow Test Data	41
15	Monthly Production Period Statistics	42
16	Pressure Buildup Data- Well B	43
17	Pressure Buildup Data- Well C	44

List of Tables (continued)

<u>Table Number</u>		<u>Page Number</u>
18	Pressure Buildup Data- Well G	45
19	Pressure Buildup Data- Well H	46
20	Pressure Buildup Data- Wells A,D,F	47
21	Water Level Depths and Surface Gas Pressures Measured in 1979 by Dead Weight Tester and Echometer	48
22	Apparent Reservoir Permeabilities-Wells A-G	49
23	Average Reservoir Pressures, June 1979	50
24	Reservoir Gas-Filled Void Volumes Based on Pressure/Production Analyses	51
25	Calculated Effective Fracture Half Lengths- Wells B, C and G	52
26	Calculated Average Fracture Widths, $-\bar{y}_f$, Wells B, C, & G	53

LIST OF FIGURES

<u>Figure Number</u>		<u>Page Number</u>
1	Cumulative Gas Production Volume vs Cumulative Production Time	54
2	Cumulative Gas Production Volume vs Cumulative Production Time	55
3	Cumulative Gas Production Volume vs Cumulative Production Time	56
4	Reservoir Rock Characteristics Distributions	57
5	Apparent Clay Fraction of Producing Gross Sands versus Slope of Log Cum. Production Volume versus Log Cumulative Time Curve.	58
6	Temperature Logs Taken During Production - Well B	59
7	Reservoir Drainage Area versus Distance from Wellbore as a Function of the Ratio of Total Sand- stone Bed Thickness to Total Producing Interval Thickness (after Knutson - 1977)	60
8	SP/Resistivity Log Character - Wells A & B	61
9	Gamma Ray/ Resistivity Log Character - Well C	62
10	SP/Resistivity Log Character - Well D	63
11	Gamma Ray/Resistivity Log Character - Well F	64
12	SP/Resistivity Log Character- Wells G & H	65
13	Cumulative Gas Production versus Actual Production Time Wells A & D	66
14	Cumulative Gas Production versus Actual Production Time Wells D, F and G.	67
15	Cumulative Gas Production versus Actual Production Time Wells B & H	68
16	Pressure Buildup - Well A	69
17	Pressure Buildup - Well B	70
18	Pressure Buildup - Well C	71
19	Pressure Buildup - Well D	72
20	Pressure Buildup - Well F	73

List of Figures (continued)

<u>Figure Number</u>	<u>Page Number</u>
21 Pressure Buildup - Well G	74
22 Pressure Buildup - Well H	75
23 $\Delta(p^2)$ versus $(\Delta t)^{\frac{1}{2}}$ - Well B (log-log)	76
24 $\Delta(p^2)$ versus $(\Delta t)^{\frac{1}{2}}$ - Well C (log-log)	77
25 $\Delta(p^2)$ versus $(\Delta t)^{\frac{1}{2}}$ - Well G (log-log)	78
26 $\Delta(p^2)$ versus $(\Delta t)^{\frac{1}{2}}$ - Well H (log-log)	79
27 $\Delta(p^2)$ versus $(\Delta t)^{\frac{1}{2}}$ - Well B	80
28 $\Delta(p^2)$ versus $(\Delta t)^{\frac{1}{2}}$ - Well C	81
29 $\Delta(p^2)$ versus $(\Delta t)^{\frac{1}{2}}$ - Well G	82
30 p/z versus Gas Production - Well A	83
31 p/z versus Gas Production - Well B	84
32 p/z versus Gas Production - Well C	85
33 p/z versus Gas Production - Well D	86
34 p/z versus Gas Production - Well F	87
35 p/z versus Gas Production - Well G	88
36 Comparison of Gas Filled Reservoir Volumes Determined by Two Methods	89

ABSTRACT

Volumes of 29 lenticular tight gas sandstone reservoirs in the Uinta Basin, Utah have been approximated from long-term pressure buildups on 6 wells. Average reservoir volume was interpreted to be about 240,000 cu. ft. per ft. of net pay. Outcrop reservoir geometry studies indicate an average reservoir volume (without any reservoir interconnection assumed) of about 30% less than the average based upon production analysis. Therefore, some reservoir interconnection may exist.

The results of this study are consistent with the Knutson lenticular reservoir model in which average reservoir width is 22 times the gross sand thickness, length is 10 times the width, and reservoir interconnection is a function of the sand fraction in the productive interval.

Apparent reservoir permeabilities, assuming radial flow, range from .009 to .052 millidarcies and actual sandstone matrix permeabilities are interpreted to range from .06 to .21 millidarcies. Fracture half lengths are interpreted to be about 0.1 ft/bbl of fluid with an average proppant load of 1.2-1.7 lb/gal. at injection rates of 18-24 BPM and injection pressures of 2,500 to 4,600 psi for each 100 ft. of gross sand in the fraced interval.

AN INVESTIGATION OF RESERVOIR
CHARACTERISTICS EXHIBITED BY PRODUCING
UINTA BASIN GAS WELLS

INTRODUCTION

This study encompasses an analysis of gas production, well log, and pressure buildup data obtained from gas wells in the Uinta Basin, Utah. The objectives were to determine 1) whether or not the more continuous sands can be identified using log data, 2) reservoir volumes, apparent reservoir permeabilities, and degree of reservoir interconnection for a number of wells and 3) the applicability of reservoir models developed from outcrop studies.

NEAR RADIAL-FLOW WELL ANALYSIS

Production data were screened and analyzed for all (total of 46) pre-Green River Formation Uinta Basin gas wells with at least 7 years generally continuous production history in order to identify radial/near radial-flow wells. A total of 5 such wells were identified based on analysis of log-log plots of cumulative production volume versus time.

Production Data

Production data through 1977 are presented for these 5 wells in Table 1. The produced gas volumes and production times shown were obtained from the Utah State Department of Natural Resources in Salt Lake City. The production times indicated are those for which the wells were actually on production. As is evident from the data presented, these wells have been on production for at least several months in each year for 15 to 18 years. The average number of production months/year ranges from 7 to 10 and the cumulative 10-year gas production volumes range from 242 to 895 MMCF. Two of the wells were dually completed in the Wasatch and Mesaverde - RH#3 and UT#1. The Wasatch only exhibits near-radial flow in RH# 3, whereas both formations exhibit it in UT#1.

As indicated in the table, the slopes of the log cumulative production volumes versus log production time curves

range from .75 to .88. (The curves from which these slopes were obtained are shown in Figures 1, 2, and 3.) Hence, there are no absolute radial flow wells (slope of 1.0). All 5 are "near radial".

Well Completion Data

Completion data for these 5 wells are shown in Table 2. As indicated in this table, the number of sands per completion range from 1 to 9. Frac jobs ranged from 6,600 gal. of fluid and 2,300 lbs. of proppant to 40,200 gal. of fluid and 50,000 lbs. of proppant. Frac fluids included oil, oil/water emulsions, and water with various additives. Proppant was primarily 20/40 mesh sand.

Calculated Reservoir Rock Characteristics

Calculated values of net pay sand thickness, sonic wave travel time (Δt_s), pseudo-static spontaneous potential (PSP), equivalent formation water resistivity (R_{wa}), SP curve character, porosity (ϕ), and apparent water saturation (S_w) are presented in Table 3. As indicated in this table, total net pay thicknesses vary between 13 and 261 ft. The well with the greatest 5 and 10 year cumulative production volumes (UT#1) also has the greatest thickness of net pay completed, whereas the well with the smallest production (CW#17) has the smallest thickness.

The apparent clay fractions of the reservoir sands as indicated by analysis of the available gamma ray logs are presented in Table 4 for 4 of the near radial-flow wells as well as for 6 of the linear/indeterminate-flow wells.

Comparison of Reservoir Rock Characteristics with the Type of Flow Exhibited

Distribution curves are shown for Δt_s , PSP and R_{wa} , and SP curve character in Figure 4. As indicated in this figure, the median values are:

Δt_s :	70 μ sec/ft.
R_{wa} :	.45 ohm-m
PSP :	25 millivolts

Also, the preponderance of the completed sands exhibit a sand grain-size "fining up" SP curve character.

By comparing these values with those previously determined (Knutson & Boardman-1978) for linear and indeterminate-flow wells, it was concluded that these parameters apparently do not constitute valid correlative tools. This comparison is shown as follows:

<u>Parameter</u>	<u>Linear</u>		<u>Indeterminate</u>		<u>Radial</u>	
	<u>Median</u>	<u>Range</u>	<u>Median</u>	<u>Range</u>	<u>Median</u>	<u>Range</u>
Δt_s	72	67-83	70	67-80	70	65-78
R_{wa}	.22	.07-.90	.17	.06-.57	.45	.03-.90
PSP	28	7-70	35	11-63	25	12-67
SP Curve Pattern (Predominant)	Fining Up		Fining Up		Fining Up	

The apparent clay fractions as indicated by gamma ray log analysis and tabulated in Table 4 are plotted versus the slopes of the log cumulative production volume vs log production time curves in Figure 5. In this figure, the data points represent the average values obtained for each gross sand in wells with no more than 2 sands completed or in wells with more than 2 sands but with the apparent clay fractions being very close to the same number. This relationship appears to indicate that the more continuous sands are "cleaner" or less shaly. The correlation coefficient is .92 for this data set.

RELATIVE CONTRIBUTION TO FLOW OF INDIVIDUAL SANDS

An attempt was made to determine which sands were contributing the most production at late time in wells with multiple sand completions. A number of Uinta Basin gas well operators were contacted and at least 6 wells were identified for analysis; 2 each exhibiting near radial, indeterminate, and linear flow.

All the operators contacted required that third party liability insurance be secured as a prerequisite for reentering the wells. Considerable difficulty was encountered in attempting to secure such insurance. However, a policy was finally obtained from Marsh and McLennan in Las Vegas which provided \$100,000 coverage per well. This was adequate for a number of wells since the calculated value of reserves left to be produced was less than this amount.

Attempts were made to log two producing wells with Birdwell's sibilation and differential temperature probes. Unfortunately, one well had a blockage in the tubing and the other had a leaky valve which precluded both wells from being logged.

NL McCullough ran gamma ray, absolute temperature, differential temperature, and noise probes to near total depth during production in another well, designated Well "B". Production rate was about 100 MSCF/D and flowing tubing pressure at the well

was about 490 psig. No mechanical problems were encountered during the logging operation. However, in running the noise probe, it was discovered that there was a column of water in the well. Also, the noise generated by gas bubbles moving up through the water column was so great and so variable in intensity that it was impossible to obtain a measure of the relative amount of noise generated by gas movement into the wellbore at each set of perforations.

The absolute and differential temperature logs are depicted in Figure 6. As indicated by this figure, there are no consistent deflections of the differential curve which might be used to determine relative production rates. As can be seen, however, there are some indications of cooling at all producing sand levels, which would be expected if all sands were contributing to the production. The column of water obviously damped the cooling effect of gas entering the wellbore.

Because of the problem of water column interference with the logging results on Well B, the decision was made to abandon this objective and to concentrate on the determination of lenticular reservoir properties under the assumption that all the completed sands were contributing to the observed production. Subsequent observations revealed that probably all the wells selected for logging had enough water standing in the wellbore to preclude quantitative determinations of relative contribution to flow.

INFERENCES FROM PRESSURE BUILDUPS IN SEVEN TIGHT WASATCH GAS WELLS IN THE UINTA BASIN

Introduction

Seven tight Wasatch gas wells were made available for pressure buildup testing and analysis by a number of Uinta Basin operators. They have been designated simply as Wells "A,B,C....", since the respective operators and locations are confidential.

All seven wells have been somewhat continuously on production for 16 to 18 years. The number of months per year each well has been on production and the respective annual production volumes are presented in Table 5. As of June, 1979, cumulative production per well ranged from 447,000 to 1,587,000 MSCF, with an average of about 1,000,000 MSCF.

* An eighth well, "Well E" was also made available but since it had a leaking wellhead, it was not included in the study.

Geology of the Wasatch Formation in the Uinta Basin

The Wasatch Formation has been assigned to the Paleocene-Eocene of the Tertiary Period. It overlies the Cretaceous Mesaverde Formation and underlies the Tertiary Green River Formation of Eocene age. Its thickness ranges from 850 ft. in the eastern portion of the Basin to more than 3,000 ft. in the central portion. It is composed of fluvial sandstones and shales.

The shales are carbonaceous, pyritic, micaceous, and generally calcareous. The sandstones are generally fine to medium-grained. They contain greater than 10% of dark minerals and rock fragments with quartz being the most abundant mineral grain. Their sorting and permeability range from fair to poor because of clay and silt. Cement is generally calcite and/or argillaceous minerals. (Murany-1964)

In the general area in which the wells of interest are located, the Wasatch is about 2,500 ft. thick. Most of the producing sands are located in the upper third of the formation.

Geometry of Reservoir Beds

Knutson (1977), in a study of fluvial sandstone outcrops on the periphery of the eastern Uinta Basin found that the average width to height ratio for sandstone beds in the Neslen and Farrer facies of the underlying Mesaverde Group is 22 and the average length to width ratio is 10. He reported that the Wasatch beds "exhibited higher length to height ratio's than the Farrer/Neslen population, but the Wasatch sample was too small to make a statistical evaluation meaningful". Because of this lack of statistically significant ratios for the Wasatch, it was assumed that the Nesler/Farrer ratios ($W/H=22, L/W=10$) were appropriate for the purpose of this analysis.

Knutson (1977) also generated a reservoir model which enables an estimate of the amount of additional reservoir rock that intersects a given bed. This model was developed by using the foregoing W/H and L/W ratios and by randomly selecting a number of lenticular bed directions and locations for a multiplicity of sandstone thickness/total interval thickness ratios. The results of his modelling are presented in Figure 7. Specific reservoir area is presented as a function of distance from the wellbore and sandstone/interval thickness ratio. Reservoir volume for a given distance from the wellbore and sandstone fraction is calculated by multiplying the specific reservoir area by total net pay thickness. This model was tested with the data and analyses developed in this study.

Basic Well Data

The seven wells tested range in depth from 5,530 to 6,473 ft. Casing diameters range from 4½" to 7" and production tubing from 2 3/8 and 2 7/8". Wells G & H only are equipped with packers in the tubing/casing annulus above the production zones; the other wells have open annuli. Available casing and tubing specifications are presented in Table 6. Perforated zones are given in Table 7 along with average midpoint depths. As indicated in the latter table, the number of perforated zones in each well ranges from one to six.

Frac job details are presented in Table 8. Diesel fuel and salt water were used as frac fluids. Proppant was primarily 20-40 mesh sand. The size of the jobs ranged from 15,000 gal. frac fluid/15,000 bls. proppant to 50,000 gal/50,000 lbs. Available injection pressures ranged from 2500-4000 psig and available average injection rates from 10.5 to 25.1 BPM. Balls were used for multiple zone treatments.

Reservoir Sand Characteristics

Logs available for use in determining reservoir characteristics are listed as follows:

<u>LOG</u>	<u>A</u>	<u>B</u>	<u>C</u>	<u>D</u>	<u>F</u>	<u>G</u>	<u>H</u>
Induction electrical	x	x		x	x	x	
Microlog	x	x				x	x
Sonic				x	x		
Electrical							x
Spontaneous potential	x	x		x	x	x	x
Gamma ray		x	x	x	x		x
Neutron			x				x

Spontaneous potential/resistivity log character of producing sands and adjoining shales is shown in Figures 8-12.

Sandstone Fraction

The ratio of gross sandstone thickness to the total thickness of the interval from the top of the uppermost sand to the base of the lowermost sand was determined for Wells A-G. These values are presented in Table 9. As indicated in this table, the sand/total interval ratio ranges from .17 to .35 and averages .28 for these wells. (Beds smaller than 5 ft. were not included in this tally.)

Initial Pressure and Temperature

Measured initial pressures were obtained for Wells A-C,

F and G. These values are shown in Table 10. Average gradient for these 5 wells was .437 psi/ft. as indicated in the table. The range was .404 to .478 psi/ft. Since no value was available for Well D, the average was assigned to this well for analytical purposes. As indicated, actual average pressures ranged from about 2,200 to 2,700 psia. The datum for these pressure values is the average depth of the midpoints of the perforated zones.

Also shown in Table 10 are calculated values for reservoir temperatures at the same datum depth. These values are based upon the gradient determined from measurements in Wells A, C, E, and F after several weeks of shut-in time. This gradient was approximately $1^{\circ}/100$ ft. depth. As indicated, temperatures ranged from 154°F to 160°F .

Net Sand Thickness, Porosity, and Water Saturation

Values for these parameters, determined by analysis of the available logs, are shown in Table 11. Portions of sands with calculated porosities less than 5% and/or water saturations in excess of 80% were excluded from the net pay sand thicknesses.

A total of 29 producing sands were analyzed. Gross sand thicknesses range from 8 to 41 ft. with a median of 22 ft. and net sand thicknesses range up to 31 ft. with a median of 11 ft. Average ratio of net pay sand thickness to gross sand thickness is 0.62.

Calculated net pay sand porosities range from 6% to 14% and water saturations from 25% to the cut off value of 70%. Average values of these two parameters for the 29 sands are 11.9% and 54%, respectively.

Gas Gravity

Available analyses of the gas indicate that its specific gravity is about 0.6.

Reservoir Volumes Based on Log Data and Outcrop Geometry

The total gas-filled void volumes of the producing sands were calculated for each well using the foregoing parameters and Knutson's ratios of reservoir width to height and length to width. These volumes were determined by assuming that the lenticular reservoir beds are elongate rectangular parallel-pipeds with heights equal to the net sand thicknesses, widths equal to 22 times the gross sand thicknesses, and lengths equal to 10 times the widths. The effect of reservoir interconnection was not included in these calculations.

Calculated lengths and widths of the gross sand beds are presented, along with areas and volumes in Table 12. The areas shown in this table were used along with net pay thickness, porosity and water saturation to determine the gas filled void volumes shown in Table 13. Calculated individual sand volumes range up to 12.5 million cu. ft. The values for single wells range from 4.7 to 22.6 million cu. ft.

The volumes of gas at initial reservoir conditions were calculated for Wells A-G using the foregoing volumes and initial pressures and temperatures presented in Table 10. These calculations were made by assigning the pressure and temperature at the average perforation midpoint depth to the entire gas-filled void volume for each well. The results were as follows:

<u>Well</u>	<u>Gas Volume, MMSCF</u>
A	1,876
B	3,954
C	1,881
D	728
F	889
G	805

Reservoir Flow Regimes

The type of flow regime (radial versus linear) was estimated for each well based on production histories. Cumulative annual production volumes shown in Table 5 were plotted versus time on a log-log basis (Figures 13-15). Slopes were determined to range from 0.43 to 0.71 and average 0.58. Under conditions of radial flow, slopes are expected to be 1.0 and under conditions of linear flow, 0.5, according to D. O. Cox of Energy Consultants, Inc. of Denver. On this basis, it appears that all seven wells exhibit near-linear flow at least after about 5 years of production (Wells A and H appear to exhibit near radial flow during the first 3 to 5 years.).

Permeability

Average permeabilities were calculated for Wells A-G by a method suggested by D. O. Cox which employs a log-log plot of dimensionless cumulative production versus dimensionless time (Knutson and Boardman-1977). These values are:

<u>Well</u>	<u>Permeability, md</u>
A	.03
B	.01
C	.02
D	.42
F	.30
G	.19

This method assumes that the fracture is infinitely conductive and that it is oriented perpendicular to the long axis of the sand body. After several years of production, Don Montan of Lawrence Livermore Laboratory has found through computer simulation that fractures which make an acute angle with the perpendicular to the long axis result in slopes similar to those for the perpendicular case. Also, Cox has found that fractures which penetrate as much as 1/3 of the width of a sand body yield slopes similar to those for complete penetration. (Knutson and Boardman-1978)

Flow Periods Utilized in Pressure Buildup Analysis

The entire production periods from start-up in the summer of 1978 to final shut-in in the summer of 1979 were used in the pressure buildup analysis for Wells A-G. For Well H, a continuous flow period of 37 days in May and June, 1979 was utilized, which followed a 52-day shut-in period.

The duration of flow periods, associated prior shut-in times, produced volumes and rates are presented in Table 14. As indicated by this table, the median shut-in time period prior to production was 170 days and the median production time period (including shut-in time) was 239 days. Median shut-in time during the production periods was 39 days.

The monthly production volumes and number of days produced per month during the flow periods are shown in Table 15. Flow volumes were determined by Mountain Fuel Supply and Colorado Interstate Gas with orifice meters and chart recorders which are used in the routine determination of gas sales volumes. As indicated in Table 15, Wells B, F and G were shut-in on about May 10, 1979 and then placed back on production for 8-9 days during June prior to final shut-in. These three wells were flowed in June in order to attempt the production logging program. When the turbulent water problem was discovered, the wells were again shut-in for pressure buildup.

In order to construct Horner plots for the subsequent pressure buildups, values for flow period t_p , were approximated from the data in Tables 14 and 15 using the cumulative production, V_p , since the last pressure equalization divided by the rate, q , just before shut-in (Earlougher-1977). Actually, none of the wells' pressures had equalized. However, except for Well H, it is believed that well pressures were within roughly 100 to 200 psi of the average reservoir pressure at the time production was begun. The flow period for Well H was merely a "convenient, relatively short time in terms of reservoir depletion" (Earlougher-1977).

Values for V_p , q and t_p are shown in Table 14. The variance of t_p from the actual production period (including "down" days) ranges from -68% to +8% with a median value of -19%. The variances for Wells A, D, F, and H are all within 19% of the actual production period.

Pressure Buildup Data

Shut-in surface tubing pressures were measured by Mountain Fuel Supply and Colorado Interstate Gas for a number of weeks immediately after shut-in on Wells B, C, G, and H. These pressures were measured with the same probes used in connection with sales volume measurements. In addition, spot surface tubing and casing pressure measurements were made on Wells A-G with a deadweight pressure tester along with casing water level measurements using an "Echometer" by Sun Oil Field Services of Vernal, Utah. The latest spot measurements were made at 157 days following shut-in on Wells A, D, and F and at 121 days following shut-in on Wells B, C, and G.

Both the continuous and the spot-measured tubing pressures for Wells B, C, G, and H are presented in Tables 16-19. The spot surface casing pressure measurements for Wells A, D, and F are presented in Table 20 and the complete set of spot pressure measurements and water level determinations are given in Table 21.

Determination of Pressures at Depth of Reservoir

Pressures, p_m , at the average midpoint depth of the perforated zones were approximated as follows:

$$p_m = p_s + (25 \times 10^{-6} p_s / \text{ft}) H_g + (.44 \text{ psi/ft.}) H_w \quad (\text{Craft \& Hawkins, 1959})$$

where

p_s = surface pressure, psia

H_g = height of gas column above water, ft.

H_w = height of water column above average midpoint depth of the perforated zones, ft.

Surface casing pressures were used for p_s in the case of Wells A, D, and F since the water levels determined were those in the casing rather than in the tubing and since no early tubing pressures were measured as was the case for Wells B, C, G, and H. In the case of these latter wells, values of H_w for the tubing were calculated for use in approximating values for p_m at early times. The following equation was used:

$$H_{wt} = \frac{p_{mc} - p_{st} (1 + 25 \times 10^{-6} D_m)}{.44 - 25 \times 10^{-6} p_{st}}$$

where

- H_{wt} = height of water column above perforations' midpoint depth in tubing, ft.
- p_{st} = surface tubing pressure psia
- D_m = depth of perforations midpoint
- p_{mc} = pressure at perforations' midpoint depth in casing, psia

Since it was impossible to measure water levels in Wells G and H, an average water column height of 364 ft. was assigned to these 2 wells in order to calculate values of p_m . The range of water column heights for the other 5 wells plus Well E was 187 - 695 ft.

Horner Plots

Pressure buildup data from Tables 16-20 were plotted as a function of $t + \Delta t / \Delta t$ in order to determine apparent reservoir permeabilities and average reservoir pressures, and to provide indications of reservoir boundaries. These plots are presented in Figures 16-22. Although the early (first 3 to 4 days after shut-in) pressures are shown in these plots, because of suspected relative water movements in the tubing and casing, it is felt that no conclusions should be drawn from these early data. As indicated by the casing water level determinations, however, it appears that the tubing and casing water levels had stabilized by at least 11 days following shut-in.

The Horner plots for Wells B, C, and G display at least 2 distinct slopes; one for Δt values of 5 to 15 days and another much steeper slope in the 100 + day- Δt range. Only the initial slope was recorded for Well H and only the "final" slope for Wells A, D, and F. The breaks in slope were used in assessing boundaries and the final slopes were used in assessing apparent reservoir permeability and effective reservoir pressures.

Agarwal-Carter-Pollock Plots

The early time buildup data were plotted in the manner recommended by Agarwal, Carter and Pollock (Agarwal, et al-1977) in order to determine the nature of the conductivity of the hydraulic fractures and to assess their effective lengths. The pressure function $\Delta(p^2)$ is plotted on a log-log basis versus $(\Delta t)^{1/2}$ in Figures 23-26. $\Delta(p^2)$ is defined as the difference in the square of the pressure at time Δt and the square of the flowing well pressure. Agarwal-Carter-Pollock point out that essentially infinite capacity fractures display a characteristic $1/2$ slope in this type of plot while those with finite capacity display much flatter slopes.

Their relationship for determining effective fracture half length, x_f , for a gas well utilizes simple $\Delta(p^2)$ vs $(\Delta t)^{1/2}$ plots (Fig. 27-29) and is:

$$x_f = \frac{40.925 qzT}{m_L h} \left[\frac{\mu}{k \phi_g c_t} \right]^{1/2}$$

where

- x_f = effective fracture half length, ft.
- q = flow rate, MSCF/day
- z = gas z factor, fraction
- T = reservoir temperature, $^{\circ}R$
- m_L = slope, $\text{psi}^2/\text{hour}^{1/2}$
- μ = viscosity, cp
- k = permeability, md
- ϕ_g = formation porosity, fraction
- c_t = total system compressibility, psi^{-1}
- h = formation thickness, ft.

* The plot for Well H is not shown since an approximation for permeability was not obtained for this well.

Reservoir Boundaries

Since the chances are high that at least a number of the lenticular reservoirs were penetrated near one side by these 7 drill holes and since by virtue of the extent of the hydraulic fractures from the wellbore, that particular side should be reflected quite early (in a matter of several days at most) in the pressure buildup response of the reservoir. The pressure buildup from this point on would then be expected to be a function of the flow toward the wellbore from roughly a 180° sector.

At the point in time when the other side of the reservoir is "hit" by the pressure transient, true near-linear flow is assumed to occur with the pressure transient then moving linearly down the long axis of the reservoir. This flow regime is interpreted as being responsible for the "final" slope observed on the Horner Plots.

With this model it can be assumed that the slope of the buildup curve prior to the pressure transients' arrival at the second side of the reservoir would be $\frac{1}{2}$ that of the final slope if it were not for the effect of the linear flow into the frac and linear flow within the frac if it is of finite conductivity (Cinco and Samaniago-1978). Also, the slope of the curve would be expected to be $\frac{1}{2}$ that of the final slope before the pressure transient arrives at the first side of the reservoir, again if it were not for the effect of the frac. It is with this model and under these assumptions that the average reservoir matrix permeability was approximated.

Apparent Overall Reservoir Permeability (Radial Basis)

Apparent reservoir permeabilities were calculated using the final slopes on the Horner plots. It is recognized that these permeabilities are merely apparent values because of the peculiar geometry of these beds. Approximations of the average reservoir matrix permeability per se are presented in the following section.

The apparent permeabilities and the parameters used to calculate them are presented in Table 22. The methodology used in the calculations is that described by Matthews and Russell (Matthews and Russell- 1967). The calculated values range from .009 to .052 millidarcies and average .025 millidarcies.

Reservoir Matrix Permeability Approximations

By assuming 1) that the final slope observed on the Horner Plots represents movement of the pressure transient

down the long axis of the reservoirs, 2) that the slope of the curve prior to the pressure transient's arrival at the farthest sides of the reservoirs is theoretically $\frac{1}{4}$ that of the observed final slope, and 3) that the slope prior to the pressure transient's arrival at the nearest sides is theoretically $\frac{1}{4}$ that of the final slope, the matrix permeabilities can be determined using the methodology of Matthews and Russell. These values, which are simply 4 times those shown in Table 22, are:

<u>Well</u>	<u>Approximations of Matrix Permeability, md.</u>
A	0.10
B	0.06
C	0.04
D	0.21
F	0.14
G	0.06

The foregoing values are those which should be compared with the permeabilities calculated using Cox's methodology which was described previously. This comparison indicates that the Cox permeabilities for Wells A, B, and C are 30%, 17% and 50% of the foregoing values and his values for Wells D, F, and G are 200%, 214%, and 317% of the foregoing values respectively.

Gas-Filled Reservoir Void Volumes

In order to estimate the gas-filled reservoir void volume from the pressure and gas production data, the average reservoir pressure was approximated for the final shut-in period of Wells A-G. Since it is not clear whether or not the pressure transient had reached the "other side" of the Well H reservoir at the time that the well was placed back on production, no attempt was made to estimate that well's average reservoir pressure.

The method used to estimate average reservoir pressures is that recommended by Matthews and Russell (Matthews and Russell-1967), i.e. obtaining p^* from the Horner plots, obtaining $p^* - \bar{p}$ from type curves, and obtaining \bar{p} by difference. As Matthews and Russell point out, in tight reservoirs the shut-in time required to obtain \bar{p} directly from the Horner plots is prohibitive.

The estimated values of average reservoir pressure for Wells A-G are presented in Table 23 along with values of

the other parameters required in the computation. Values of these various parameters were obtained as follows:

- ϕ_g - average for all sands obtained by log computations
- \bar{A} - average area for all reservoirs (weighted by net sand thickness). Width is 22 x gross sand height and length is 10 x width.
- t_p - gas volume produced during flow period divided by rate for last 10 days
- μ - Erlougher - 1977, page 234
- c_g - Erlougher - 1977, page 233
- c_w - Erlougher - 1977, page 232
- c_f - Erlougher - 1977, page 229
- c_t - $S_g c_g + S_w c_w + c_f$
- p^* - Horner plot extrapolated to $t + \Delta t / \Delta t = 1$
- k - Table 22
- $\frac{p^* - \bar{p}}{m/2.303}$ - Matthews and Russell - 1967, page 44 (type curve for reservoir with a 5 to 1 length to width ratio)
- m - final slope on Horner plots

As indicated in the table, the average pressures obtained are very close to the values of p^* . They range from 912 to 1518 psia. In terms of percentage of the initial reservoir pressures, the range is 41% to 67% and the average is 53%.

The initial pressures shown in Table 10, the cumulative gas production volumes in Table 5, and the values of \bar{p} for June 1979 shown in Table 23 were used to develop the plots of \bar{p}/z versus cumulative production (Craft and Hawkins- 1959) shown in Figures 30-35. The initial volumes of gas-in-place were obtained from these curves at the point of intersection with the abscissa ($\bar{p}/z=0$). These values are presented in Table 24 along with the estimated gas-filled reservoir volumes and the parameters required for the computation.

As indicated in Table 24, the estimated gas-filled reservoir volumes range from 5.1 to 18.9 million cubic ft. The specific volumes₃ (volume per ft of net pay) range from 70,000 to 370,000 ft³ and average 240,000 ft³. These volumes

are compared with those determined using log properties and outcrop reservoir geometry, but excluding reservoir interconnection effects, Fig. 36.

The Horner plots utilized for the previous calculations tend to under-estimate the reservoir pressure, p^* , since an incremental time should have been added to the production life, t , used for the $t + \Delta t/\Delta t$ calculation. This would have resulted in a steeper slope, m , and a higher pressure (as well as a lower calculated permeability)*.

Reservoir Interconnection

For the observed average ratio of gross sand thickness to total interval thickness for Wells A-G of .28, the expected average reservoir drainage area in a 640-acre circular pattern would be about 100 acres of 4,400,000 sq. ft. per foot of net sand thickness, based on the Knutson drainage model (See Fig. 7). The total thickness of net sand for these 6 wells is 355 ft. Therefore, it would be expected that the total gas-filled reservoir volume would be $4.4 \times 10^6 \text{ ft.}^2 \times 355 \text{ ft.} \times .055$, or $86 \times 10^6 \text{ ft.}^3$. This compares favorably with the total volume for all 6 wells based on pressure buildup analysis of $75.3 \times 10^6 \text{ ft.}^3$.

The total volume for all 6 wells within a 640 acre circular drainage area based upon log values of porosity and water saturation and outcrop geometries without lens interconnection is $53.4 \times 10^6 \text{ ft.}^3$. (This value excludes those portions of reservoir sand which are estimated to extend beyond 5,960 ft. so as to be consistent with the 640-acre circular drainage area limitation. This excess volume is calculated to be $7.4 \times 10^6 \text{ ft.}^3$.) Therefore, it appears that a model utilizing some interconnection is suggested, since the production reservoir volume falls between the no-interconnection and the interconnected outcrop reservoir volumes (the no-interconnection volume is 71% and the interconnected volume is 114% of the "production" volume).

Fracture Conductivity

The log-log slope of the $\Delta(p^2)$ vs time data for Well G (Fig 25) is 0.49 or about $\frac{1}{2}$. For Wells B, C and H, the slopes are 0.2, 0.11, and 0.03 respectively (Fig 23, 24 and 26.). It appears, therefore, that the Well G fractures are essentially infinitely conductive and that those of Well B and C have finite conductivities. Because of the lack of late-time pressure data, the conductivities of the Well H fracture is questionable.

Effective Fracture Half Lengths

The Agarwal-Carter-Pollack gas well equation was used to calculate effective fracture half lengths for Wells B, C, and D. These are the only wells for which early-time buildup data plus permeability approximations are available.

* Personal communication R. D. Carter.

Two separate approximations for matrix permeability were utilized in this calculation. The first approximation, k_1 , is 4 times the apparent permeability (radial basis). This approximation applies in the case of a frac which is oriented in such a manner that the early-time linear flow into it would not be reduced by the boundary effect of either side of the channel. The second approximation, k_2 , is 2 times the apparent reservoir permeability (radial basis). It applies in the case of a frac oriented such that one boundary of the reservoir is fully reflected in the linear flow into the frac at early times. These two approximations should effectively bracket the effective apparent early time permeabilities.

The values of q used are those obtained by dividing the total volumes of gas produced during the production "test" periods by the total time including both time on production as well as time when the well was temporarily shut-in. Values assigned to the remaining parameters are the same as those used in the permeability calculations.

Calculated effective fracture half lengths are presented in Table 25. These calculated values range from 121 to 488 ft. for the k_1 permeability case and from 167 to 694 ft. for the k_2 case.

As a check on these estimated half lengths, corresponding fracture widths were determined. These values were first approximated by assuming 1) that the hydraulic fractures were contained within the sandstone reservoirs and 2) the void fraction in the fracs is .37. These assumptions are inherent in the expression:

$$\bar{y}_f = \frac{.685 V_s}{\bar{x}_f h_g}$$

where

h_g = gross sand thickness, ft.

\bar{y}_f = average fracture width, ft.

V_s = volume of proppant sand minus voids, ft^3 .

A second approximation was made by assuming that the fracs also penetrated the shales above and below each pay sand to the extent that the frac height for each sand is equal to the length.

The calculated values for these 2 cases, are presented in Table 26. They range from .003' to .019' for the first case and .0002' to .003' for the second case.

The first case lower value (.003') does not appear to be credible, since the maximum grain diameter in the predominant sand size fraction used (20-40 mesh) is .0027". This would only allow for a one maximum size grain-diameter fracture width. It is expected that this could not occur since the frac jobs would have probably sanded out at this width. Therefore, the calculated frac half length for well G is probably too large. On the other hand, the first case frac widths for Wells B and C are more credible in that they are the equivalent of 6 to 9 maximum size grain diameters. The lower value for Case 2 is obviously nonsensical. The higher value is also incredible in line with the foregoing reasoning.

It is probable that the fracs did indeed penetrate the overlying and underlying shales. Therefore, the actual frac widths for Wells B and C would be expected to be less than the value for the first case and considerably greater than the second case value. If true, the approximations for frac lengths for Well's B and C hold up under the "frac width" test.

SUMMARY AND CONCLUSIONS

Only 10% of the Uinta Basin tight gas sand wells that have been produced for at least 7 years exhibit near radial flow. Neither Δt , R_{wa} , PSP, nor SP curve character appear to be diagnostic indicators of near radial-flow sands in these wells. However, based upon a limited data set, the more continuous sands appear to have a lower clay content.

Standing water in a gas well substantially hampers definitive determination of relative contribution of individual sand to flow by noise and differential temperature logging.

Assuming radial flow for a sampling of Wasatch gas wells, the overall apparent reservoir permeabilities range from .009 to .052 millidarcies and the approximations for apparent matrix permeabilities for use in linear flow models range from .06 to .21 millidarcies.

After approximately 18 years of production, the average reservoir pressures in six Wasatch gas wells have declined roughly 50%. The average specific gas-filled reservoir void volume is 240,000 cu.ft. per ft. of net pay thickness and average specific area for these wells is 100 acres. The average additional amount of reservoir volume attributable to lens interconnection and included in this specific volume is about 40%.

At least one wells' fractures exhibit essentially infinite conductivity while at least two wells' fractures exhibits finite conductivity. The average fracture half-lengths based on data from 2 wells appear to be about 0.1 ft/bbl of diesel fuel with an average proppant load of 1.2 - 1.7 lbs/gal at injection rates of 18-24 BPM and injection pressures of 2,500 to 4,600 psi for each 100 ft. of gross sand in the fraced interval.

Knutsons' lenticular reservoir model for the Neslen and Farrer facies of the Mesaverde Group appears to be adequate for evaluation of Wasatch reservoir behavior.

ACKNOWLEDGEMENTS

Mr. Charles Atkinson of the DOE provided technical direction and made helpful suggestions for the pressure buildup data analysis.

Belco Petroleum Corporation, Gas Producing Enterprises and Diamond Shamrock Oil and Gas Company very generously made their gas wells and well data available for this study.

Colorado Interstate Gas Company shut in a producing well for buildup analysis and recorded the pressure buildups. Mountain Fuel Supply Company recorded pressure buildups and put wells on production specifically for this study during a time of low gas demand.

Mr. Paul Branigan of CER Corporation provided an independent computer check of a number of the determinations from the pressure buildup data and made helpful suggestions regarding analysis techniques. He critically read the manuscript.

The assistance in the field of Leo Jorgenson (Mountain Fuel), Al Maxfield (Belco), Karl Oden (Gas Producing Enterprises), and Bill Swim (Colorado Interstate) is gratefully acknowledged.

REFERENCES

Agarwal, R. G., R.D. Carter, and C. B. Pollock, "Evaluation and Prediction of Performance of Low Permeability Gas Wells Stimulated by Massive Hydraulic Fracturing", SPE 6838, SPE-AIME Fall Technical Conference, Denver Colo., October 9-12, 1977.

Cinco, Heber and Fernando Samaniego, "Transient Pressure Analysis for Fractured Wells", SPE 7490, SPE-AIME 53rd Annual Fall Conference, Houston, Tx. October 1-3, 1978.

Craft, B. C. and M. F. Hawkins, Applied Petroleum Reservoir Engineering, Prentice Hall, Inc., Englewood Cliffs, N. J., 1959.

Erlougher, R. C., Jr. Advances in Well Test Analysis, SPE-AIME Monograph Volume 5, Henry L. Doherty Series, 1977

Knutson, C. F., "Outcrop Study of Fracture Patterns and Sandstone Geometry, Eastern Uinta Basin, Utah", C. K. GeoEnergy Corporation, Las Vegas, Nevada, September 23, 1977.

Knutson, C. F., and C. R. Boardman, "Continuity and Permeability Development in the Tight Gas Sands of the Eastern Uinta Basin, Utah", DOE Report No. NVO/0011-1, May 1, 1978.

Knutson, C. F., and C. R. Boardman, "Rock Geometry/Mechanics Study of the Western Tight Gas Reservoirs", Lawrence Livermore Laboratory Report UCRL 13778, September 1977.

Matthews, C. S. and D. G. Russell, Pressure Buildup and Flow Tests in Wells, SPE-AIME Monograph Volume 1, Henry L. Doherty Series, 1967

Murnay, E. E., "Wasatch Formation of the Uinta Basin", Guidebook to the Geology and Mineral Resources of the Uinta Basin, Intermountain Association of Petroleum Geologists, Salt Lake City, Utah, 1964.

NOMENCLATURE

- \bar{A} : average area of sand reservoirs in a well
 B_g : gas formation volume factor
 c_f : formation rock/pore volume compressibility
 c_g : gas compressibility
 c_t : total system compressibility
 c_w : water compressibility
 D_m : depth of perforations' midpoint
 H_g : height of gas column in wells
 H_w : height of water column above average midpoint depth of the perforated zones.
 H_{wt} : height of water column above perforation midpoint depth in tubing
 h : net pay sand thickness
 h_g : gross sand thickness
 k : permeability
 m : slope of curve
PSP: pseudo-static spontaneous potential
 p^* : pressure at time when $t_p + \Delta t / \Delta t = 1$
 \bar{p} : average reservoir pressure
 P_i : initial reservoir pressure
 P_m : pressure at depth of midpoint of perforated zones
 P_{mc} : pressure at perforations' midpoint depth in casing
 P_r : pseudoreduced pressure
 P_s : pressure at surface
 P_{st} : surface pressure in tubing
 P_{wf} : flowing well pressure
 q : flow rate
 R_{wa} : apparent formation water resistivity
 S_w : water saturation
SP : spontaneous potential
 T : absolute temperature, $^{\circ}R$
 T_r : pseudoreduced temperature

(Nomenclature continued)

t_p : gas volume produced during flow period divided
by last 10 day's rate

V_p : volume of gas produced prior to pressure buildup

V_s : volume of proppant minus voids

x_f : effective fracture half length

y_f : fracture width

z : gas deviation factor

$\Delta(p^2)$: difference in the squares of the flowing well
pressure and the pressure at any time after shut-in.

Δt : cumulative time after shut-in.

Δt_s : sonic wave interval travel time

ϕ : porosity

ϕ_g : gas-filled porosity

PRODUCTION DATA

TABLE 1.

NEAR RADIAL FLOW JUNTA BASIN GAS WELLS

Well	Fm	Twp-Rge-Sec	Operator	Cumulative Production, MMCF		1977 Production Rate, MCF/D	Slope of Log Cumulative Production Volume vs Log Time Curve
				5 yr.	10 yr.		
RH#3	W	11S 23E 11	Shamrock	230	400	33	.79
CV#17	W	9S 22E 25	Belco	146	242	24	.80
CV#21	W	9S 22E 23	Belco	269	448	53	.75
UT#1	W	10S 22E 8	GPE	564	895	111	.88
UT#1	M	10S 22E 8	GPE	338	714	152	.81
GP#1	W	12S 15E 11	Texaco	195	338	63	.78

CUMULATIVE PRODUCTION TIME, MONTHS/CUMULATIVE GAS PRODUCTION VOLUMES THROUGH 1977, MMSCF

Well	1961	1962	1963	1964	1965	1966	1967	1968	1969	1970	1971	1972	1973	1974	1975	1976	1977
RH#3 (W)	2/ 8	12/ 69	22/ 111	33/ 139	41/ 160	49/ 192	58/ 222	63/ 243	68/ 265	74/ 287	80/ 307	86/ 325	92/ 342	98/ 357	104/ 374	109/ 389	112/ 392
CV#17 *		7/ 32	14/ 46	22/ 60	24/ 63	30/ 78	39/ 96	48/ 117	55/ 136	57/ 143	67/ 154	75/ 170	86/ 186	93/ 202	104/ 222	115/ 238	126/ 246
CV#21		2/ 22	13/ 86	25/ 133	34/ 164	43/ 197	48/ 221	58/ 261	69/ 306	77/ 336	82/ 349	91/ 375	103/ 404	115/ 434	126/ 464	138/ 493	150/ 512
UT#1 (W)	2/ 32	14/ 159	25/ 258	35/ 357	45/ 443	51/ 493	55/ 521	60/ 564	64/ 611	70/ 656	75/ 691	81/ 729	88/ 771	95/ 804	100/ 835	106/ 860	115/ 890
UT#1 (M)	2/ 32	14/ 143	23/ 164	33/ 209	44/ 230	51/ 265	59/ 331	65/ 372	71/ 423	77/ 470	83/ 517	88/ 555	94/ 591	100/ 624	106/ 654	113/ 682	120/ 714
GP#1		4/ 29	15/ 48	26/ 68	26/ 98	38/ 134	48/ 163	60/ 195	72/ 221	84/ 244	89/ 254	95/ 275	100/ 287	107/ 307	113/ 323	119/ 336	128/ 353

* Additional zones completed in 1974. Production data through 1973 only were used in the analysis.

W - Wasatch
M - Mesaverde

TABLE 2

WELL COMPLETION DATA

NEAR RADIAL FLOW UINTA BASIN GAS WELLS

<u>Well</u>	<u>No. of Sands</u>	<u>Completed Zones Depth, ft.</u>	<u>Frac Fluid Volume, gal.</u>	<u>Proppant (20/40 sand) Weight, lbs.</u>
RH#3	5	4096-4106	6,600 diesel	2,000
		4368-74,4296-4306	14,900 diesel	13,700
		4458-62	8,360 diesel	3,730
		4528-38	18,360 diesel	10,800
CW#17	1*	6201	18,930 water	15,000
CW#21	2	5327-65,5396-5429	40,200 water	50,000
UT#1(W)	4	5060-81	37,200 water	50,000
		5242-62	16,800 water	14,000
		6720-30,6747-70	15,850 oil & water	9,750
UT#1(M)	9	7004-82	7,900 petrogel	13,000
		7320-40	13,000 water	10,100
		7720-50,7798-7817,7832-40	21,000 water	28,000
		7889-7905,7920-40,8040-50	22,260 water	48,000
		7720-8110	24,150 water	29,300
		8078-8110		
GP#1	5	3782-97, 3813-37	25,000 water	24,000
		4036,44		
		4336-54,4426-45	20,000 water	20,000

* Until 1974.

TABLE 3. SOME RESERVOIR ROCK CHARACTERISTICS

NEAR RADIAL FLOW WELLS

WELL	Completed Sand Depths, ft.	Thickness Net Pay* Sands, ft.	Δt_s , msec/ft.	PSP, millivolts	R_{we} , ohm-m	SP Curve Character	ϕ , %	S_w , %
RH#3	4095-4106	11	77	29	.67	Fining Up	15	65
	4292-4299	7	72	21	.84	Fining Up	11	58
	4300-4306	6	75	24	.76	Indeterminate	13	68
	4368-4375	7	71	38	.48	Fining Up	10	62
	4458-4464	6	76	49	.38	Symmetrical	14	41
	4532-4538	6 43	78	67	.21	Symmetrical	16	37
CW#17	6197-6210	13	67	29	40	Fining Down	7	55
CW#21	5334-5354	20	71	12	.05	Fining Up	10	76
	5410-5422	12 32	71	27	.03	Fining Up	10	60
UT#1	5055-5090	27	72	-	-	Fining Up	11	-
	5242-5272	22	68	12	.68	Symmetrical	8	58
	6721-6732	0	-	-	-	-	-	-
	6748-6769	19	68	44	.22	Fining Down	8	41
	7007-7023	16	-	24	.37	Fining Down	-	48
	7032-7038	6	-	20	.38	Symmetrical	-	40
	7058-7081	23	-	20	.38	Fining Down	-	55
	7324-7334	10	-	28	.30	Fining Up	-	40
	7718-7727	9	-	23	.35	Symmetrical	-	69
	7735-7754	16	-	21	.35	Complex	-	72
	7796-7815	19	-	15	.50	Fining Up	-	80
	7822-7831	9	-	14	.52	Symmetrical	-	80
	7872-7947	63	-	16	.47	Fining Up	-	71

* $\phi > 5\%$, Apparent $S_w \leq 80\%$

(Table 3 continued)

SOME RESERVOIR ROCK CHARACTERISTICS-NEAR RADIAL FLOW UINTA BASIN GAS WELLS

WELL	Completed Sand Depths, ft.	Thickness Net Pay* Sands, ft.	Δt_s , μ sec/ft.	PSP, millivolts	Rwe, ohm-m	SP Curve Character	$\bar{\Phi}$, %	\bar{S}_w , %
UT#1	8054-8060	6	69	22	.33	Fining Up	9	65
(cont)	8094-8110	16	74	30	.27	Fining Up	13	58
		261						
GP#1	3781-3800	19	70	30	.9	Symmetrical	10	48
	3810-3840	26	70	58	.37	Fining Up	10	36
	4030-4054	15	70	47	.55	Fining Down	10	50
	4331-4351	15	65	35	.85	Fining Up	6	72
	4423-4426	7	66	40	.6	Fining Up	7	58
		82						

* $\Phi > 5\%$, Apparent $S_w \leq 80\%$

TABLE 4- APPARENT CLAY FRACTION-PRODUCING GROSS SANDS

Well	Slope of Log Cum. Production Volume vs Log Time	Gross Sand Depth, ft.	Net Sand Depth, ft.	Apparent Clay Fraction
CW#21	.75	5327-65	5334-40	.22
			5340-54	.09
		5396-5429	5410-16	.18
			5416-22	.09
CW#17	.80	6196-6210	6197-6210	.13
GP#1	.78	3781-3800	3781-3800	.29
		3810-40	3810-40	.15
		4030-54	4030-54	.10
		4331-51	4331-51	.13
		4423-46	4423-46	.17
RH#3	.79	4095-4107	4095-4106	.33
		4292-4300	4292-99	.46
		4300-06	4300-06	.42
		4364-76	4368-75	.19
		4458-66	4458-64	0
		4525-48	4532-38	.06
CW#16	.59	5262-73	5262-69	.14
		5373-87	5374-86	.09
		5440-87	5450-55	.21
			5460-67	.09
			5473-77	.29
		5534-51	5534-41	.09
		5830-42	5830-35	.01
		5848-71	5850-54	.05
			5856-61	.06
			5861-68	.20
		SU#6	.65	5330-60
	5353-59			0
5402-45	5407-18			.40
	5423-30			.29
	5435-43			.57
5505-15	5504-08			.14
	5509-13			.14
5635-55	5637-47			.20
	5644-55	.14		
CW#2	.67	5065-5117	5066-84	.17
UT#83 X 9H	.50	4868-86	4868-86	.30
		4894-4903	4894-4903	.37
RW#212	.56	9158-82	9162-67	.22
			9168-74	.27
			9174-80	.33
		9265-87	9266-82	.24
		9365-94	9372-92	.26
B#3	.43	4916-26	4916-26	.29

Table 5

GAS PRODUCTION STATISTICS - 7 UINTA BASIN WASATCH WELLS

CUMULATIVE PRODUCTION TIME, MONTHS/CUMULATIVE GAS PRODUCTION, MMCF

Well	1961	1962	1963	1964	1965	1966	1967	1968	1969	1970	1971	1972	1973	1974	1975	1976	1977	1978	1979**
A	1/ 13/	23/ 134	23/ 196	34/ 262	41/ 310	51/ 381	61/ 437	71/ 497	82/ 557	93/ 613	104/ 630	114/ 676	125/ 723	136/ 767	147/ 811	158/ 851	169/ 879	175/ 899	179/ 915
B	1/ 5	12/ 84	22/ 130	34/ 175	43/ 203	52/ 244	62/ 278	72/ 314	83/ 349	94/ 384	105/ 394	115/ 421	127/ 450	138/ 477	149/ 503	160/ 527	171/ 546	176/ 556	180/ 566
C	1/ 16	13/ 176	24/ 268	36/ 346	45/ 398	55/ 449	66/ 508	76/ 561	87/ 616	97/ 665	101/ 680	110/ 717	121/ 757	132/ 793	143/ 828	154/ 860	165/ 879	171/ 886	175/ 892
D	10/ 383	20/ 532	31/ 646	40/ 712	49/ 792	60/ 883	71/ 955	82/ 1043	93/ 1116	104/ 1177	115/ 1231	126/ 1288	136/ 1380	147/ 1453	157/ 1529	164/ 1555	169/ 1571	173/ 1587	
* F	1/ 46	12/ 293	23/ 412	33/ 502	43/ 596	45/ 679	56/ 779	65/ 864	77/ 938	88/ 1022	99/ 1093	109/ 1158	120/ 1222	131/ 1294	142/ 1342	153/ 1393	164/ 1436	170/ 1479	
G	1/ 15	13/ 117	24/ 165	35/ 216	42/ 237	47/ 248	56/ 269	65/ 296	73/ 319	86/ 328	94/ 339	105/ 358	116/ 378	127/ 400	138/ 421	146/ 438	149/ 443	151/ 445	151/ 447
H	2/ 63	13/ 365	25/ 571	35/ 717	47/ 847	58/ 958	69/ 1002	80/ 1060	90/ 1119	101/ 1187	113/ 1259	124/ 1329	136/ 1396	148/ 1459	160/ 1460	172/ 1473	178/ 1494	184/ 1503	184/ 1511

* An eighth well, "Well E", was also tested but was found to have a leaky valve.

** Through June only.

Table 6 WELL CASING AND TUBING SPECIFICATIONS

Well	Plugged Depth, ft. (KB)	CASING		TUBING	
		o.d., in.	Depth, ft. (KB)	o.d., in.	Depth, ft. (KB)
A	5,765	5 1/2	7,200	2 3/8	5,742
B	6,330	5 1/2	6,365	2 (?)	6,329
C	5,889	7 4 1/2	5,150 5018-6257	(not available)	
D	5,530	4 1/2	5,592	2 3/8	5,510
F	6,407	4 1/2	6,444	2 3/8	5,456
G	5,603	5 1/2	5,703	2 3/8	5,597 *
H	6,473	7	6,473	2 7/8	5,661 **

* Packer at 4,536'

** Packer at 5,661'

TABLE 7 PERFORATION DEPTHS

<u>Well</u>	<u>Perforated Zone Depths, ft.(KB)**</u>	<u>Average Midpoint Depth of Perforated Zones,* ft.(KB)**</u>
A	5462-72, 5579-96, 5709-25	5,595
B	5504-08, 5654-60, 5693-96, 5841-52, 5902-24, 6288-94	5,899
C	5424-34, 5480-88, 5550-52, 5764-68, 5798-5803, 5862-78	5,651
D	5098-5100, 5124-26, 5238-40* 5252-53*, 5402-04, 5476-78, 5510-11	5,313
F	5484-94, 5544-54, 5730-34, 5940-56, 6347-51	5,794
G	5428-59, 5595-5612	5,520
H	6345-6375	6,360

* Single Complex Sand

** Depth from Kelly Bushing (KB). Distance from Kelly Bushing to ground level was 12 ft. for Wells A & G and was 11 ft. for all the others.

TABLE 8. FRAC JOB DETAILS

Well	Zones No.*	FLUID		PROPPANT		Available Injection Pressures, psig	Available Injection Rates, BPM
		Volume, gal.	Type	Weight, #	Type		
A	1, 2, 3	21, 000	diesel	27, 000	20-40 sand		
B	1, 2, 3	17, 925	diesel	28, 500	20-40 sand	3700-4000	25.1
				8, 500	10-20 sand		
C	4, 5	16, 750	diesel	30, 000	20-40 sand	Max. 4000	22
				17, 300	20-40 sand	Max. 4600	18.4
C	1, 2, 3	36, 950	diesel	50, 000	20-40 sand	2500-3400	22
				6, 800	20-40 sand	4000-4600	
				50, 000	20-40 sand	3000-3700	24
				800	walnut hulls		
D	1, 2, 3	36, 000	salt water	42, 000	20-40 sand	Max. 4400	20
				25, 000	diesel	20, 000	20-40 sand
F	1, 2, 3	50, 000	salt water	50, 000	20-40 sand	3000-4200	17
				40, 000	20-40 sand	2900-4200	20
				600	walnut hulls		
G	1, 2	20, 000	diesel	25, 000	20-40 sand		
H	1	15, 000	salt water	15, 000	20-40 sand		10.5

* Zones numbered in sequence from uppermost to lowermost.

TABLE 9. FRACTIONAL SANDSTONE CONTENT IN PRODUCTION INTERVALS*

	Well						
	A	B	C	D	F	G	
Depth of Interval, ft.	5460-5740	5495-6296	5410-5880	5096-5518	5474-6352	5425-5618	
Thickness of Interval, ft.	280	801	470	422	878	193	
Gross Sandstone Thickness, ft.	85	281	161	115	150	63	
Ratio Gross Sandstone Thickness to Interval Thickness	.30	.35	.34	.27	.17	.33	
Average:	$\frac{855}{3044} =$		$\frac{.28}{}$				

*From top of uppermost sand to base of lowermost sand.

TABLE 10. INITIAL RESERVOIR PRESSURES AND TEMPERATURES AT AVERAGE DEPTH OF PERFORATIONS

	WELL					
	A	B	C	D	F	G
Depth of Perforations Midpoint, ft (GL)	5583	5888	5640	5302	5783	5508
Initial Pressure, psia	2254	2625	2696	2317*	2575	2203
Prior Shut-in time, hrs.	-	1800	504	-	-	6552
Gradient, psi/ft	.404	.446	.478	.437**	.445	.400
T, °R	617	620	617	614	619	616
T _r	1.71	1.72	1.71	1.71	1.72	1.71
P _r	3.36	3.92	4.02	3.46	3.84	3.29
z	.86	.86	.86	.86	.86	.86
P ₁ /z, psia	2621	3052	3135	2694	2994	2562

* Estimated value

** Average - Wells A-C, F-G.

TABLE 11. COMPLETED RESERVOIR SAND PROPERTIES CALCULATED FROM LOG DATA

Well	Gross Sand Depth, ft.	Gross Sand Thickness, ft.	Net Sand * Thickness, ft.	Net Sand Porosity, %	Net Sand Water Saturation, %
A	5460-86	26	8	14	51
	5576-5608	32	17	13	49
	5709-36	27	22	12	46
	All Zones	85	47	12.7	48
B	5495-5510	15	15	13	50
	5652-63	11	11	13	44
	5674-98	24	6	12	25
	5825-54	29	29	14	60
	5898-5935	37	31	13	53
	6285-96	11	11	9	30
	All Zones	127	103	12.8	50
C	5410-40	30	30	13	52
	5472-94	22	10	14	58
	5543-54	11	5	14	54
	5758-76	18	6	9	65
	5796-5806	10	4	10	58
	5858-80	22	8	6	69
	All Zones	113	63	11.8	56
D	5096-5108	12	2 **	9	70
	5116-33	17	15	13	60
	5234-62	28	18	11	65
	5396-5412	16	13	12	69
	5474-84	10	2 **	11	70
	5504-18	14	8	11	70
All Zones	97	58	11.6	65	

* Porosity cutoff of 5% and water saturation cut off of 70% were used in net sand thickness approximations.

** Assumed values (calculated water saturation for entire sand thickness was more than 70%)

TABLE 11. (continued)

Completed Reservoir Sand Properties Calculated from Log Data

Well	Gross Sand Depth, ft.	Gross Sand Thickness, ft.	Net Sand * Thickness, ft.	Net Sand Porosity, %	Net Sand Water Saturation, %
F	5474-5500	26	11	10	50
	5540-60	20	10	7	70
	5726-39	13	12	12	39
	5936-63	27	13	8	45
	6344-52	8	8	13	35
	All Zones	94	54	9.9	46
G	5425-66	41	9	14	70
	5596-5618	22	22	14	67
	All Zones	63	31	14	68
H	6345-75	30	25	10	45

* Porosity cutoff of 5% and water saturation cut off of 70% were used in net sand thickness approximations.

TABLE 12 RESERVOIR GROSS SAND GEOMETRIES ESTIMATED FROM ROCK OUTCROP STUDIES

Well	Sand No. #	Gross Thickness, ft.	Estimated Width, ft.	Estimated Length, ft.	Estimated Area 10 ⁶ ft. 2	Estimated Volume, 10 ⁶ ft. 3
A	1	26	572	5720	3.27	85.1
	2	32	704	7040	4.96	158.6
	3	27	594	5940	3.53	95.3
Total		85				339.0
B	1	15	330	3300	1.09	16.3
	2	11	242	2420	0.59	6.4
	3	24	528	5280	2.79	66.9
	4	29	638	6380	4.07	118.0
	5	37	814	8140	6.63	245.2
	6	11	242	2420	0.59	6.4
Total		127				459.2
C	1	30	660	6600	4.36	130.7
	2	22	484	4840	2.34	51.5
	3	11	242	2400	0.59	6.4
	4	18	396	3960	1.57	28.2
	5	10	220	2200	.48	4.8
	6	22	484	4840	2.34	51.5
Total		113				273.1
D	1	12	264	2640	.70	8.4
	2	17	374	3740	1.40	23.8
	3	28	616	6160	3.79	106.2
	4	16	352	3520	1.24	19.8
	5	10	220	2200	.48	4.8
	6	14	308	3080	.95	13.3
Total		97				176.3

TABLE 12. (continued)

Reservoir Gross Sand Geometries
Estimated From Rock Outcrop Studies

<u>Well</u>	<u>Sand No.*</u>	<u>Gross Thickness, ft</u>	<u>Estimated Width, ft.</u>	<u>Estimated Length, ft.</u>	<u>Estimated Area 2 10⁶ ft.</u>	<u>Estimated Volume 3 10⁶ ft.</u>
F	1	26	572	5720	3.27	85.1
	2	20	440	4400	1.94	38.7
	3	13	286	2860	.82	10.6
	4	36	594	5940	3.53	95.3
	5	8	176	1760	.31	2.5
Total		103				232.2
G	1	41	902	9020	8.14	333.6
	2	22	484	4840	2.34	51.5
Total		63				385.1
H	1	30	660	6600	4.34	130.7

* Sands numbered in sequence from uppermost to lowermost.

TABLE 13. RESERVOIR GAS-FILLED VOID VOLUMES* BASED ON LOG VALUES OF NET SAND THICKNESS, POROSITY, AND WATER SATURATION AND GEOMETRY DETERMINED FROM OUTCROPS

Well	Sand No.	Estimated Area 106 ft. 2	Net Sand Thickness, ft.	Net Sand Volume 106 ft. 3	Fractional Gas Saturated Porosity	Gas Filled Pore Volume 106 ft. 3
A	1	3.27	8	26.16	.069	1.81
	2	4.96	17	84.32	.066	5.57
	3	3.53	22	77.66	.065	5.05
Total			47	188.14		12.43
B	1	1.09	15	16.35	.065	1.06
	2	0.59	11	6.49	.073	.47
	3	2.79	6	16.74	.090	1.51
	4	4.07	29	118.03	.056	6.61
	5	6.63	31	205.53	.061	12.54
	6	0.59	11	6.49	.063	.41
Total			103	369.63		22.60
C	1	4.36	30	130.80	.062	8.11
	2	2.34	10	23.40	.059	1.38
	3	0.59	5	2.95	.064	.19
	4	1.57	6	9.42	.032	.30
	5	0.48	4	1.92	.042	.08
	6	2.34	8	18.72	.019	.36
Total			63	187.21		10.42
D	1	0.70	2	1.40	.027	.04
	2	1.40	15	21	.052	1.09
	3	3.79	18	68.22	.039	2.66
	4	1.24	13	16.12	.037	.60
	5	0.48	2	0.96	.033	.03
	6	0.95	8	7.60	.033	.25
Total			58	115.30		4.67

* Excludes effect of reservoir interconnection.

Table 13. (continued)

Reservoir Gas-Filled Void Volumes Based on Log Values of Net Sand Thickness, Porosity, and Water Saturation and Geometry Determined From Outcrops

Well	Sand No.	Estimated Area, 10 ⁶ ft. ²	Net Sand Thickness, ft.	Net Sand Volume, 10 ⁶ ft. ³	Fractional Gas Saturated Porosity	Gas Filled Pore Volume, 10 ⁶ ft. ³
F	1	3.27	11	35.97	.050	1.80
	2	1.94	10	19.40	.021	.41
	3	0.82	12	9.84	.073	.72
	4	3.53	13	45.89	.044	2.02
	5	.31	8	2.48	.085	.21
Total			54	113.58		5.16
G	1	8.14	9	73.26	.042	3.08
	2	2.34	22	51.48	.046	2.37
Total			31	124.74		5.45
H	1	4.34	25	108.50	.055	5.97

TABLE 14. FLOW TEST DATA

Well	Prior Shut in Time, days	Production		Production Period Days Produced/ Days Shut in	Calculated Flow Period, t_p^* days	Latest Average Flow Rate, q^{**} , MCF/day	Volume Produced, V_p , MCF
		Start Date	Stop Date				
A	170	9/18/78	5/14/79	213/42	209	138	28,903
B	192	9/16/78	6/21/79	208/41	180	103	18,554
C	169	9/17/78	6/22/79	212/65	104	110	11,457
D	170	9/17/78	5/14/78	206/33	267	103	27,474
F	166	9/14/78	5/14/79	230/14	251	142	25,639
G	249	11/21/78	6/21/79	99/112	67	50	3,348
H	52	5/15/79	6/20/79	37/0	30	114	3,434

* $t_p = V_p/q$

** Latest 10 days of actual production.

TABLE 15. MONTHLY PRODUCTION PERIOD STATISTICS

<u>Month</u>	<u>Well A</u>	<u>Well B</u>	<u>Well C</u>	<u>Well D</u>	<u>Well F</u>	<u>Well G</u>	<u>Well H</u>
Sept. 1978	2115/ 12	851/ 14	994/ 13	2145/ 13	4027/ 16	- -	*
Oct. 1978	2716/ 21	2834 31	1376/ 31	3139/ 22	5013/ 31	- -	*
Nov. 1978	4041/ 26	1079/ 28	919/ 27	2940/ 24	3274/ 28	437/ 9	*
Dec. 1978	3684/ 28	2641/ 28	733/ 21	2814/ 23	3998/ 28	988/ 27	*
Jan. 1979	4271/ 31	2778/ 31	977/ 18	4050/ 31	4682/ 31	572/ 21	*
Feb. 1979	3118/ 28	2089/ 28	1346/ 24	3830/ 27	3554/ 25	325/ 12	*
Mar. 1979	3256/ 27	2080/ 28	1448/ 29	3148/ 26	3308/ 29	200/ 12	*
Apr. 1979	4357/ 30	2482/ 30	2015/ 30	4377/ 30	4443/ 30	146/ 3	- -
May 1979	1345/ 10	810/ 10	626/ 10	1031/ 10	1340/ 10	290/ 7	1597/ 17
June 1979	- -	912/ 8	1023/ 9	- -	- -	390/ 8	1837/ 20

* Data not available

TABLE 16

PRESSURE BUILDUP DATA-Well B

 $t_p = 180$ days

Δt , days	$\frac{t + \Delta t}{\Delta t}$	Measured Tubing Pressure, psia	Calculated Gas Column Pressure, psi	Calculated Water Column Pressure, psi	Calculated Pressure at Perforations' Midpoint, psia
1	181	655	88	232	975
2	91.0	700	94	"	1026
3	61.0	723	97	"	1052
4	46.0	782	105	"	1119
5	37.0	805	108	"	1145
6	31.0	809	108	"	1149
7	26.7	819	110	"	1161
8	23.5	825	111	"	1168
10	19.0	833	112	"	1177
11	17.4	837	112	"	1181
12	16.0	843	113	"	1188
13	14.8	845	113	"	1190
15	13.0	853	114	"	1199
16	12.3	854	114	"	1200
17	11.6	857	115	"	1204
105	2.71	943	127	230	1300
121	2.49	953	128	230	1311

Note: (1) Water level in the casing was measured at 5,615 ft. on June 30, 1979 ($\Delta t=11$) and at 5,611 ft. on October 2, 1979 ($\Delta t=105$). Tubing water level was calculated to have been 5,362 ft. and 5,366 ft. respectively on these dates.

TABLE 17 PRESSURE BUILDUP DATA-Well C

$t_p = 104$ days

Δt , days	$\frac{t + \Delta t}{\Delta t}$	Measured Tubing Pressure, psia	Calculated Gas Column Pressure, psi	Calculated Water Column Pressure, psi	Calculated Pressure at Perforations' Midpoint, psia
1	105	700	87	306	1093
2	53.0	805	99	"	1210
3	35.7	864	107	"	1277
4	27.0	870	108	"	1284
5	21.8	876	108	"	1290
6	18.3	881	109	"	1296
7	15.9	888	110	"	1304
10	11.4	893	110	"	1309
12	9.67	900	111	"	1317
13	9.00	903	112	"	1321
14	8.43	905	112	"	1323
16	7.50	910	112	"	1328
17	7.12	914	113	"	1331
105	1.99	983	122	304	1409
121	1.86	994	123	304	1421

Note: Casing water level was measured at 4,945 ft. on June 30, 1979 ($\Delta t=11$ days) and at 4,949 ft. October 2, 1979 ($\Delta t=105$ days). The June 30th level was assumed to hold from $\Delta t=1$ through $\Delta t=17$.

TABLE 18 PRESSURE BUILDUP DATA-Well G

$t_p = 67$ days

Δt , days	$\frac{t + \Delta t}{\Delta t}$	Measured Tubing Pressure, psia	Calculated Gas Column Pressure, psi	Assumed Water Column Pressure, psi	Calculated Pressure at Perforations' Midpoint, psia
0	∞	480	62	160	702
1	68	512	66	"	738
2	34.5	525	68	"	753
3	23.3	528	68	"	756
4	17.8	533	69	"	762
5	14.4	535	69	"	764
6	12.2	536	69	"	765
7	10.6	538	69	"	767
8	9.38	539	69	"	768
105	1.64	623	80	"	863
121	1.55	630	81	"	871

Note: 1- Well was worked on at $\Delta t=8$ days.

2- Average water column height of 363 ft. for Wells A-F was assumed throughout entire buildup.

TABLE 19 PRESSURE BUILDUP DATA-Well H

$t_p = 30$ days

Δt , days	$\frac{t + \Delta t}{\Delta t}$	Measured Tubing Pressure, psia	Calculated Gas Column Pressure, psi	Assumed Water Column Pressure, psi	Calculated Pressure at Perforations' Midpoint, psia
.25	121	740	111	160	1011
.42	72.4	774	116	"	1050
.96	32.3	774	116	"	1050
1	31.0	801	120	"	1081
2	16.0	817	123	"	1100
3	11.0	824	124	"	1108
4	8.50	835	125	"	1120
6	6.00	837	126	"	1123
8	4.75	839	126	"	1125
10	4.00	839	126	"	1125
12	3.50	839	126	"	1125
14	3.14	844	127	"	1131
30	2.00	848	127	"	1135
40	1.75	850	128	"	1138
50	1.60	852	128	"	1140

Note: Average water column height for Wells A-F of 363 ft. was assumed throughout entire buildup.

TABLE 20 PRESSURE BUILD-UP DATA - WELLS A, D, F

Well	(1)		Measured Casing Pressure, psia	(2)		Calculated Gas & Water Column Pressures, psi		Calculated Pressure at Perforations Midpoint, psia
	t, days	Δt , days		t + Δt	Pressure, psia	Gas (3)	Water (4)	
A	209	98	1069	3.13	144	90	1303	
		141	1120	2.48	151	90	1361	
		157	1131	2.33	152	90	1373	
D	267	98	810	3.72	104	82	996	
		141	836	2.89	107	82	1025	
		157	843	2.70	108	82	1033	
F	251	98	816	3.56	110	164	1090	
		141	848	2.78	115	164	1127	
		157	859	2.60	116	164	1139	

Note: (1) Total volume produced divided by latest rate (latest 10 days)
 (2) Measured at wellhead.
 (3) P = (.000025) (depth to water, ft.) (casing pressure, psi)
 (4) (.44) (height of water column in ft.)

TABLE 21. WATER LEVEL DEPTHS AND SURFACE GAS PRESSURES MEASURED IN 1979 BY DEAD WEIGHT TESTER AND ECHOMETER.

<u>Well</u>	<u>Date</u>	<u>Tubing Pressure, psia</u>	<u>Casing Pressure, psia</u>	<u>Depth of Water Level In Casing, ft.</u>
A	8/20/79	1069	1069	5379
	10/2/79	1118	1120	5379
	10/18/79	1112	1131	*
B	6/30/79	*	*	5615
	10/2/79	943	1035	5611
	10/18/79	953	1050	*
C	6/30/79	*	*	4945
	10/2/79	983	986	4949
	10/18/79	994	996	*
D	8/20/79	561	810	5115
	10/2/79	550	836	5115
	10/18/79	541	843	*
F	8/20/79	816	816	5410
	10/2/79	851	848	5410
	10/18/79	859	859	*
G	10/2/79	623	*	*
	10/18/79	630	*	*

* not measured

TABLE 22 APPARENT RESERVOIR PERMEABILITIES
WELLS A, B, C, D, F, G

	<u>Well A</u>	<u>Well B</u>	<u>Well C</u>	<u>Well D</u>	<u>Well F</u>	<u>Well G</u>
T, °R	617	620	617	614	619	616
p*, psia	1572	1427	1525	1146	1288	925
P _{wf} , psia	898	923	980	808	852	725
p*, P _{wf} /2, psia	1235	1175	1253	977	1070	825
T _r	1.71	1.72	1.71	1.71	1.72	1.71
P _r	1.84	1.75	1.87	1.46	1.60	1.23
z	.90	.90	.90	.92	.91	.93
B _g	.0127	.0134	.0125	.0163	.0148	.0196
q, mcf/d	113	75	41	115	105	16
μ, cp	.0155	.0152	.0155	.0145	.0151	.0144
m, psi/cycle	542	293	393	262	352	295
kh, md.ft.	1.19	1.51	.59	3.01	1.94	.44
h, ft	47	103	63	58	54	31
k, md	.025	.015	.009	.052	.036	.014

TABLE 23 AVERAGE RESERVOIR PRESSURES, JUNE 1979

	<u>WELL</u>					
	<u>A</u>	<u>B</u>	<u>C</u>	<u>D</u>	<u>F</u>	<u>G</u>
ϕ_g , fraction	.066	.064	.052	.050	.053	.045
\bar{A} , million ft ²	4.0	3.6	2.5	1.8	2.3	6.1
t_p , hrs	5016	4320	2496	6408	6024	1608
μ , cp	.0155	.0152	.0155	.0145	.0151	.0144
c_g , psi ⁻¹ x10 ⁻⁶	723	776	776	970	806	1090
c_w , psi ⁻¹ x10 ⁻⁶	3	3	3	3	3	3
c_f , psi ⁻¹ x10 ⁻⁶	5	5	5	5	5	5
c_t , psi ⁻¹ x10 ⁻⁶	340	364	364	453	378	508
p^* , psia	1572	1427	1525	1146	1288	925
k , md	.025	.021	.009	.055	.036	.012
$\frac{.000264 k t_p}{\phi_g \mu c_t \bar{A}}$.023	.020	.008	.157	.082	.002
$\frac{p^* - \bar{p}}{m/2.303}$.23	.23	.10	0	.10	.10
m , psi/cycle	542	293	393	262	352	295
$m/2.303$	235	127	171	114	153	128
$p^* - \bar{p}$, psi	54	30	17	0	15	13
\bar{p} , psia	1518	1397	1508	1146	1273	912
z	.88	.89	.88	.91	.90	.92
\bar{p}/z , psia	1725	1570	1714	1259	1414	991

Note: 70.6 q_{4B}/kh= m/2.303

TABLE 24 RESERVOIR GAS FILLED VOID VOLUMES BASED ON PRESSURE/PRODUCTION VOLUME ANALYSES

	Well					
	A	B	C	D	F	G
Reservoir Gas Volume, BSCF	2.64	1.17	1.95	2.95	2.80	0.75
Initial Reservoir Pressure, psia	2254	2625	2696	2317	2575	2203
Initial z	.86	.86	.86	.86	.86	.86
Reservoir Temperature, °R	617	620	617	614	619	616
Calculated Gas- Filled Reservoir Volume, 10 ⁶ ft. ³	17.5	6.7	10.8	18.9	16.3	5.1

TABLE 25 CALCULATED EFFECTIVE FRACTURE HALF LENGTHS
WELLS B, C, & G

	WELL		
	<u>B</u>	<u>C</u>	<u>G</u>
q, MSCF/D	75	41	16
z, fraction	.89	.88	.92
T, °R	620	617	616
m _L , psi ² /hr ^{1/2}	14,500	12,000	2,500
μ, cp	.0152	.0155	.0144
k ₁ , md	.06	.04	.06
k ₂ , md	.03	.02	.03
φ _g , fraction	.064	.052	.045
c _t , psi ⁻¹	.000364	.000364	.000508
h, ft.	103	63	31
x _{f1} , ft.	121	172	488
x _{f2} , ft	167	243	695
\bar{x}_f , ft.	144	208	592

TABLE 26 CALCULATED AVERAGE FRACTURE WIDTHS,
 \bar{y}_f , WELLS B, C, & G

	<u>B</u>	<u>C</u>	<u>G</u>
V_p^* , ft. ³	505	654	150
\bar{x}_f , ft	144	208	592

CASE 1 (sands only penetrated by fracs)

h_g , ft	127	113	63
\bar{y}_f , ft	.019	.019	.003

CASE 2 (sands and shales penetrated by fracs)

Number of sands	6	6	2
\bar{y}_f , ft	.003	.002	.0002

*Grain density of sand assumed to be 2.67 g/cc and that of walnut hulls, 0.9 g/cc.

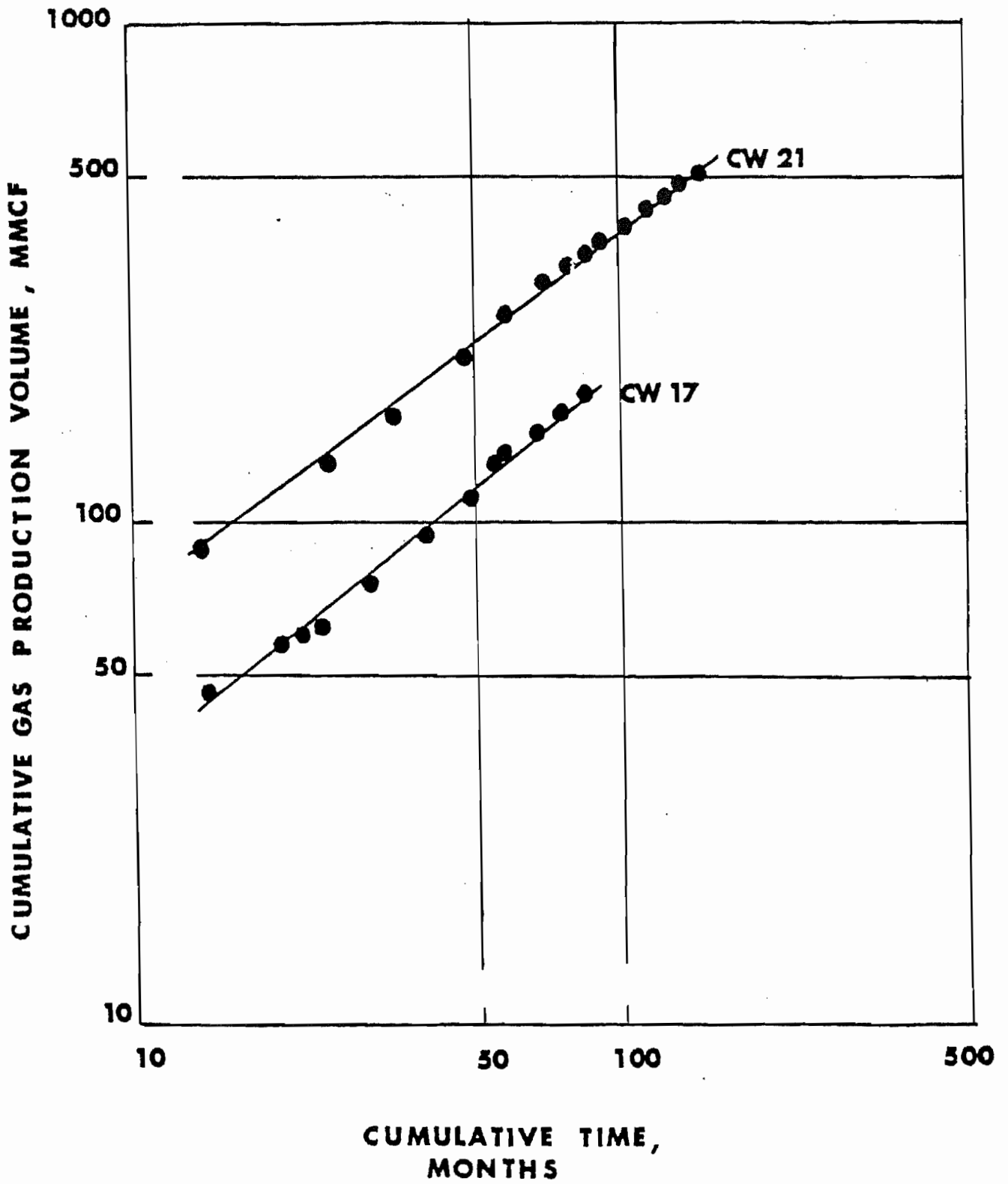


FIG. 1 Cumulative Gas Production Volume vs
Cumulative Production Time - Wells CW 21 & 17

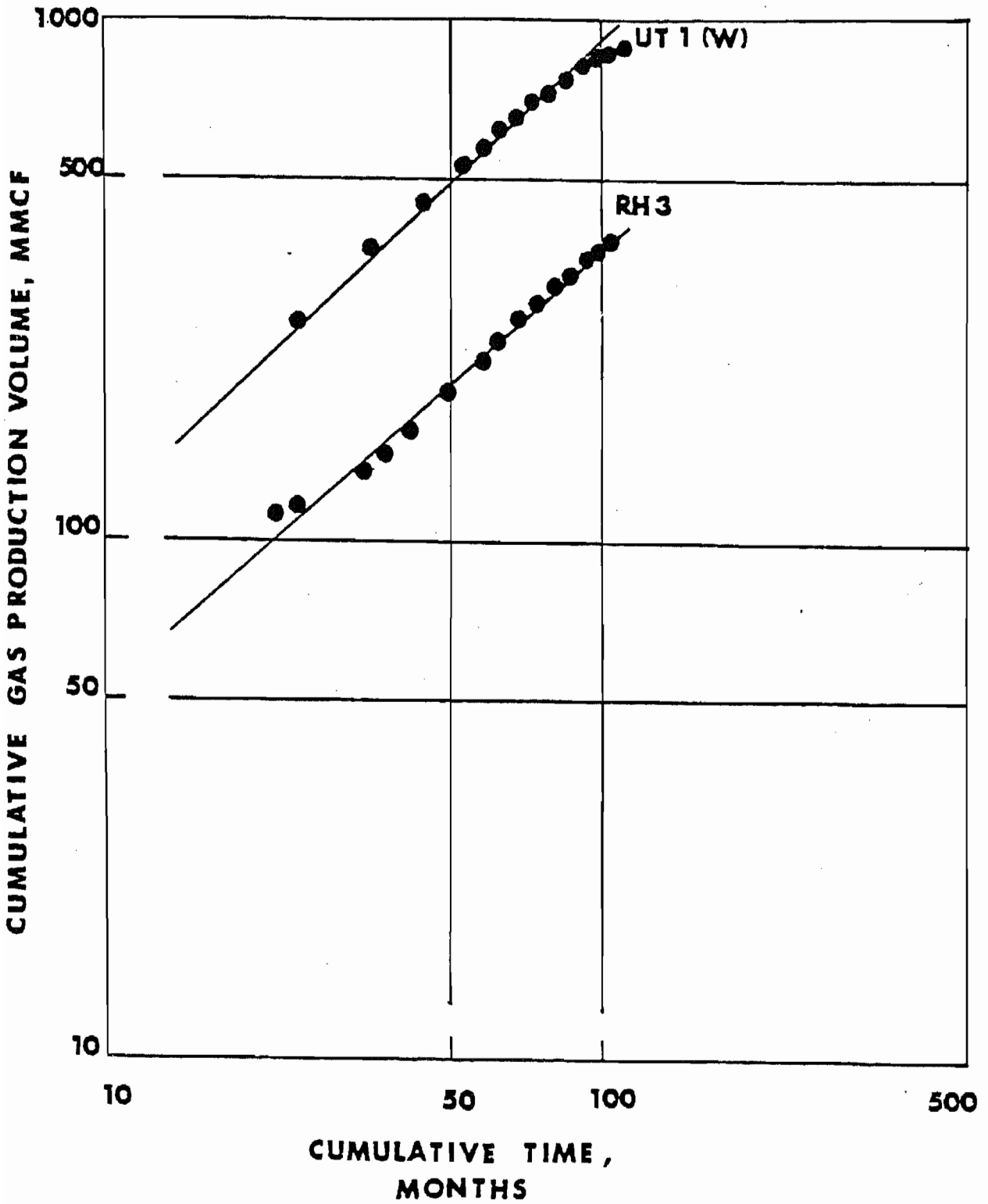


FIG. 2 Cumulative Gas Production Volume vs. Cumulative Production Time - Wells UT 1 (Wasatch only) and RH 3

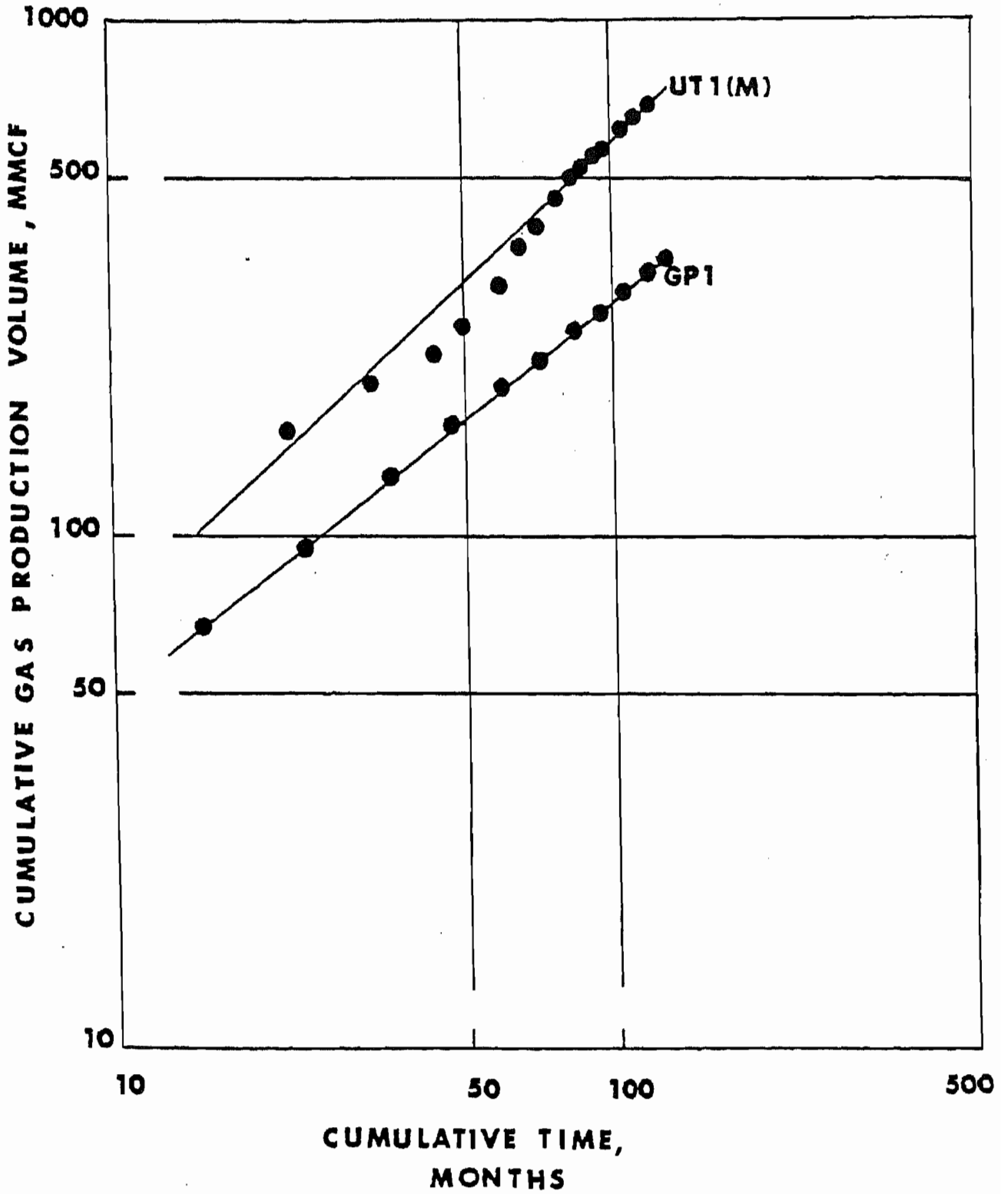


FIG. 3 Cumulative Gas Production Volume vs. Cumulative Production Time - Wells GP 1 & UT 1 (Mesaverde only)

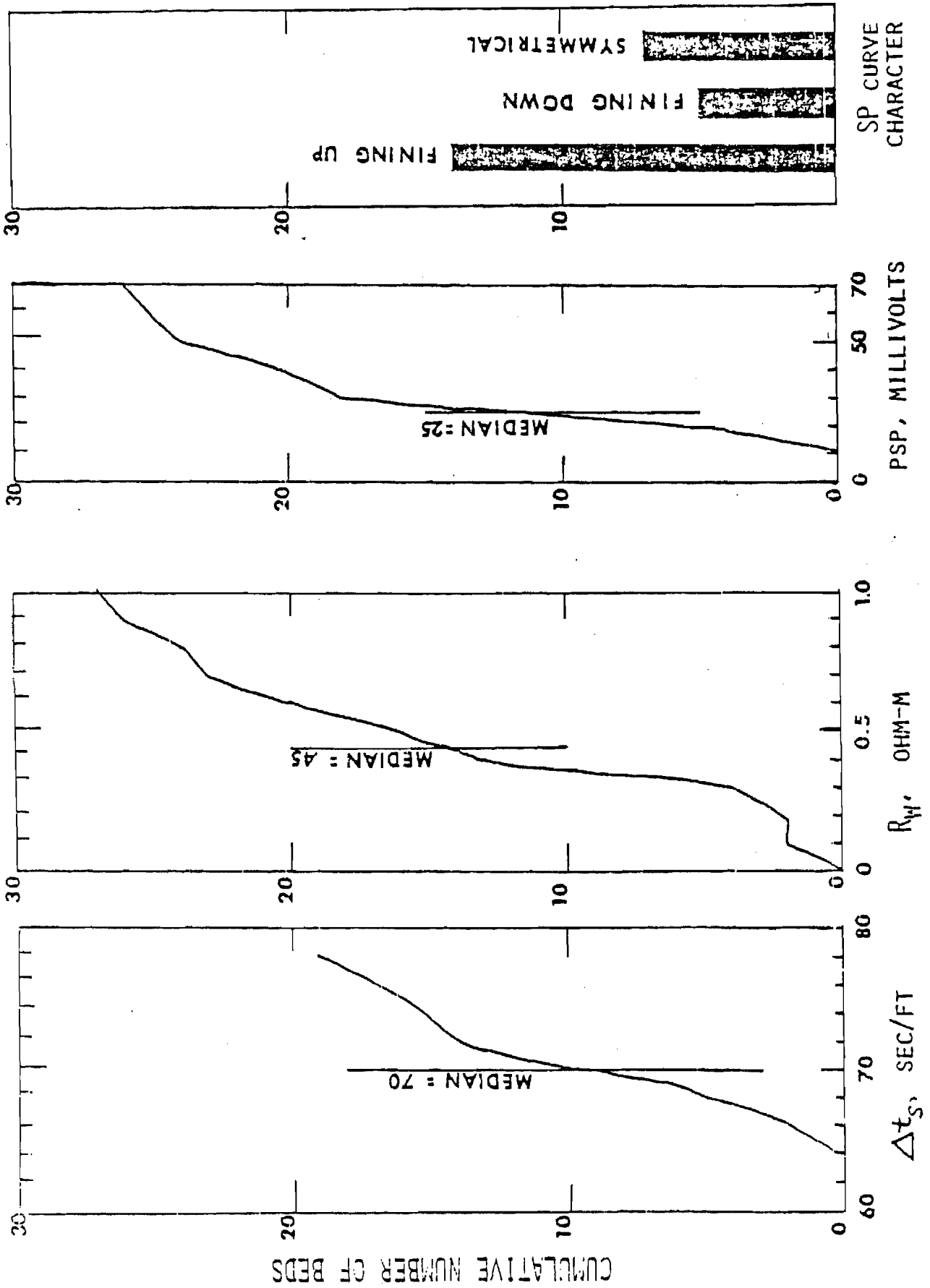


FIG. 4 Reservoir Rock Characteristics Distributions - Near Radial-Flow Wells

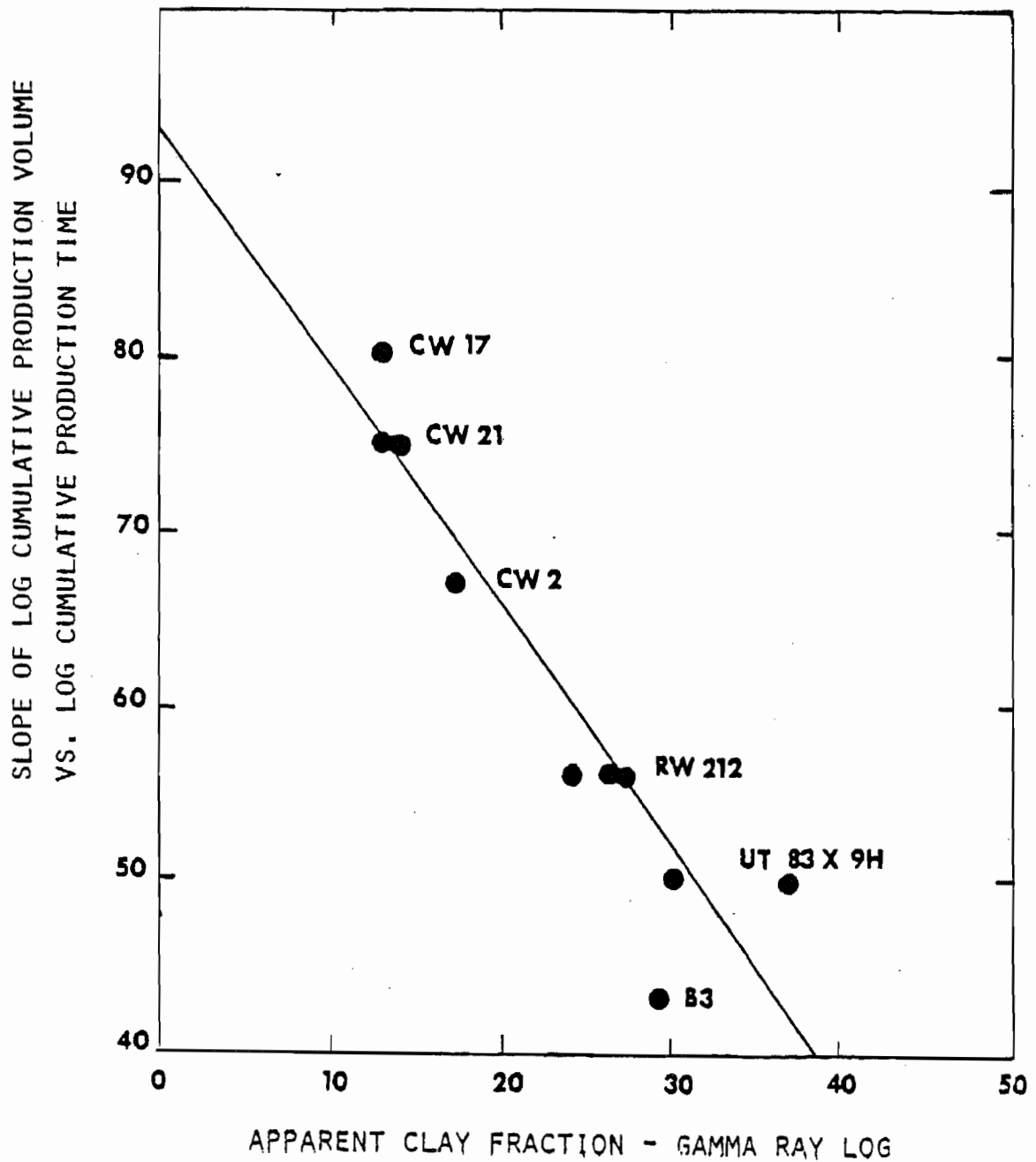


FIG. 5 Apparent Clay Fraction of Producing Gross Sands versus Slope of Log Cum. Production Volume versus Log Cumulative Time Curve.

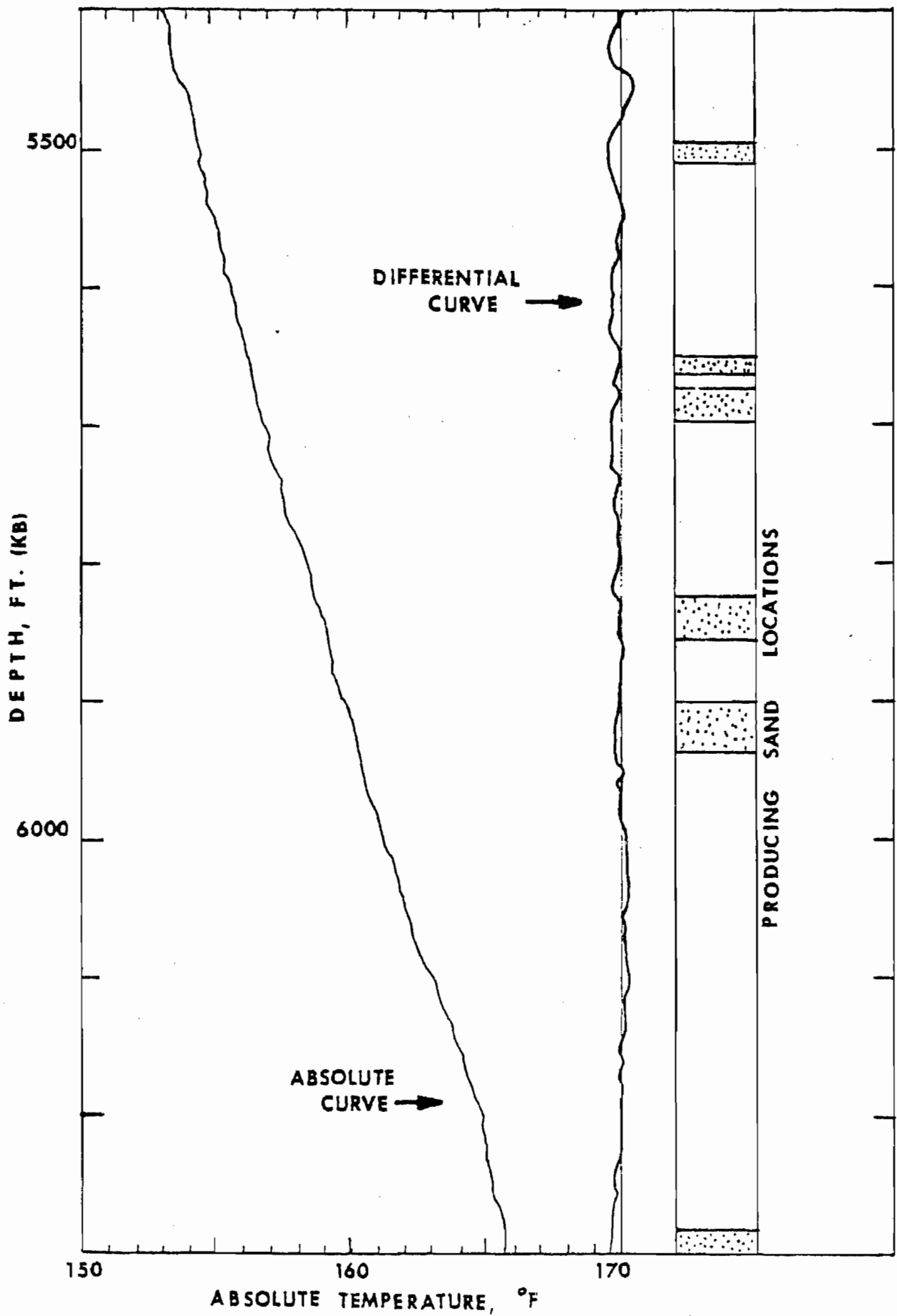


FIGURE 6. Temperature Logs Taken During Production- Well B
-59-

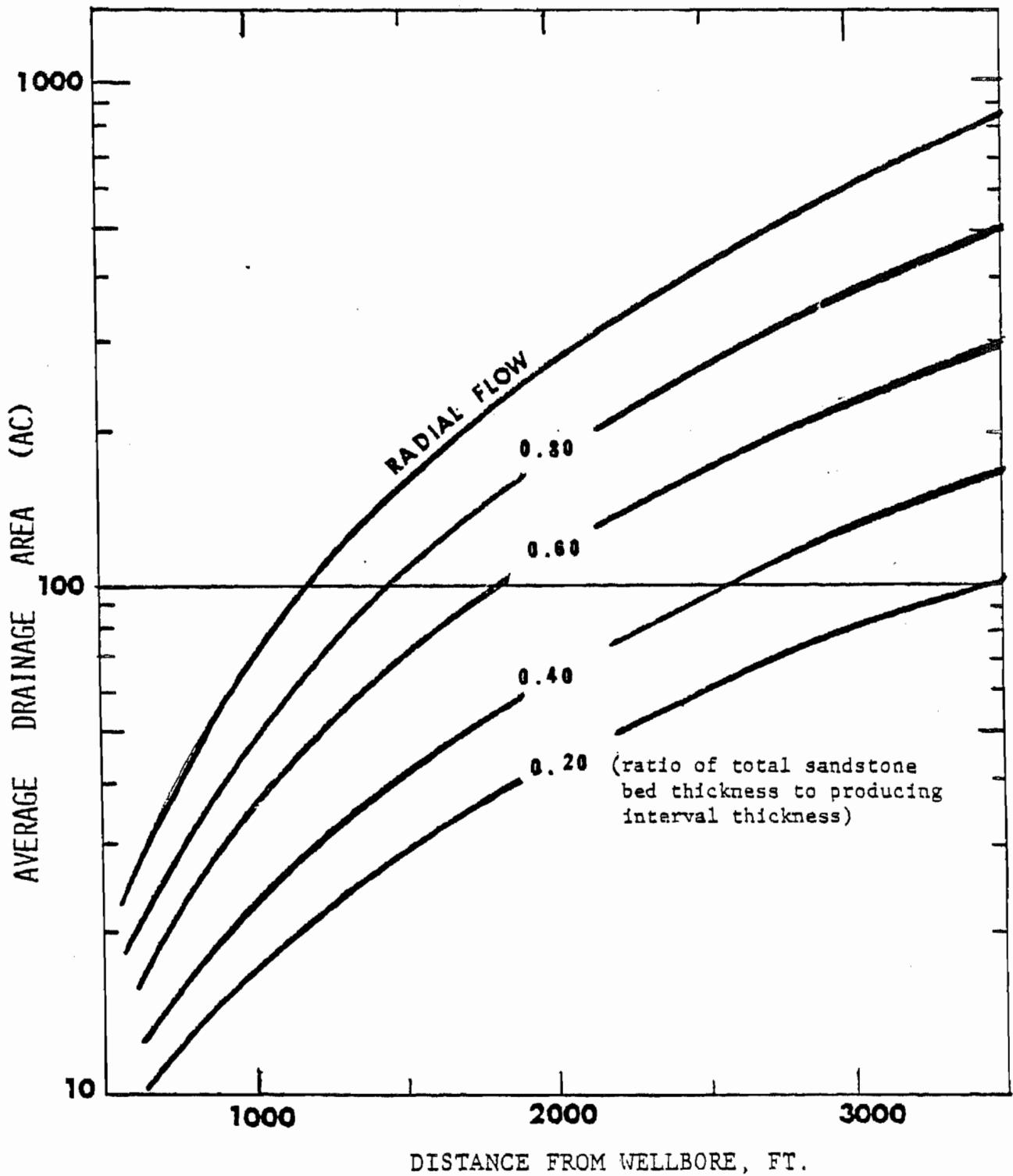


FIG. 7 Reservoir Drainage Area versus Distance from Wellbore as a Function of the Ratio of Total Sandstone Bed Thickness to Total Producing Interval Thickness (after Knutson- 1977)

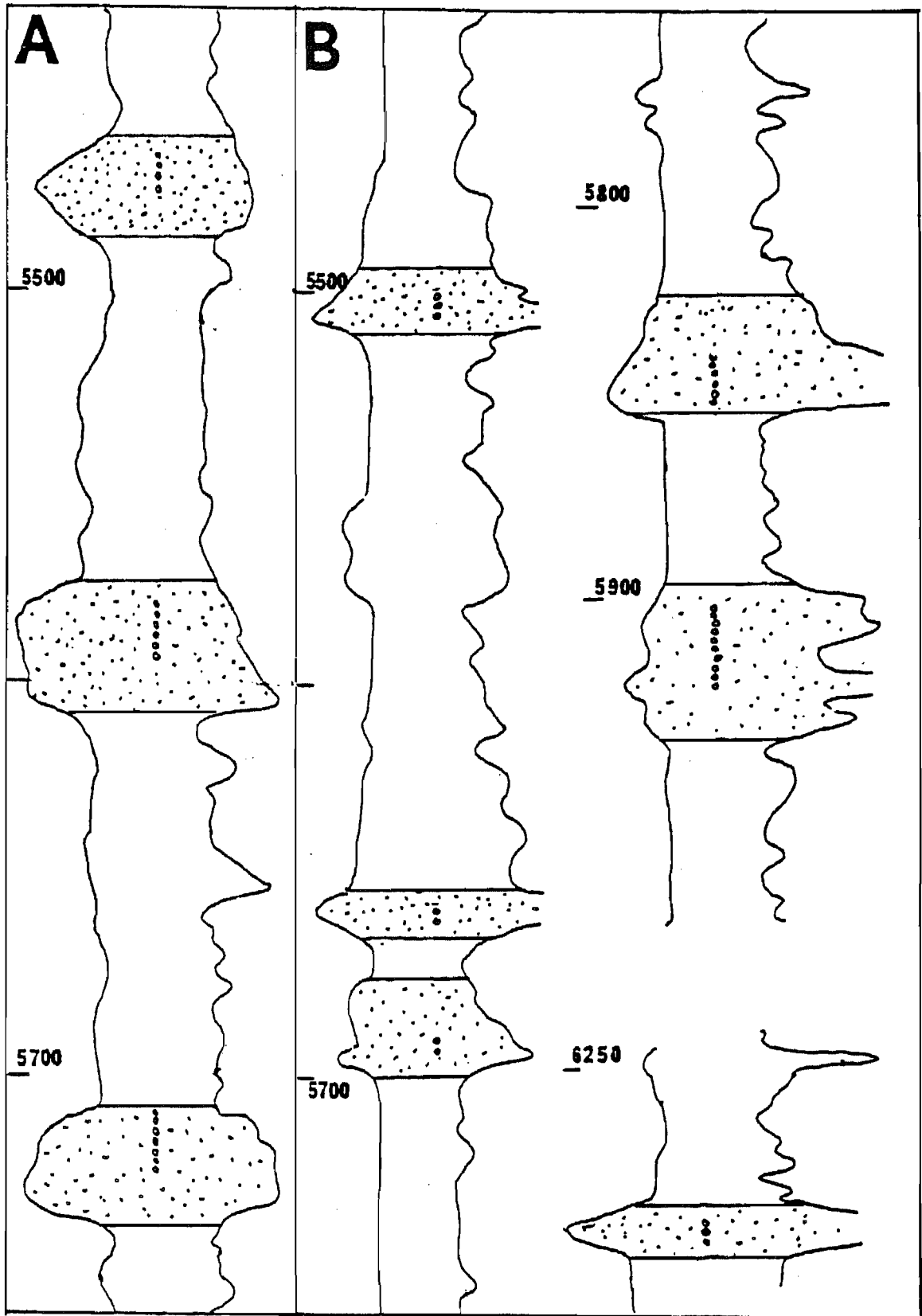


FIG. 8 SP/Resistivity Log Character - Wells A and B

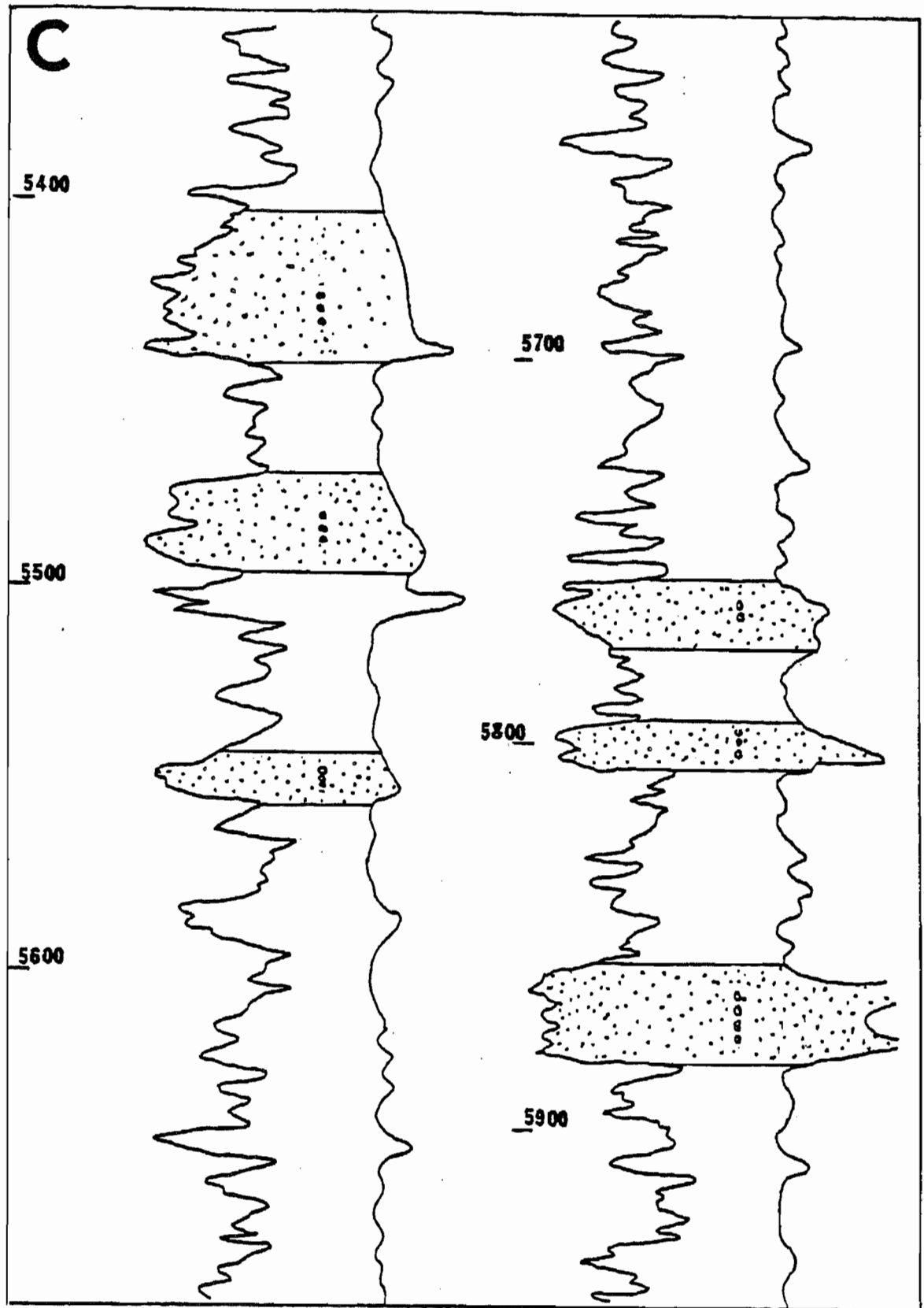


FIG. 9 Gamma Ray/Resistivity Log Character - Well C

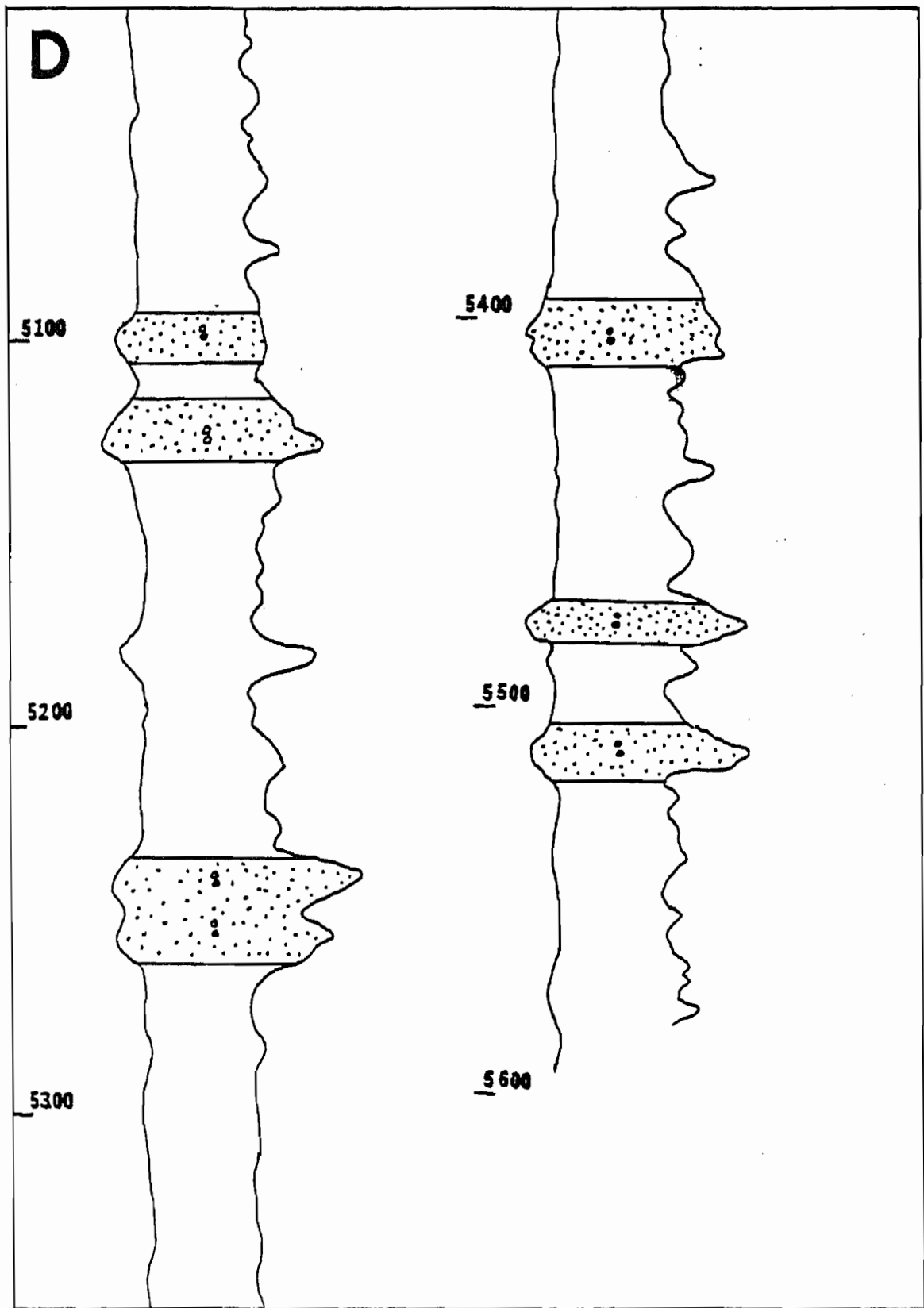


FIG. 10 - SP/Resistivity Log Character - Well D
-63-

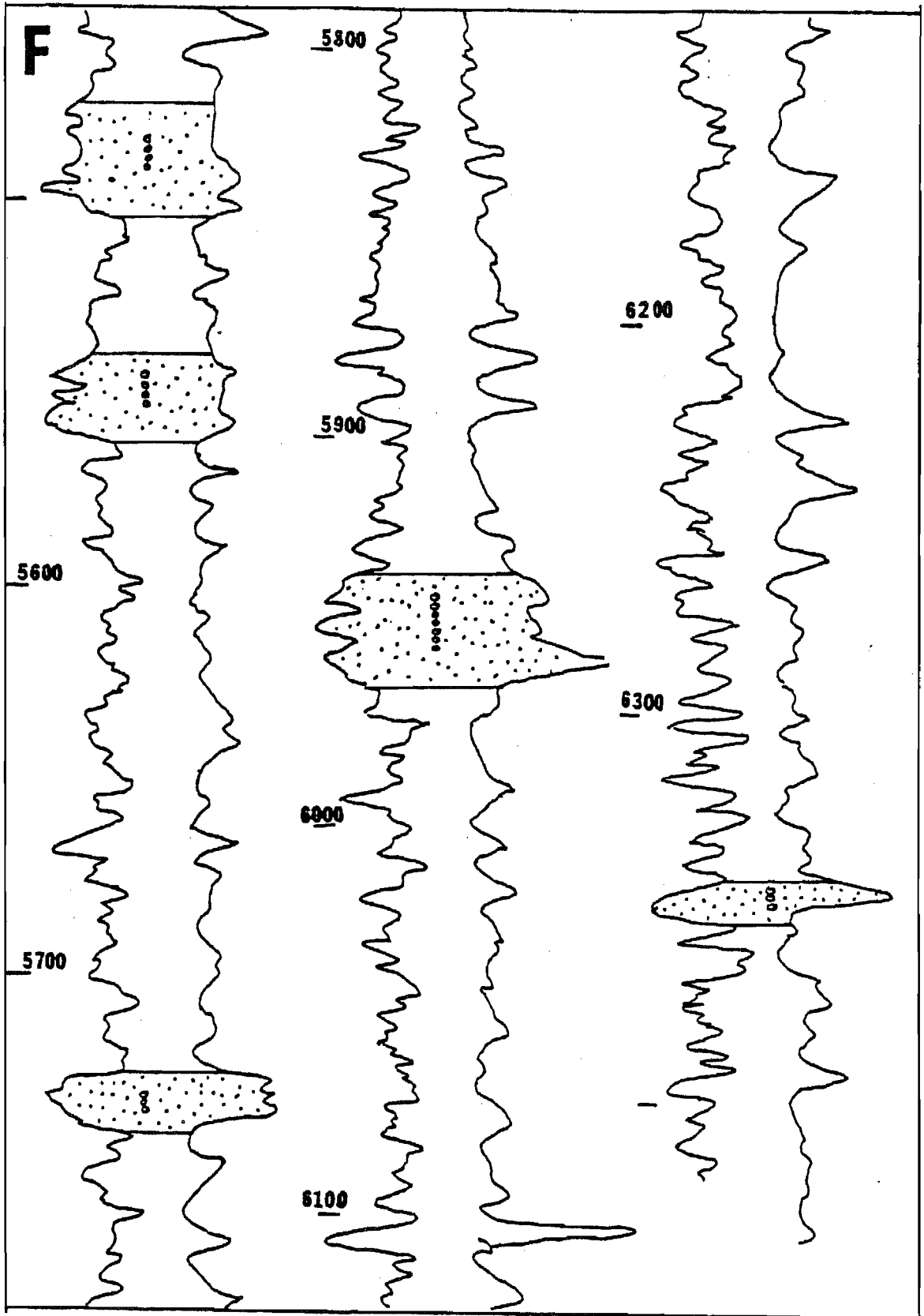


FIG. 11 Gamma Ray/Resistivity Log Character - Well F

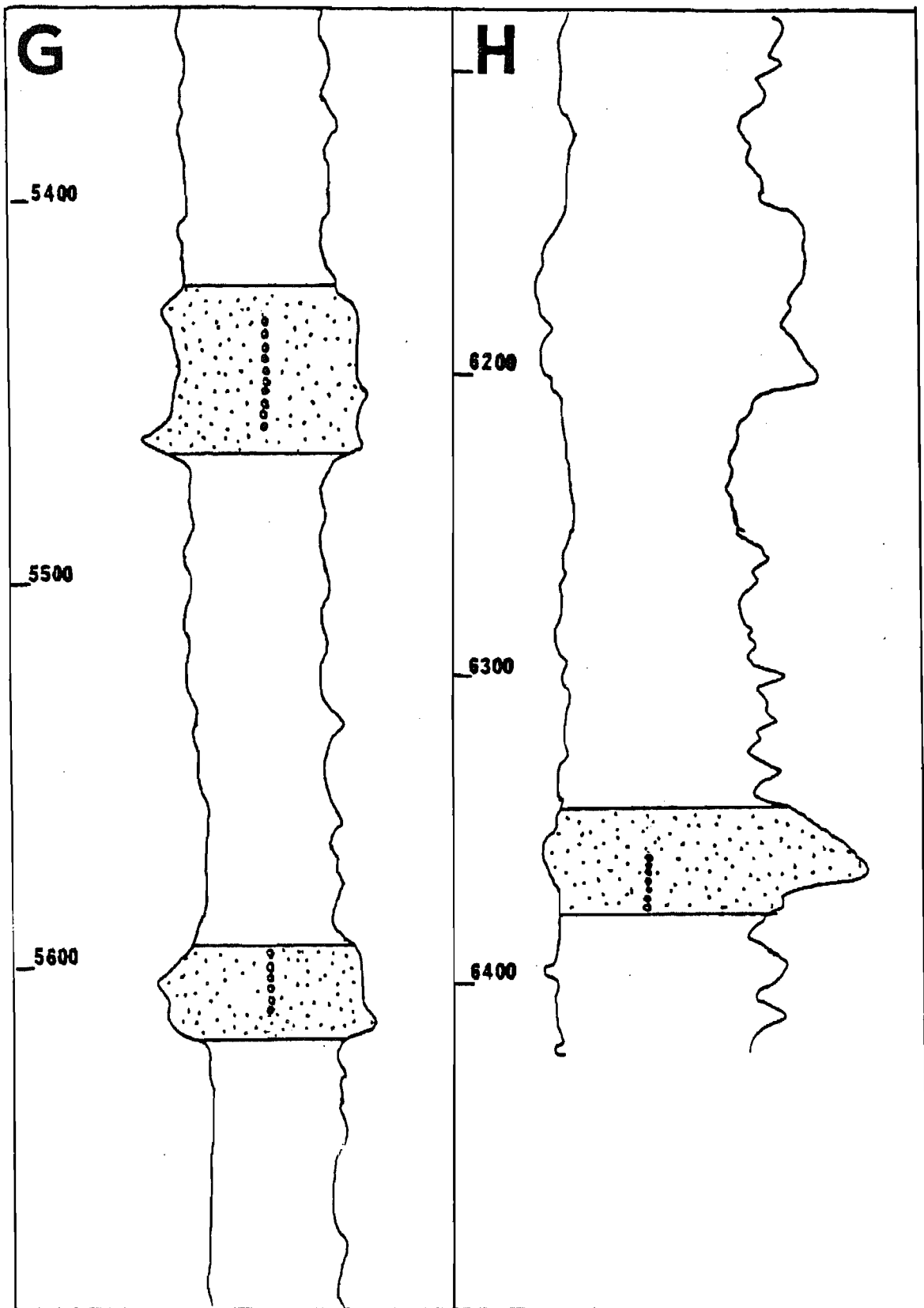


FIG. 12 SP/Resistivity Log Character -Wells G and H

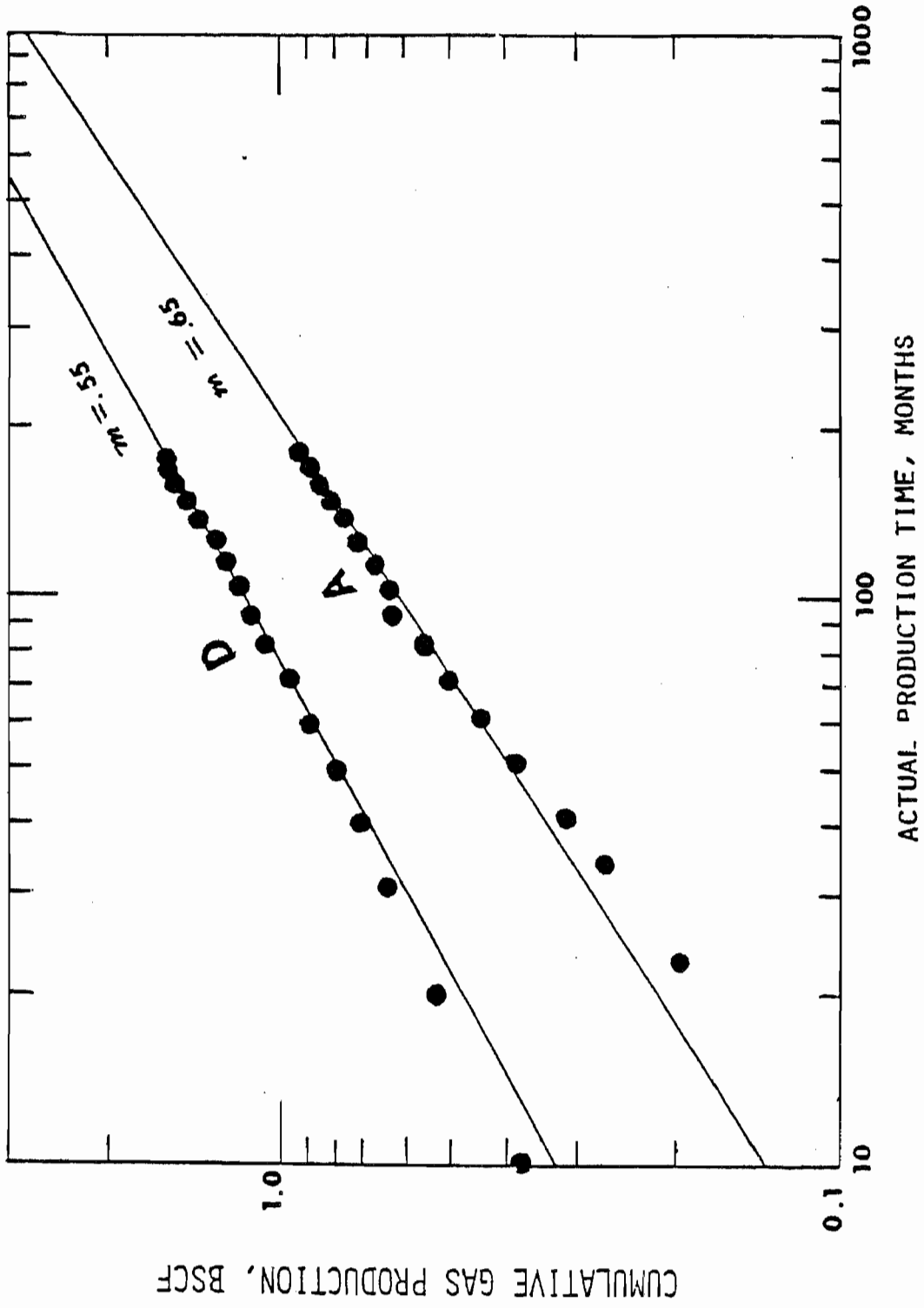


FIG. 13 Cumulative Gas Production versus Actual Production Time Wells A and D

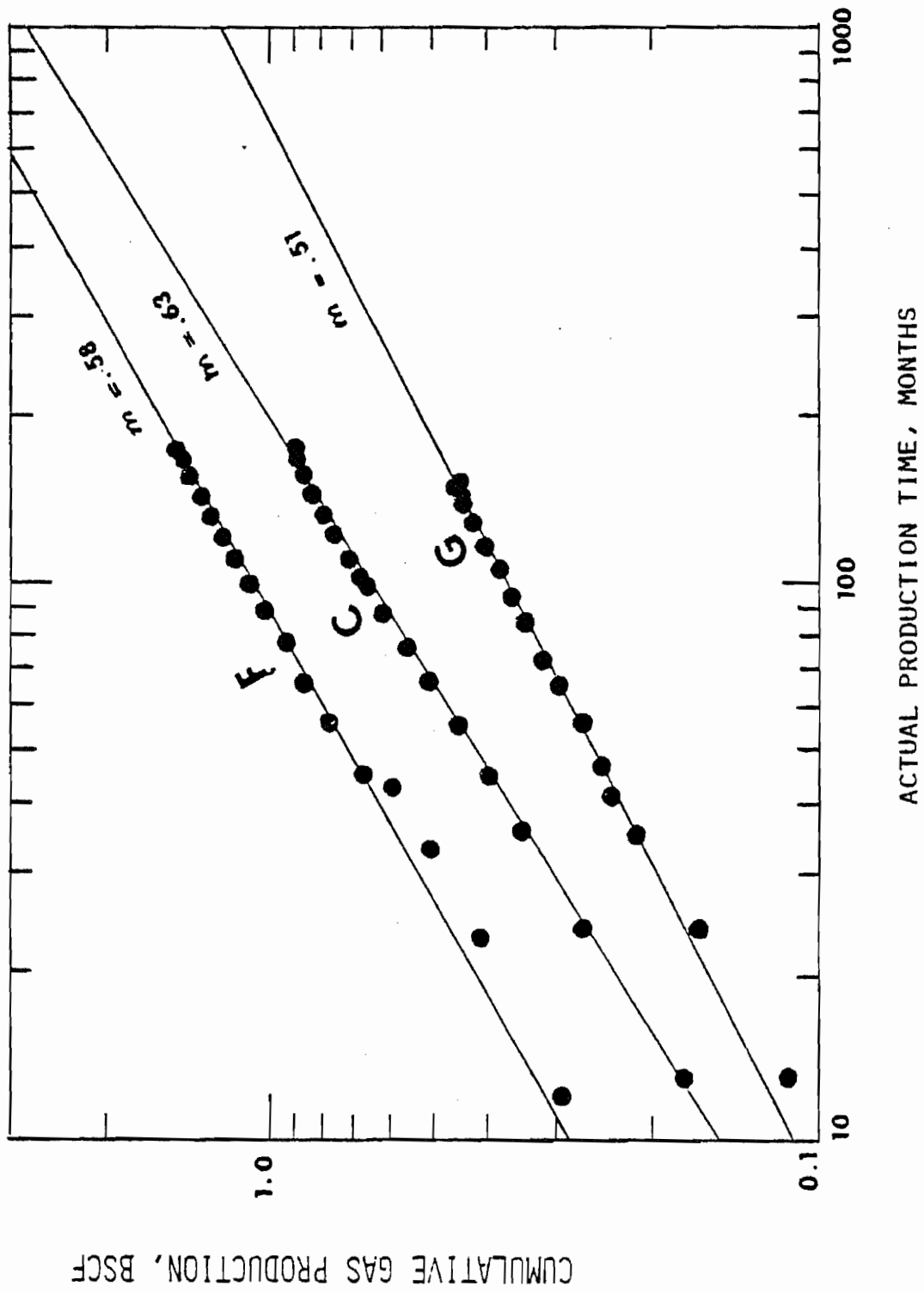


FIG. 14 Cumulative Gas Production versus Actual Production Time
Wells D, F and G.

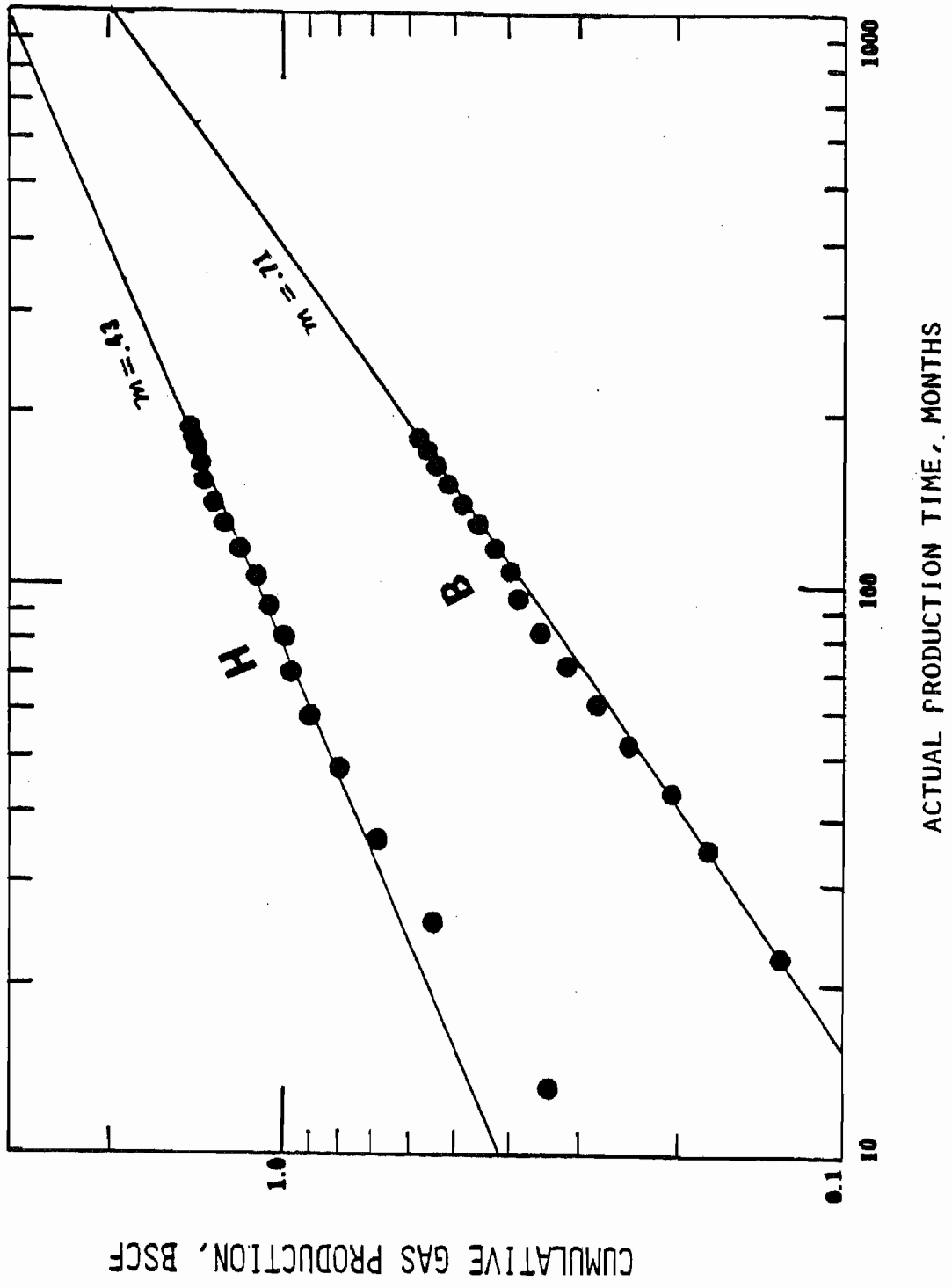
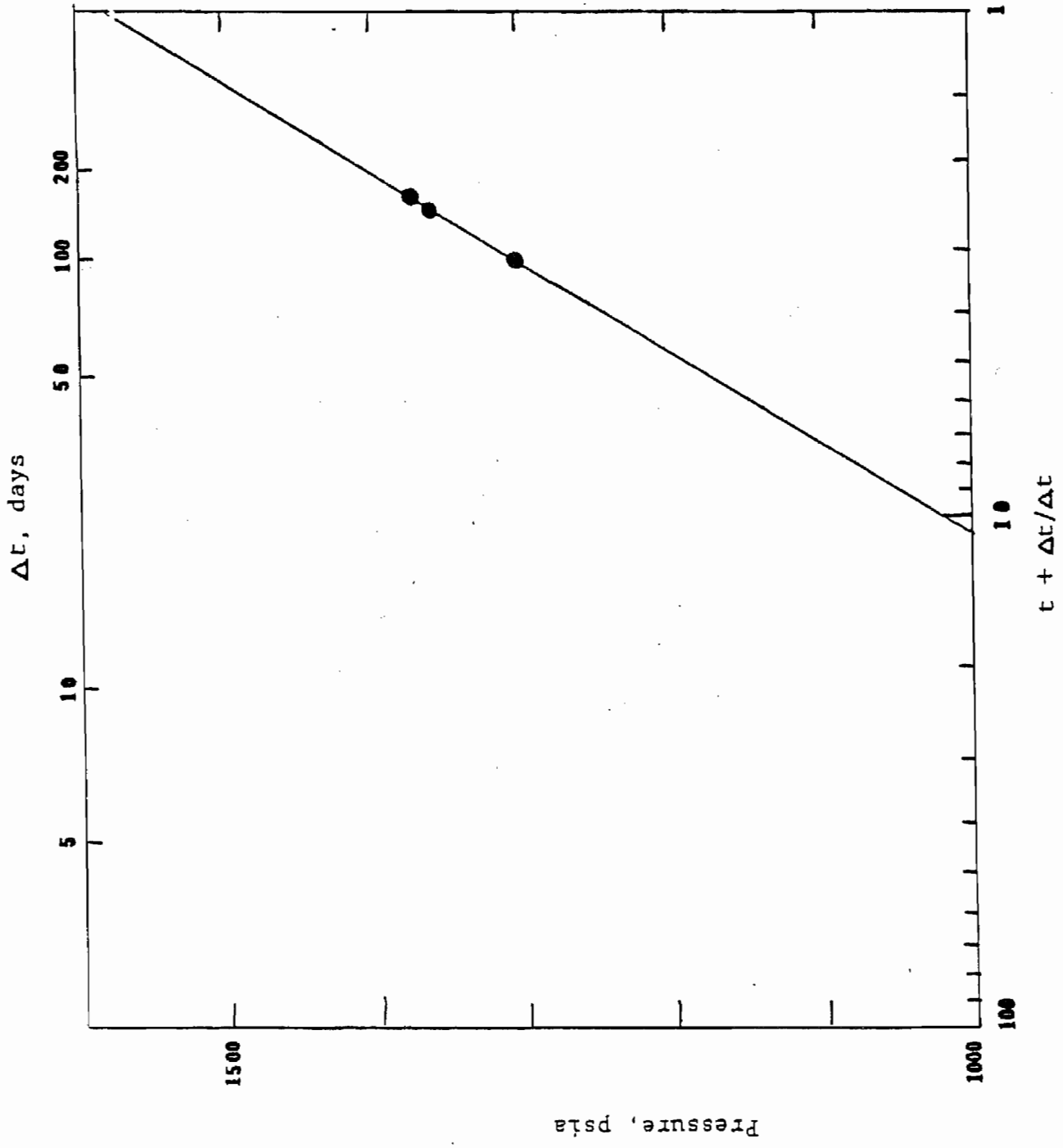
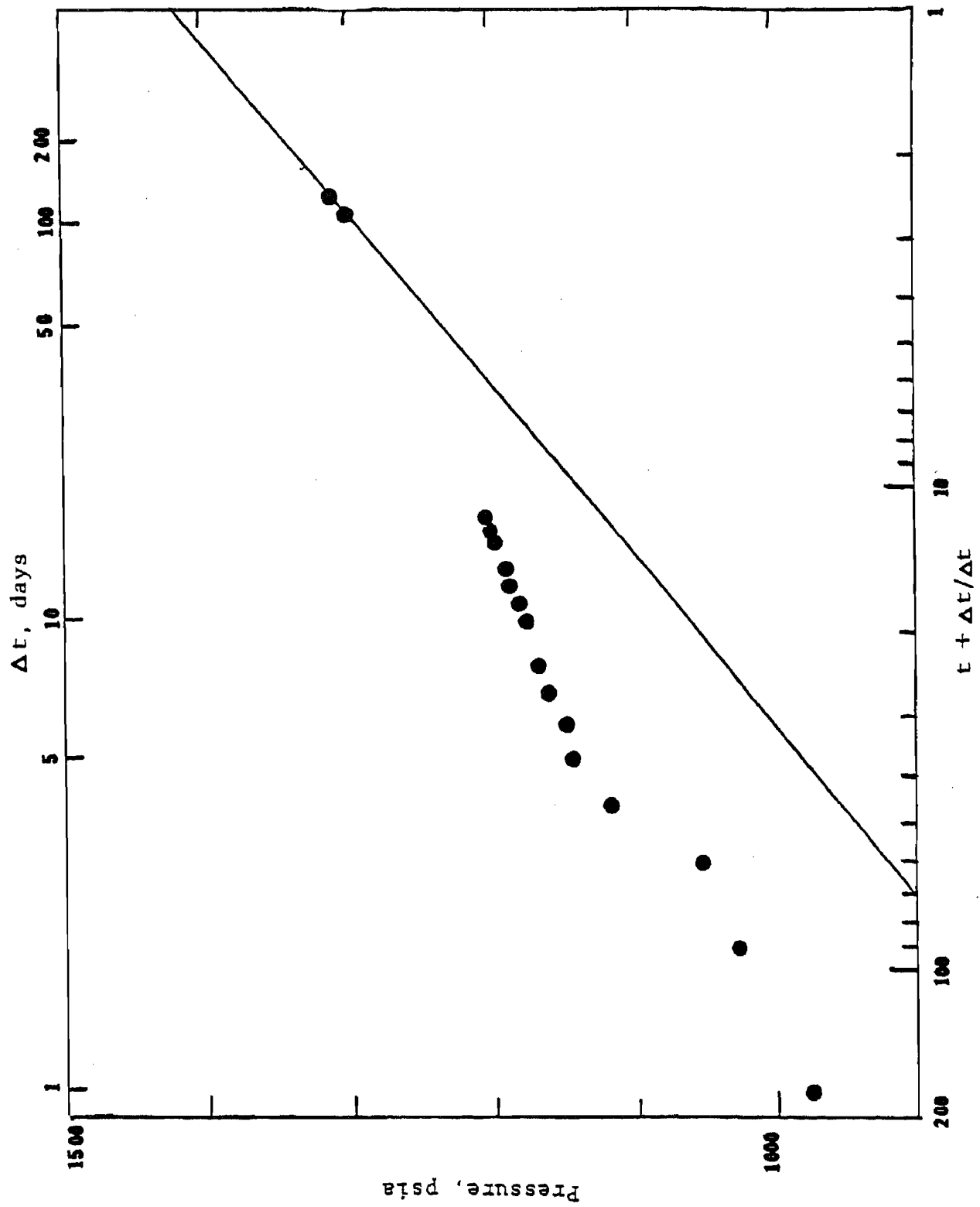


FIG. 15 Cumulative Gas Production versus Actual Production Time Wells B and H.



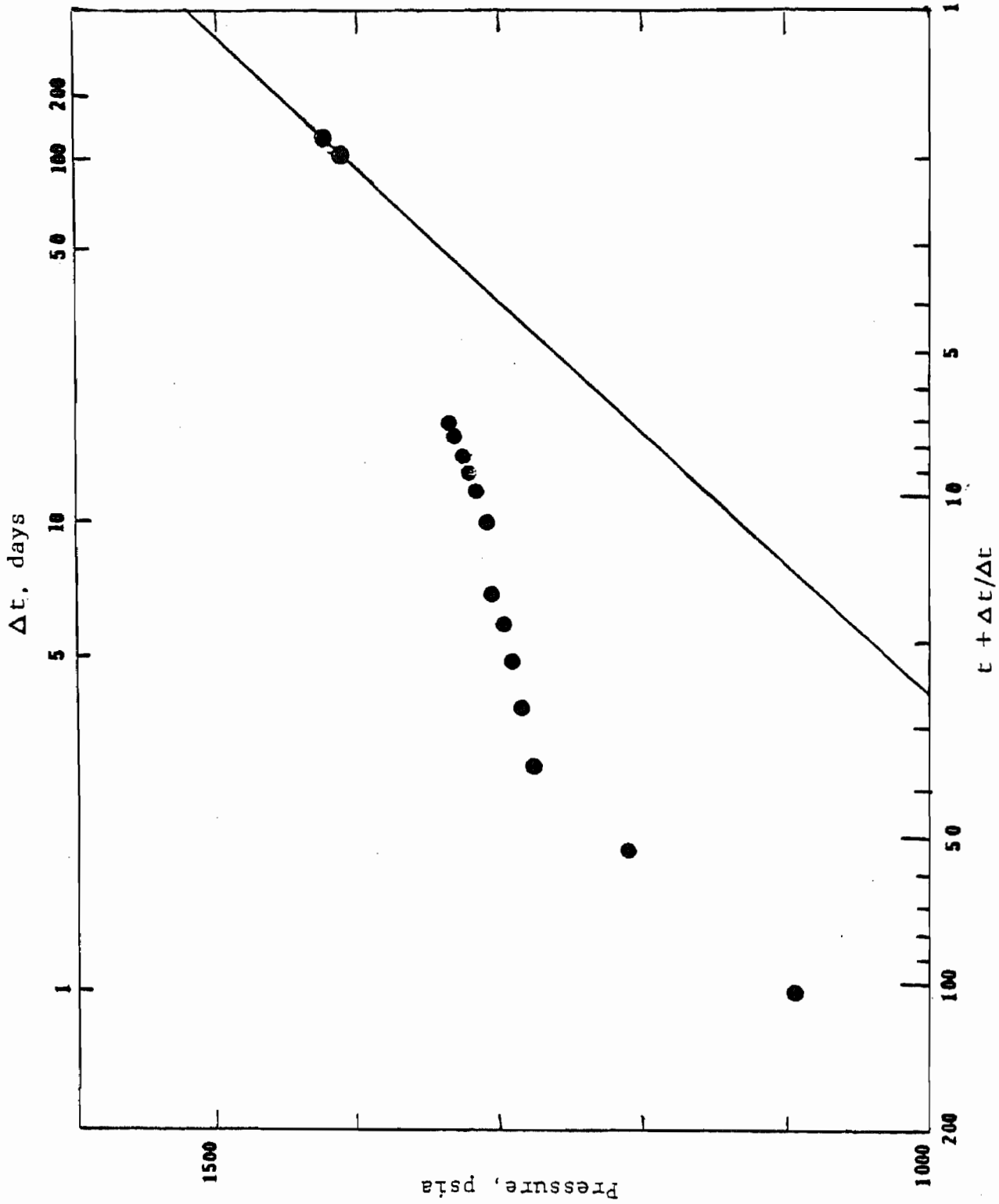
Pressure Buildup - Well A

FIG. 16



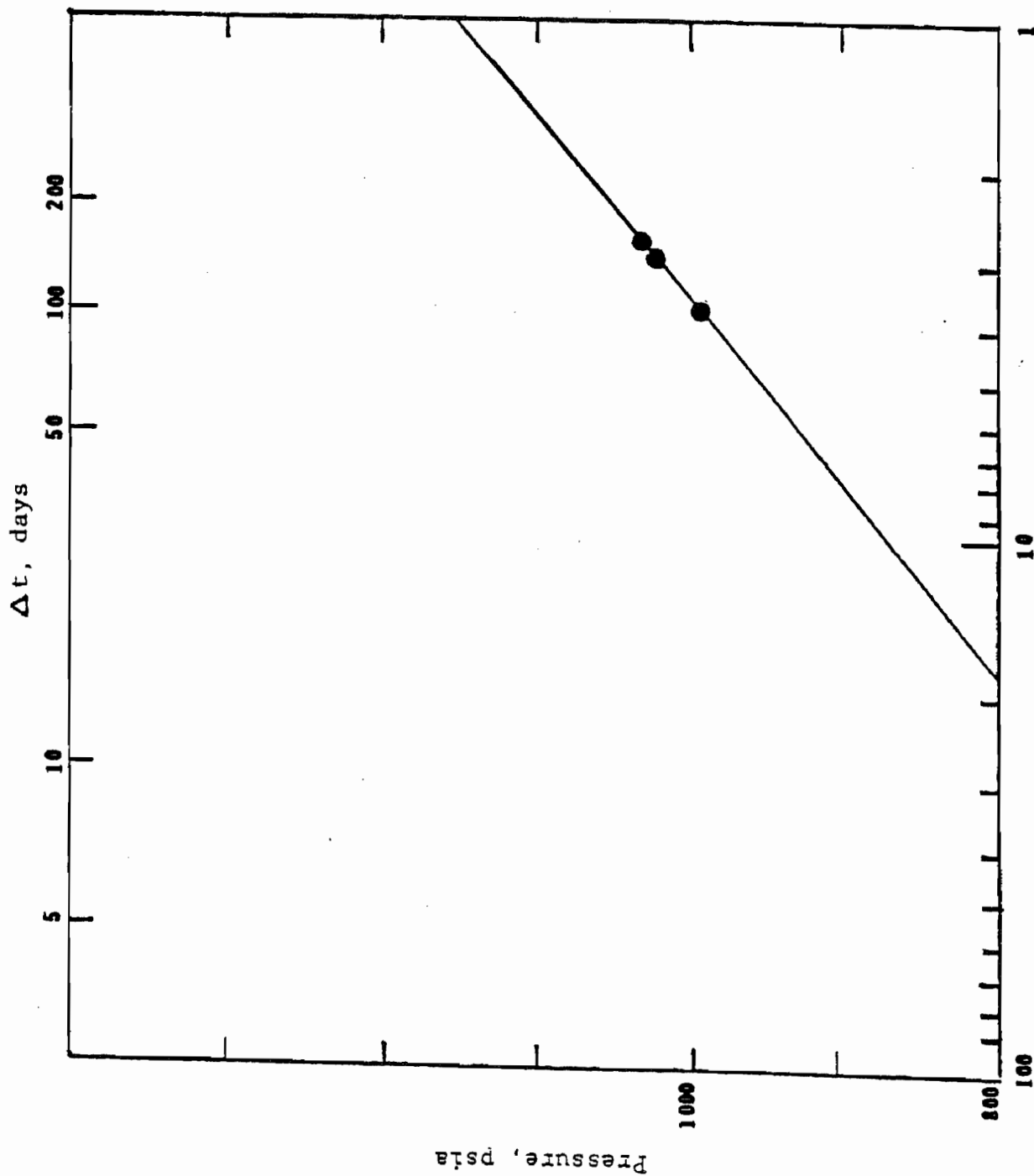
Pressure Buildup - Well B

FIG. 17



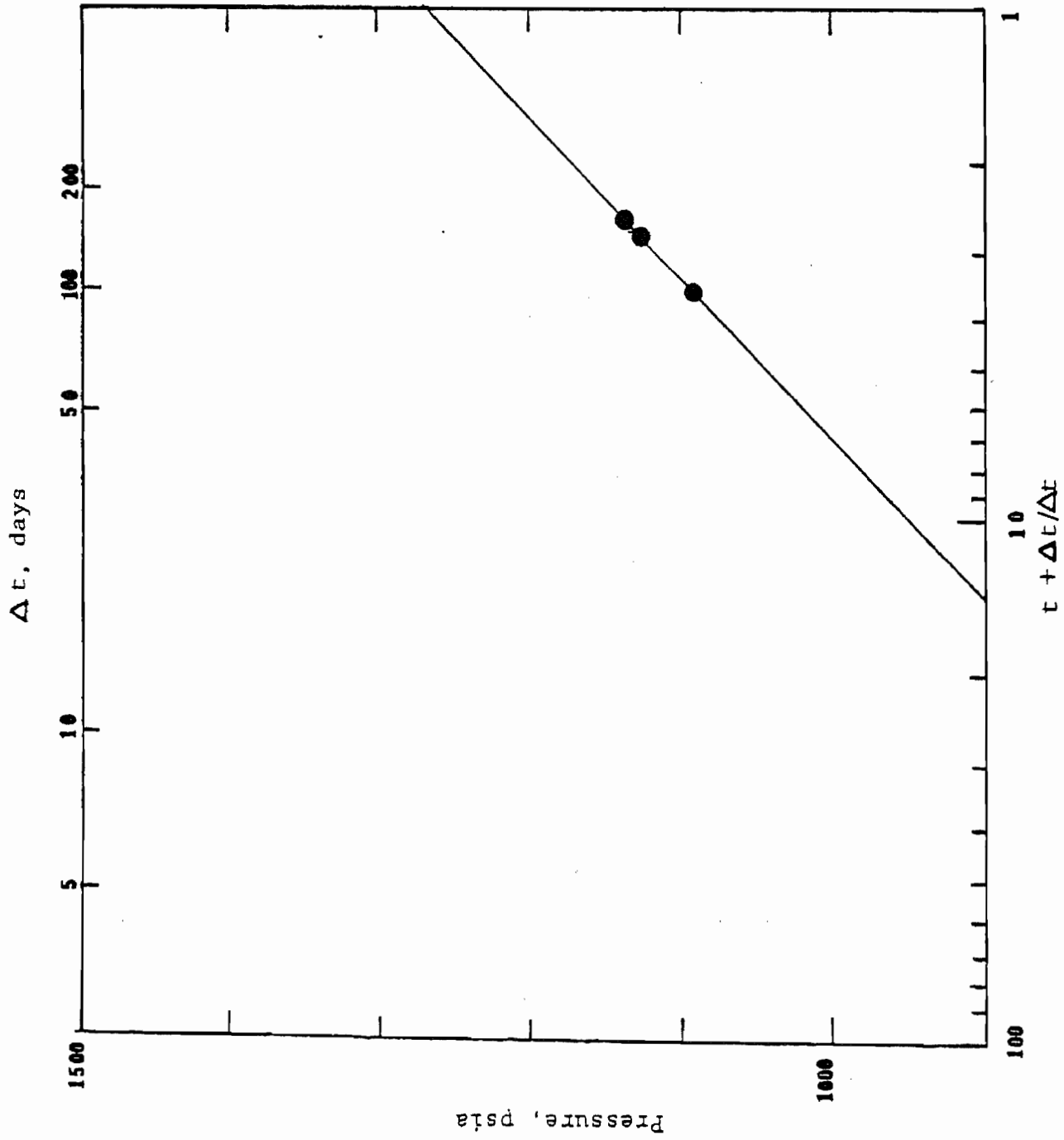
Pressure Buildup - Well C

FIG. 18



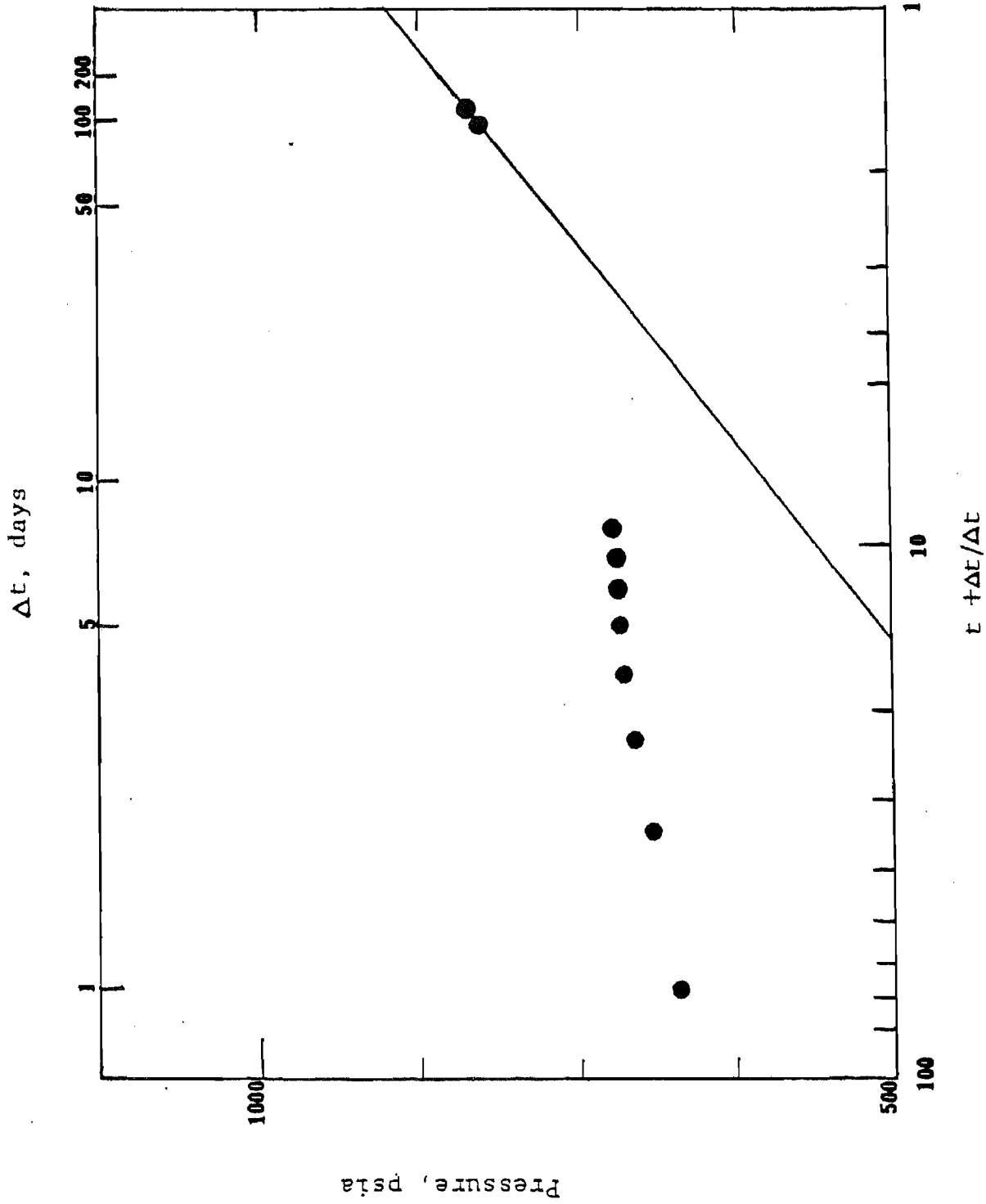
Pressure Buildup - Well D

FIG. 19.



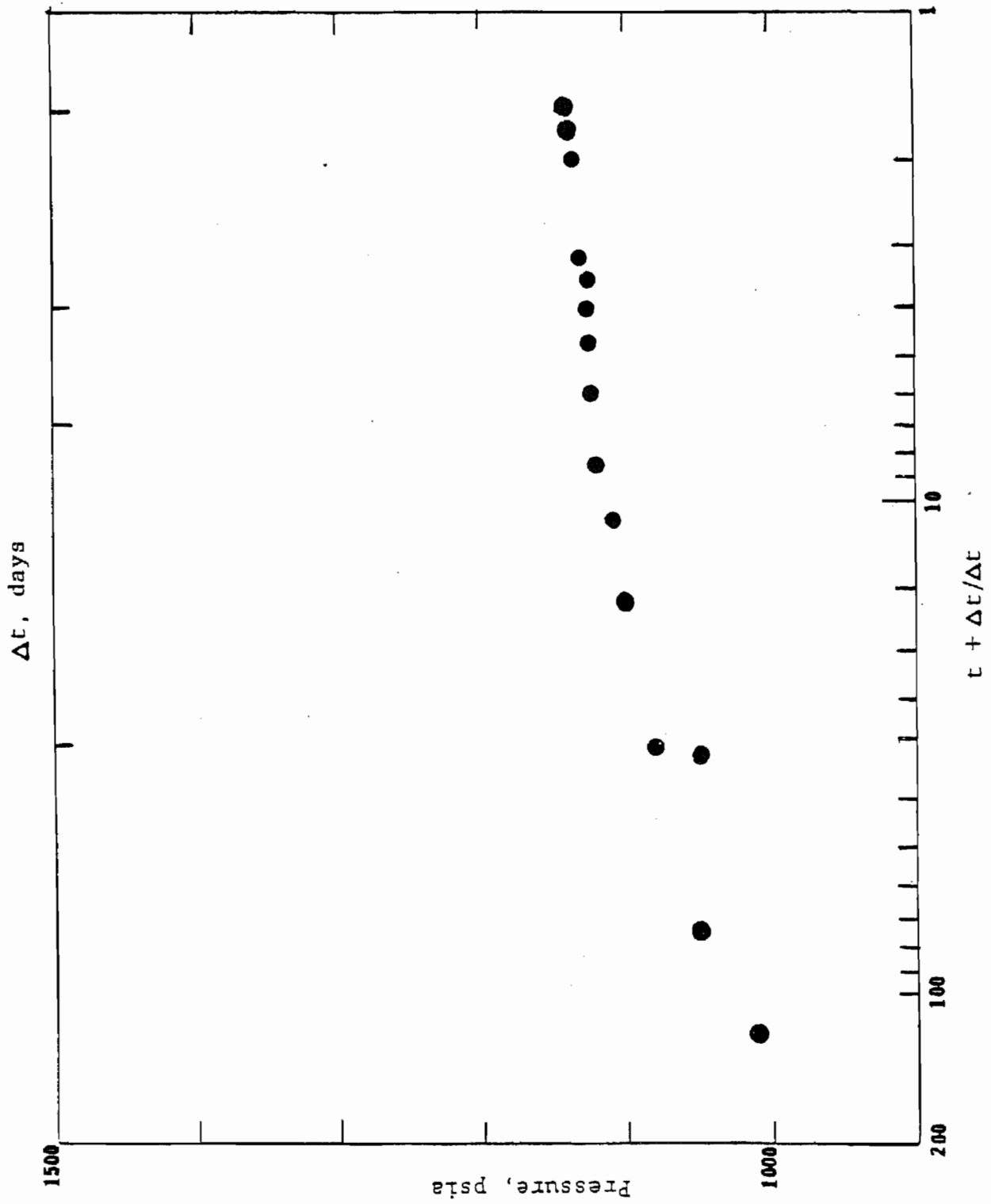
Pressure Buildup - Well F

FIG. 20



Pressure Buildup - Well G

FIG.21.



Pressure Buildup - Well H

FIG. 22

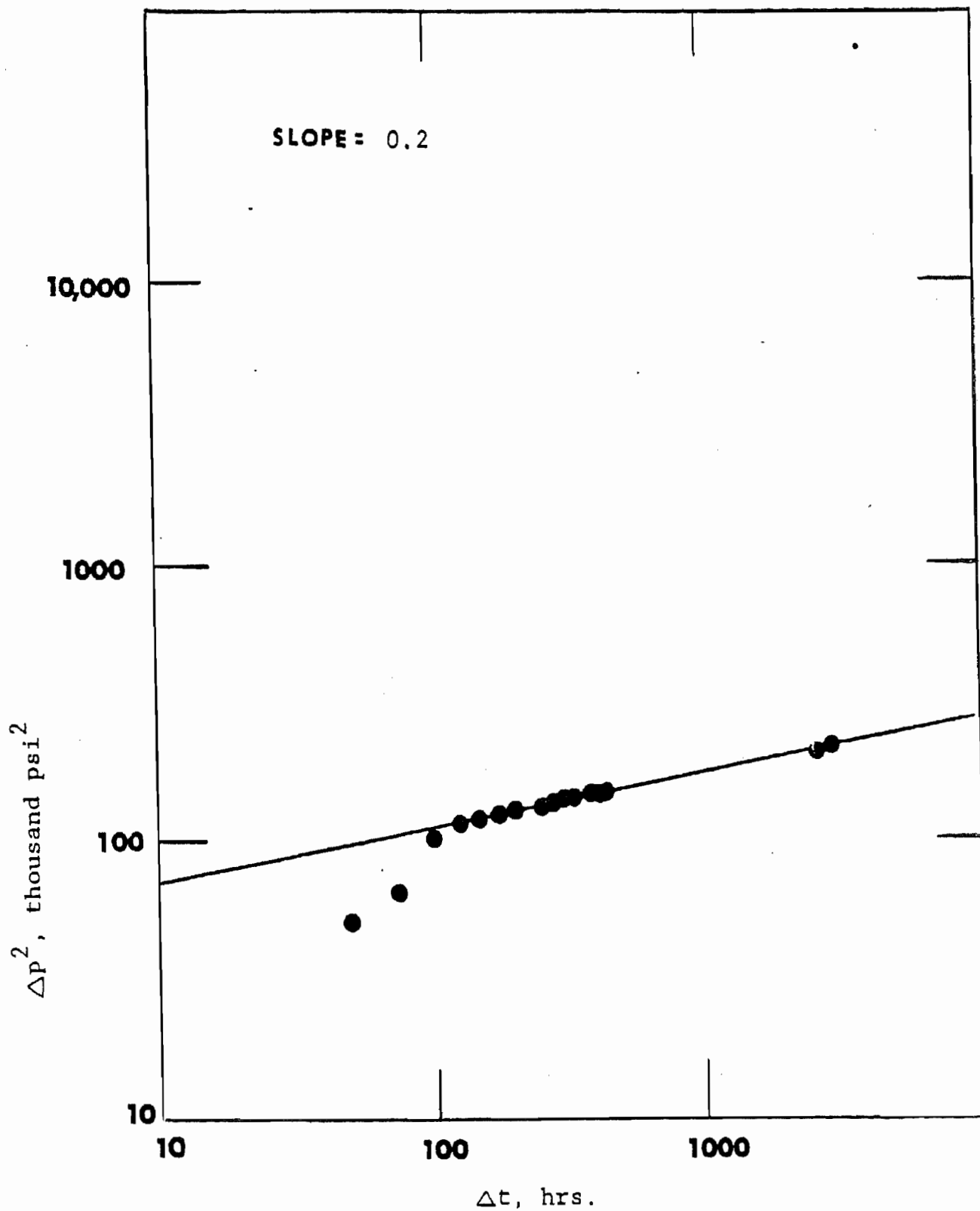


FIG. 23 Δp^2 versus Δt - Well B

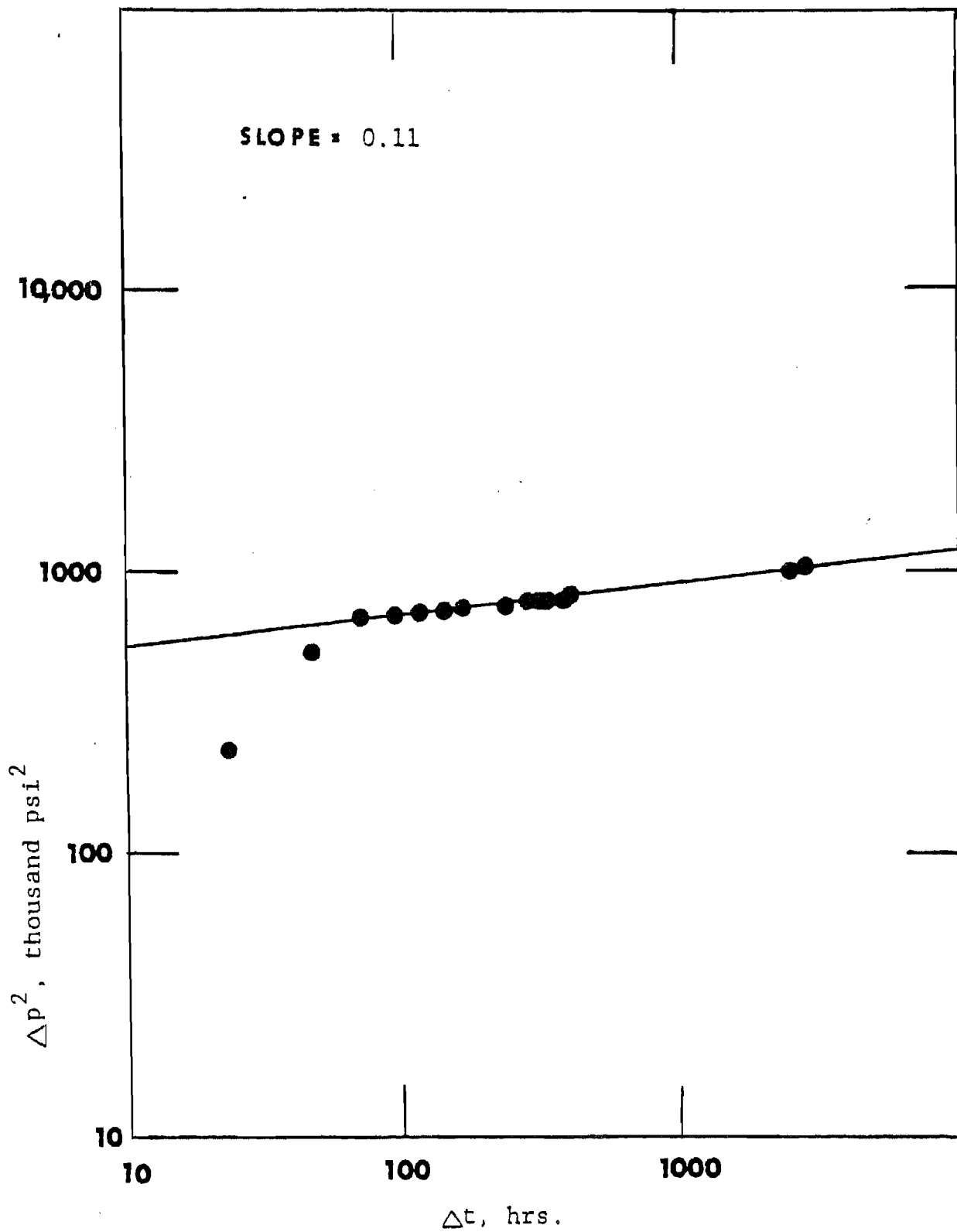


FIG. 24 Δp^2 versus Δt - Well C

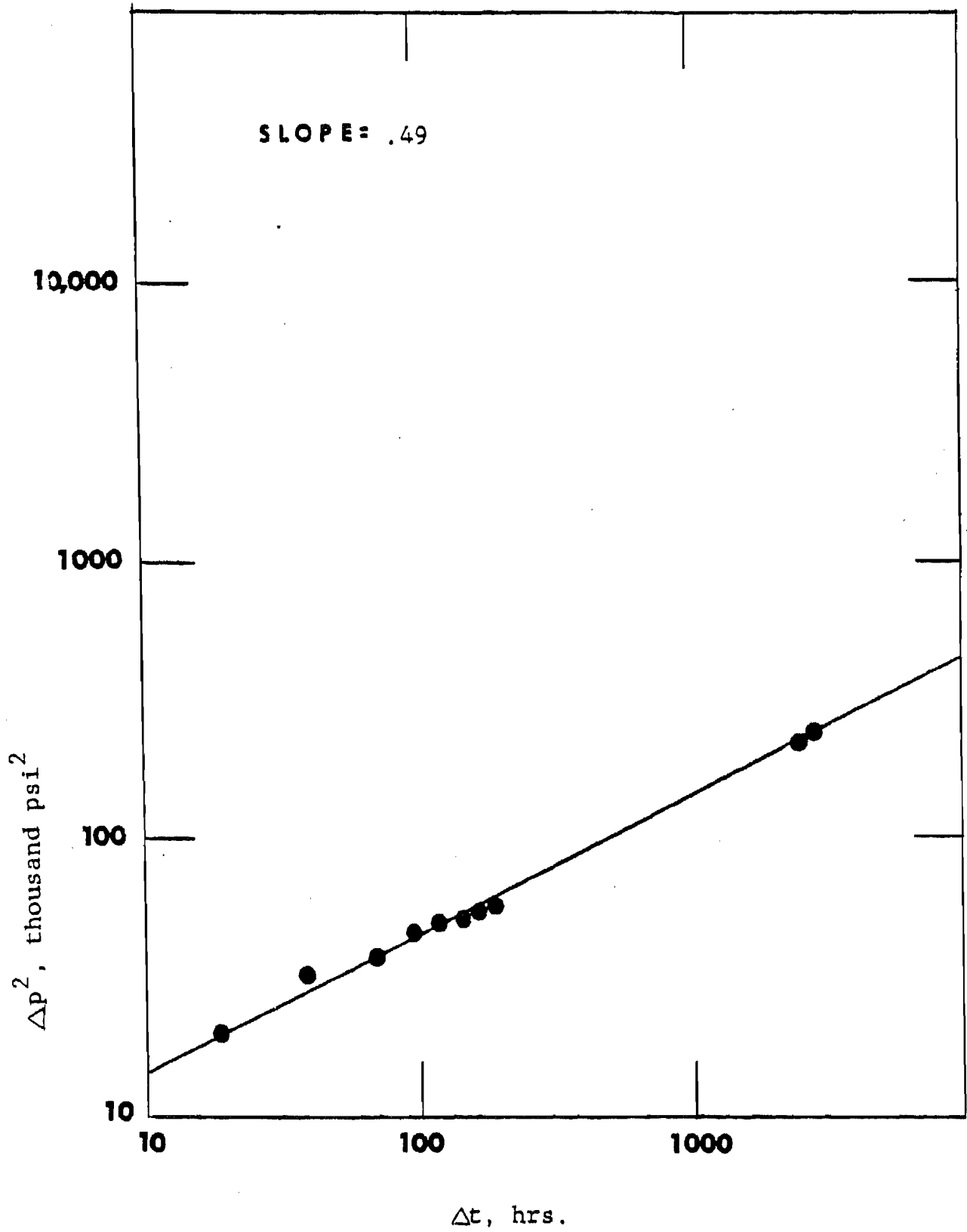


FIG. 25 ΔP^2 versus Δt - Well G

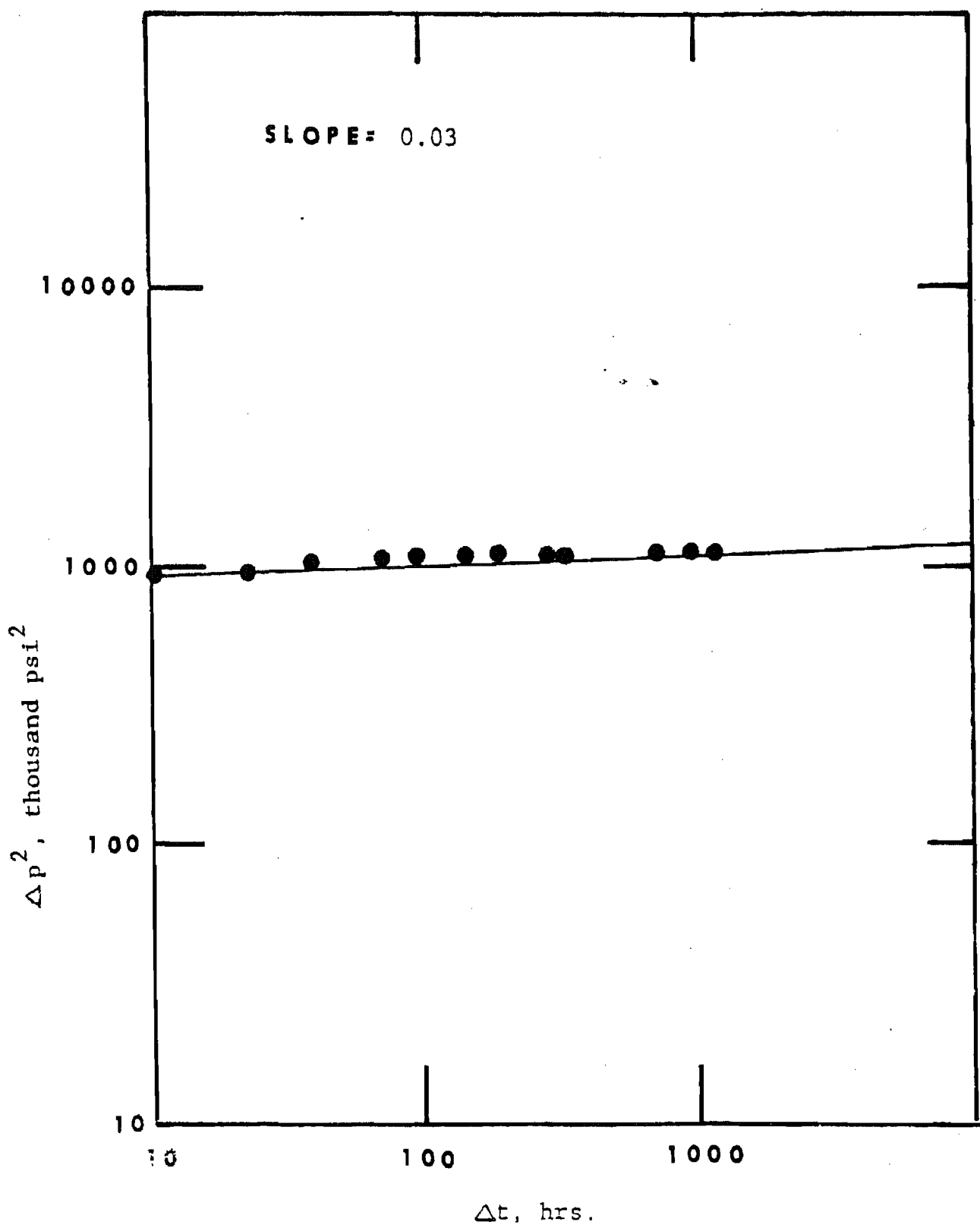


FIG. 26 Δp^2 versus Δt - Well H

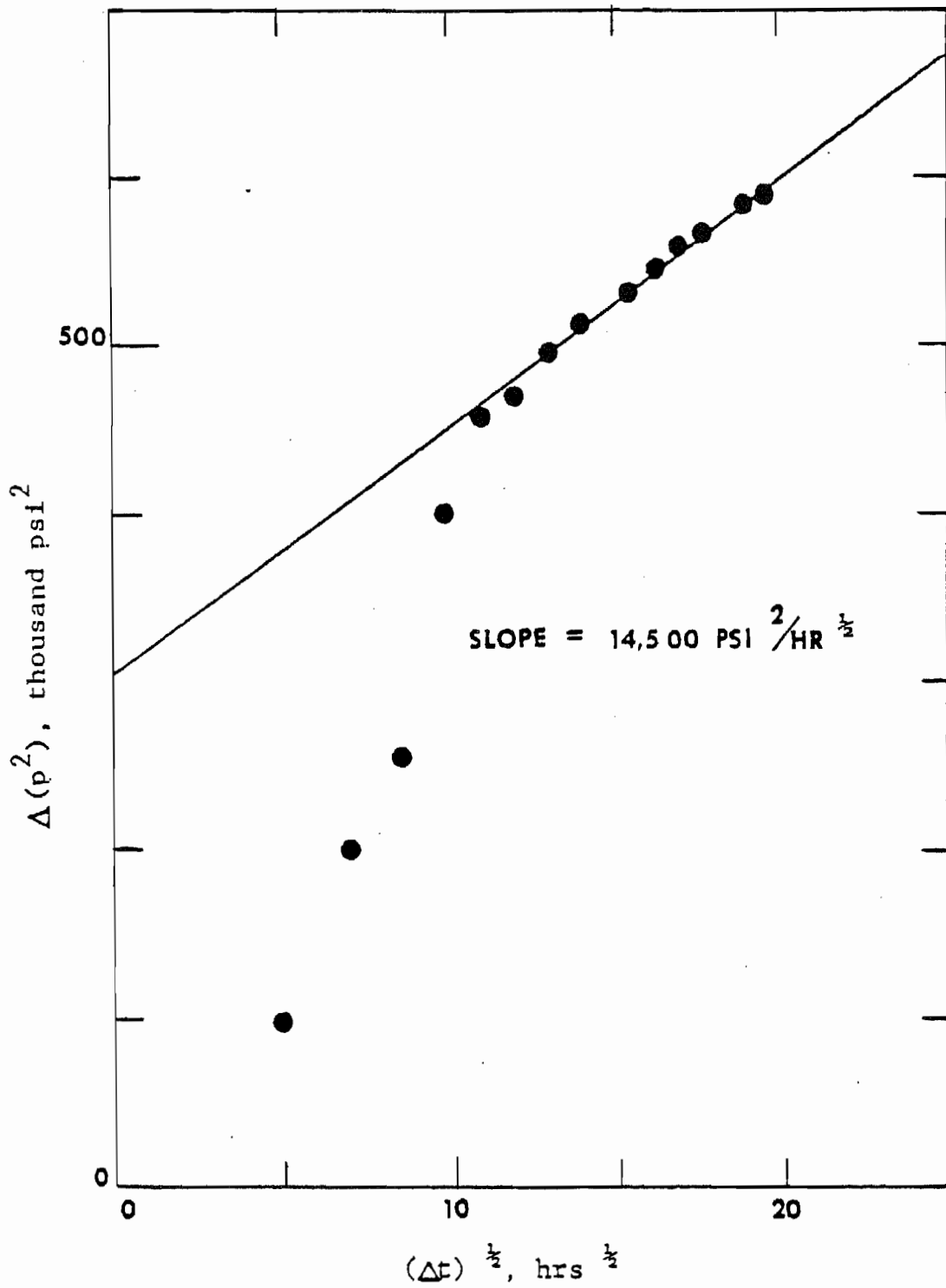


FIG. 27 $\Delta(p^2)$ versus $(\Delta t)^{\frac{1}{2}}$ = Well B

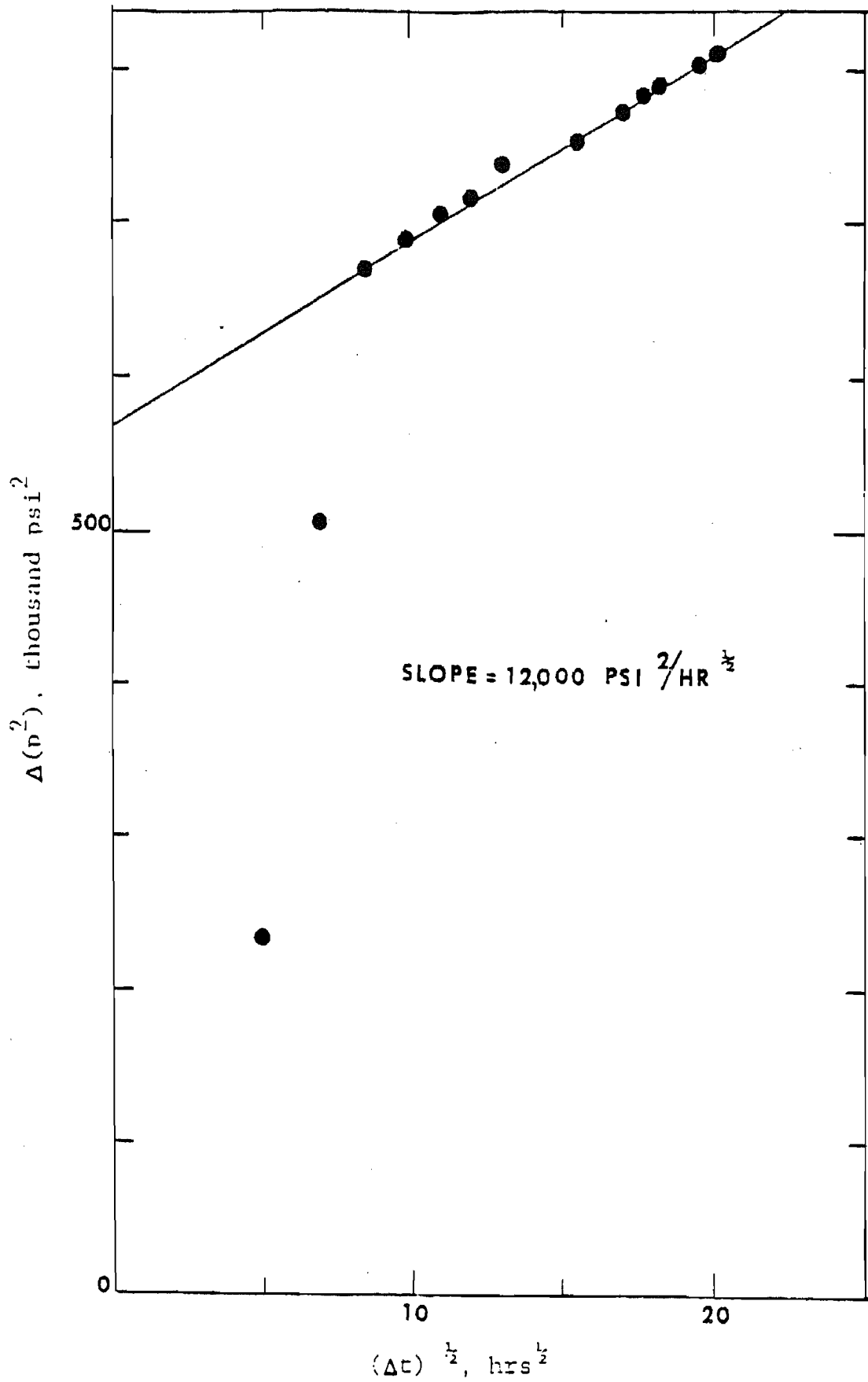


FIG. 28 $\Delta(p^2)$ versus $(\Delta t)^{1/2}$ - Well C
 -81-

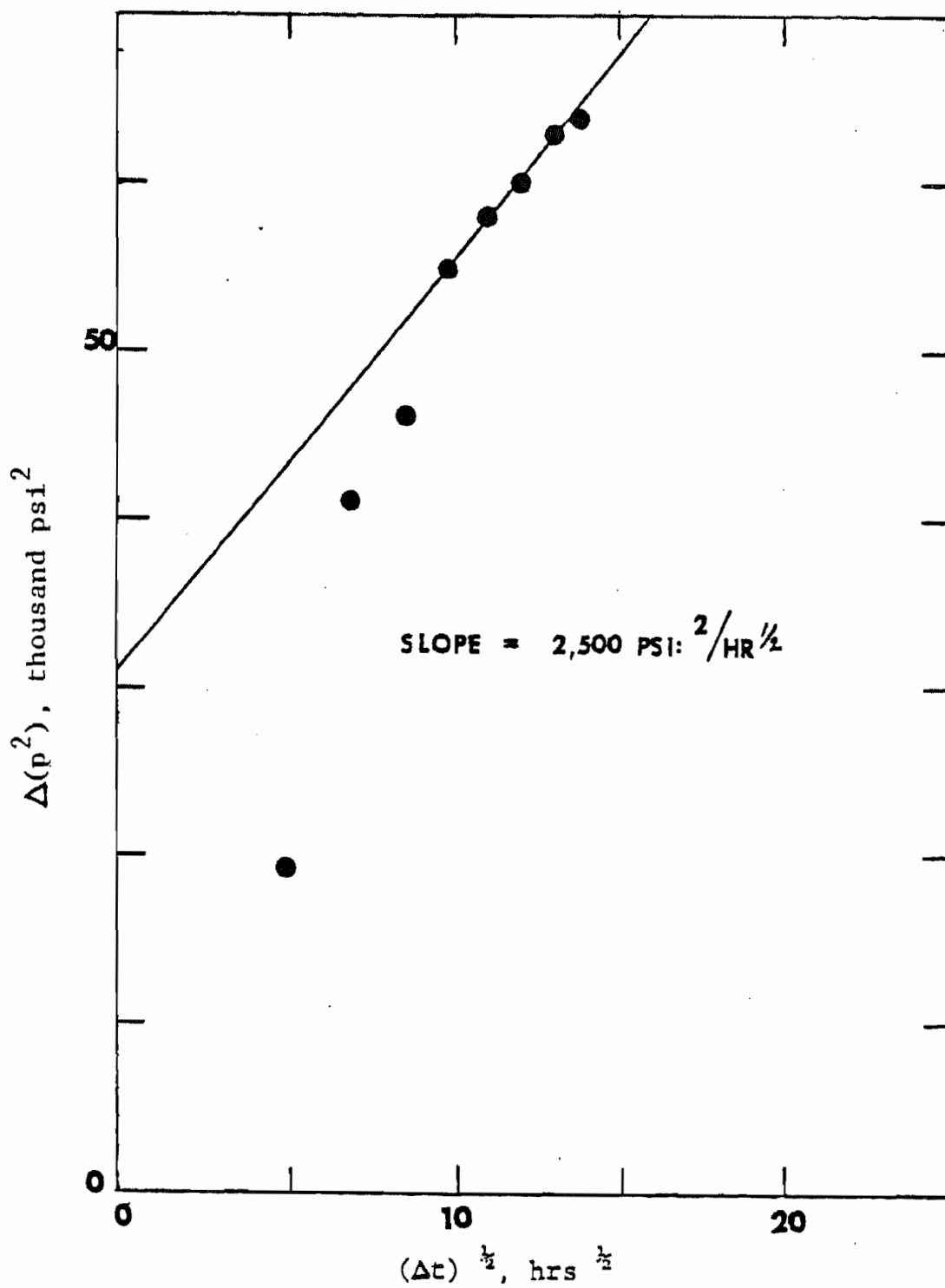


FIG. 29 $\Delta(p^2)$ versus $(\Delta t)^{1/2}$ - Well G

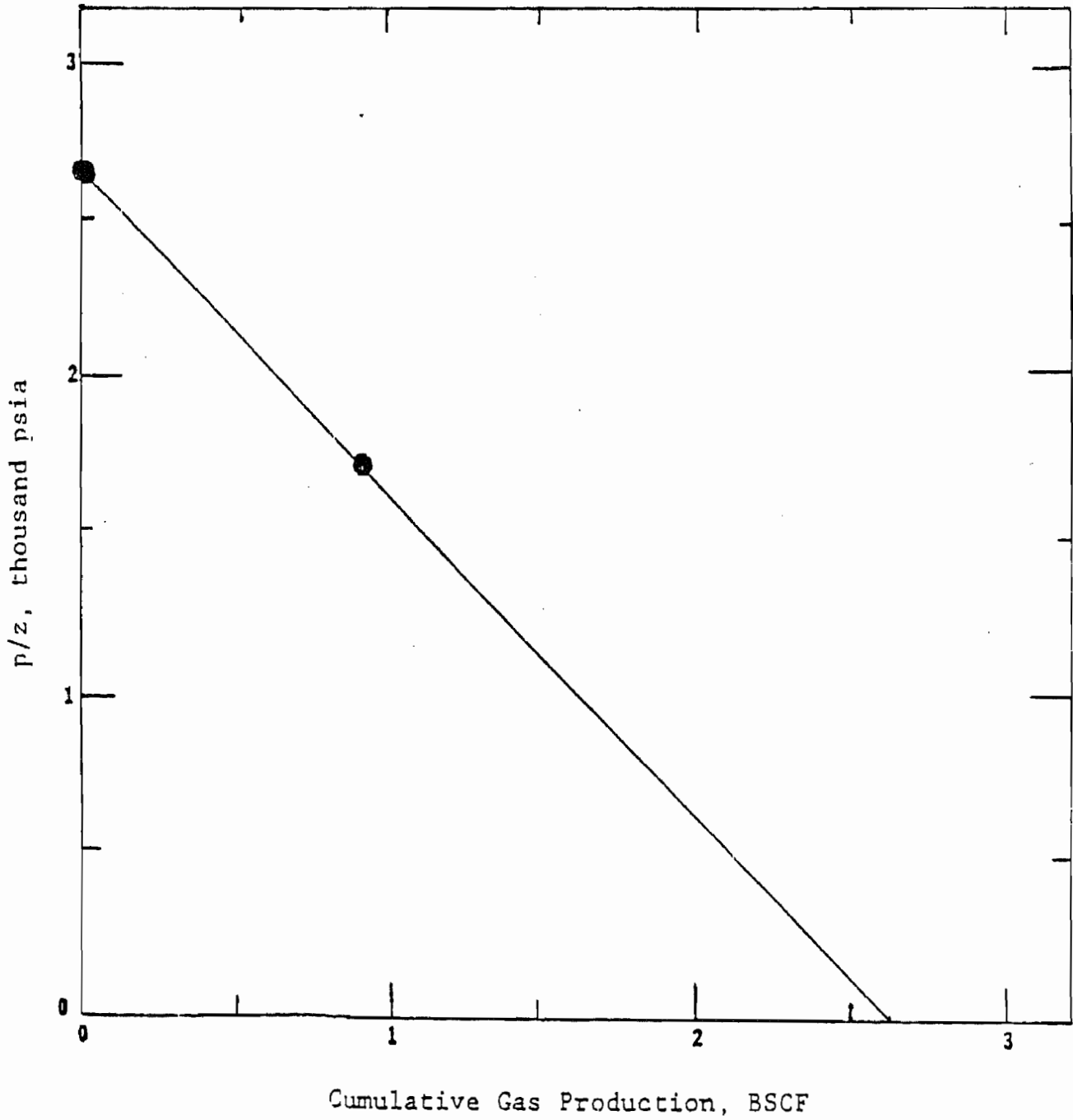


FIG. 30 p/z versus Gas Production - Well A

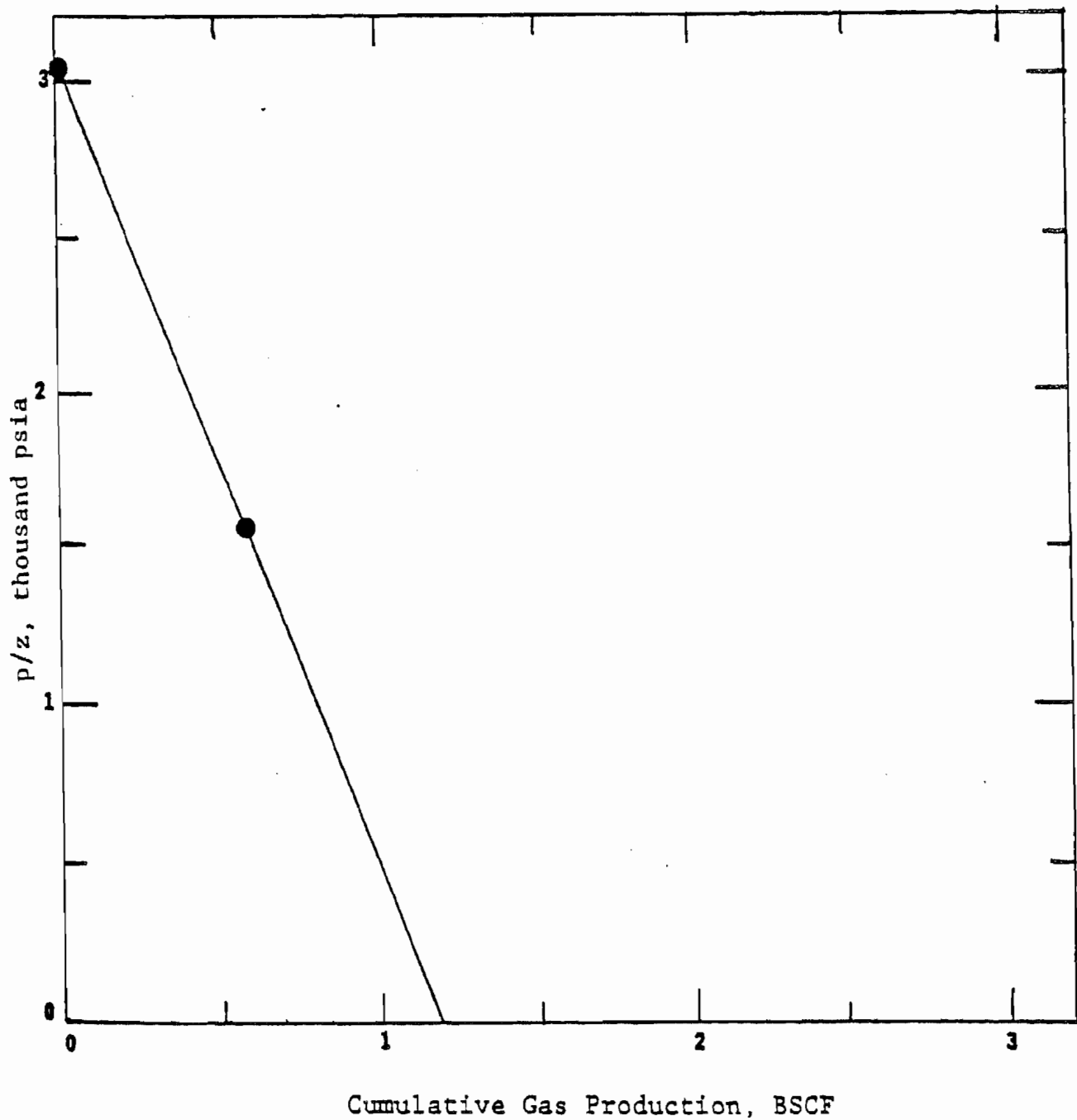


FIG. 31 p/z versus Gas Production - Well B

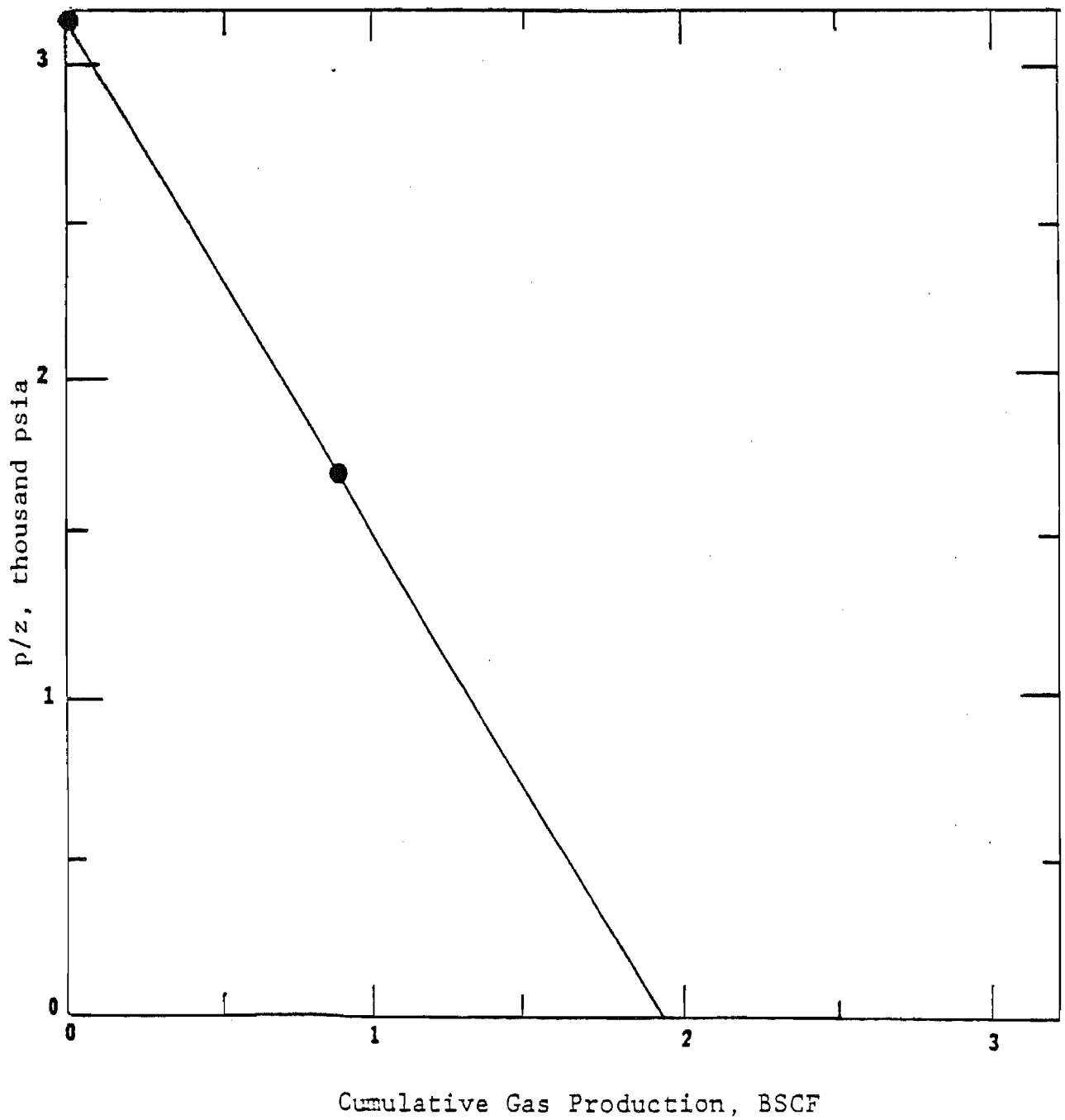


FIG. 32 p/z versus Gas Production - Well C

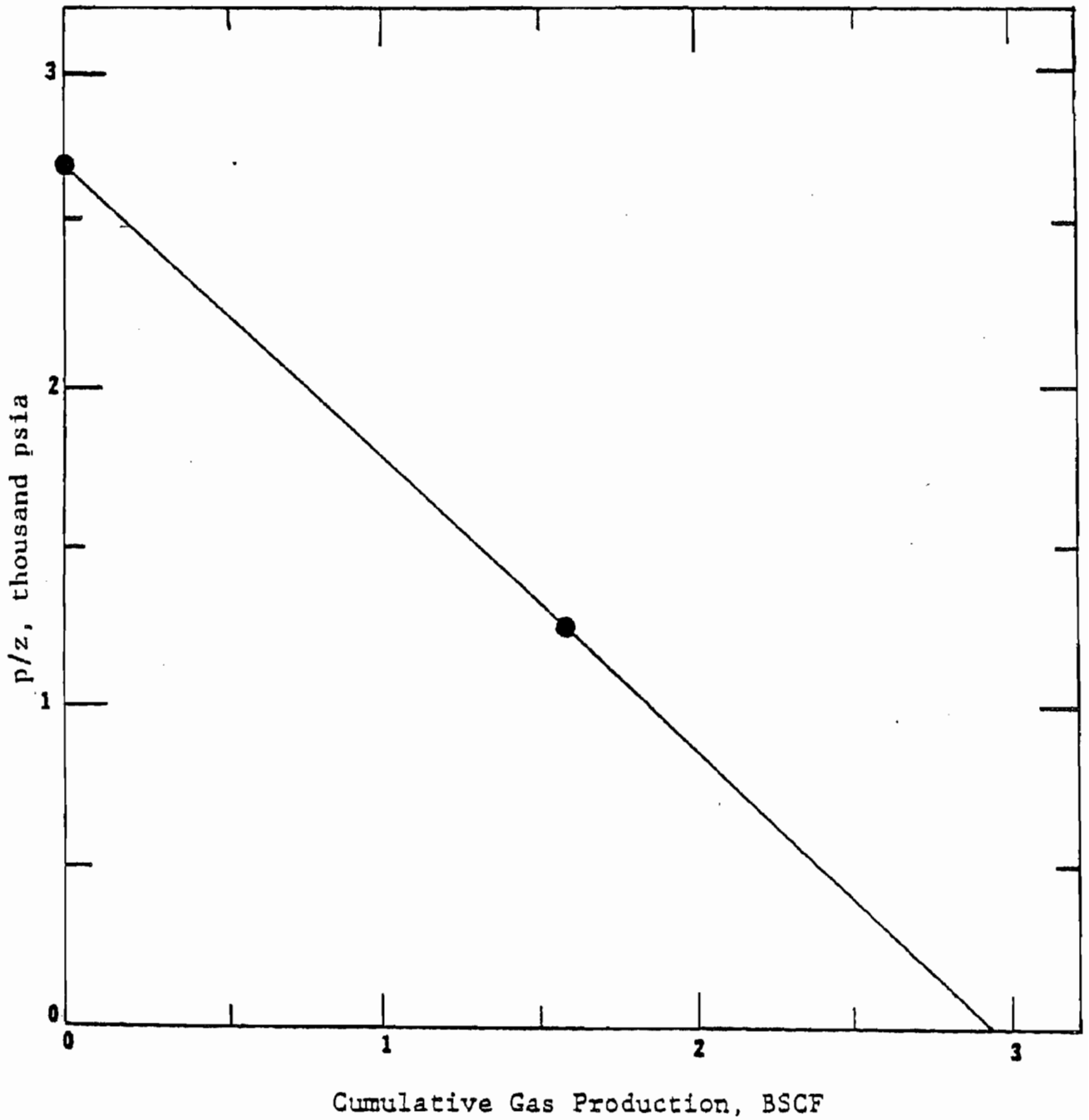


FIG. 33 p/z versus Gas Production - Well D

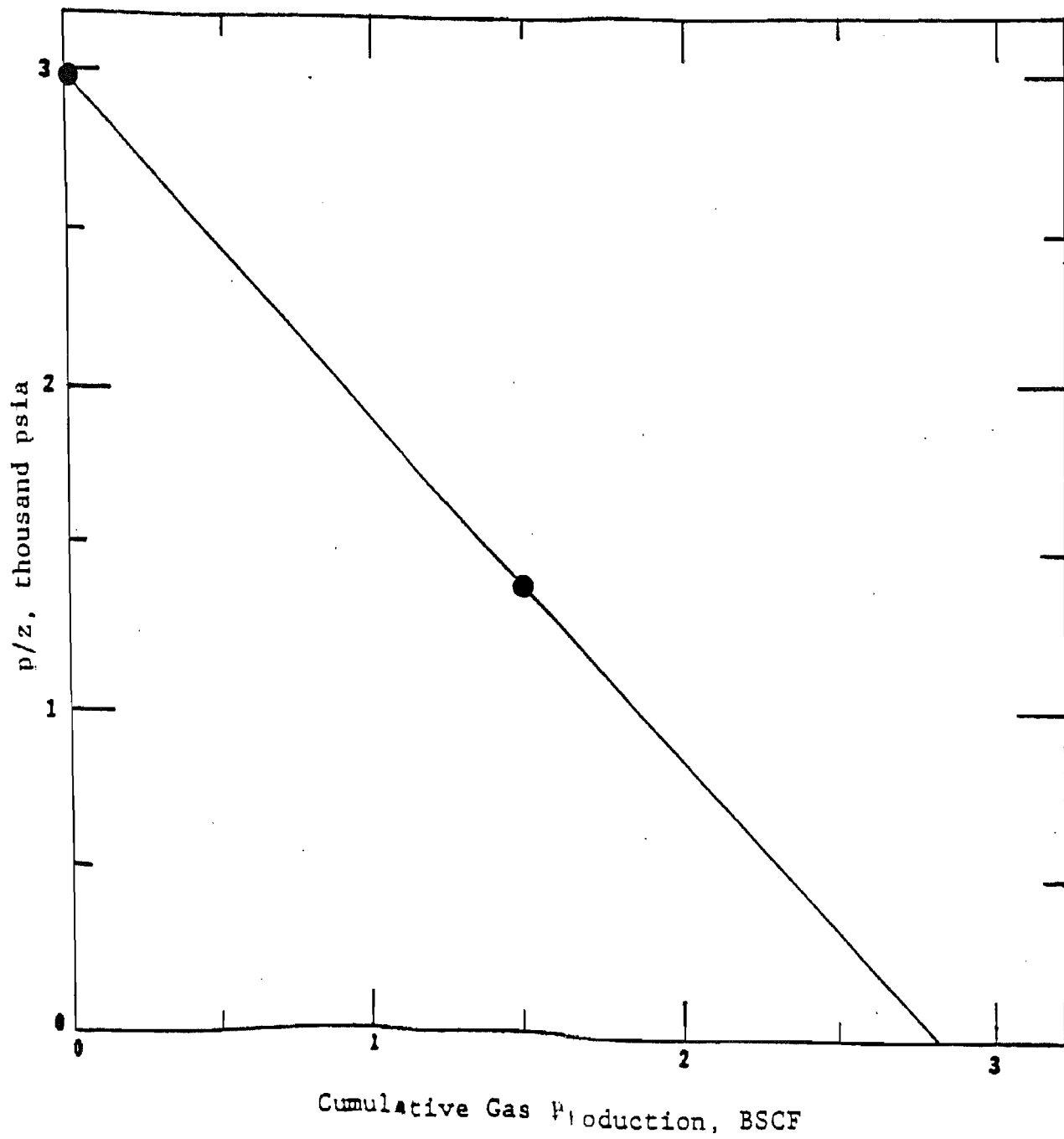


FIG.34 p/z versus Gas Production - Well F

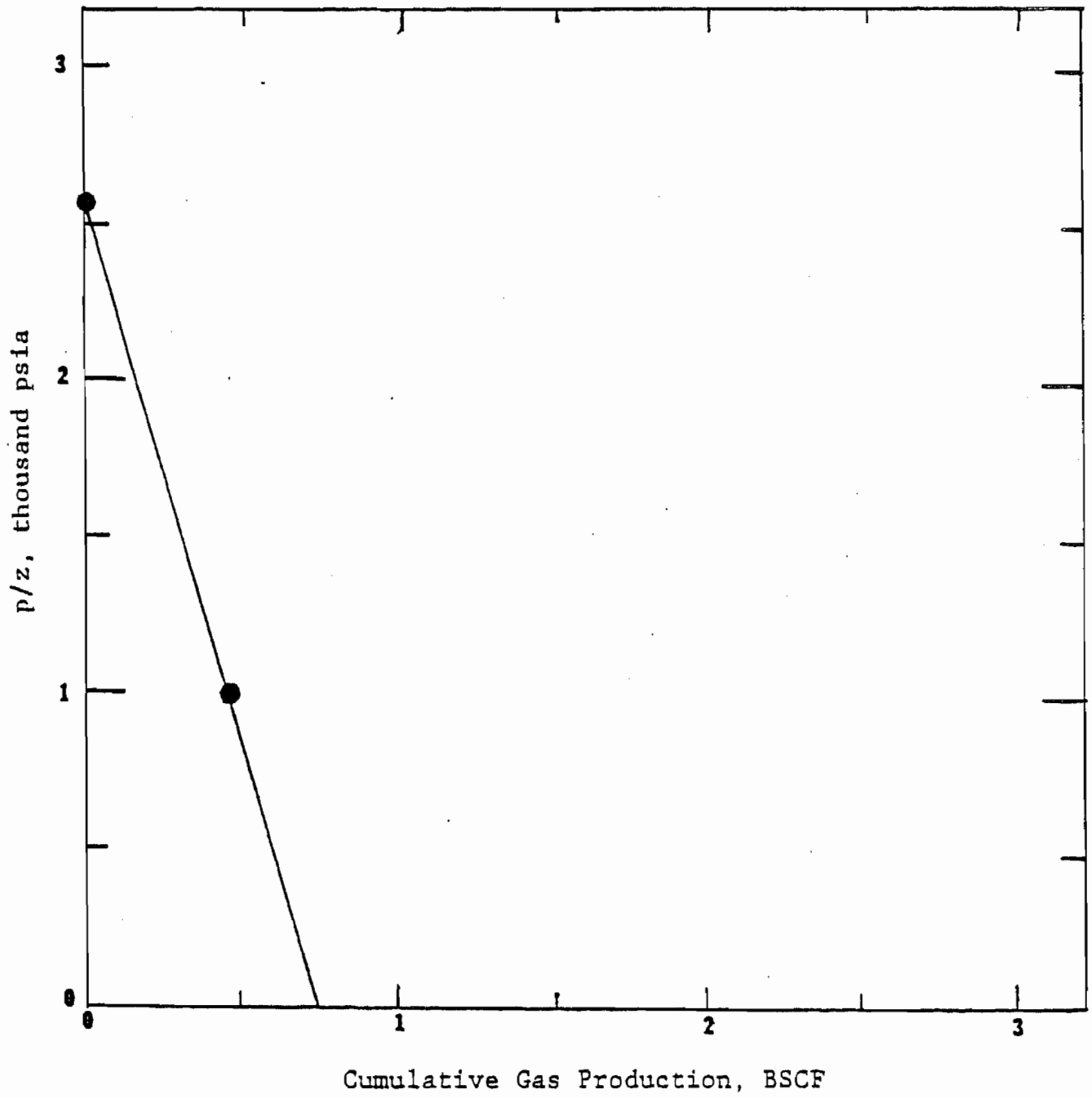


FIG. 35 p/z versus Gas Production - Well G

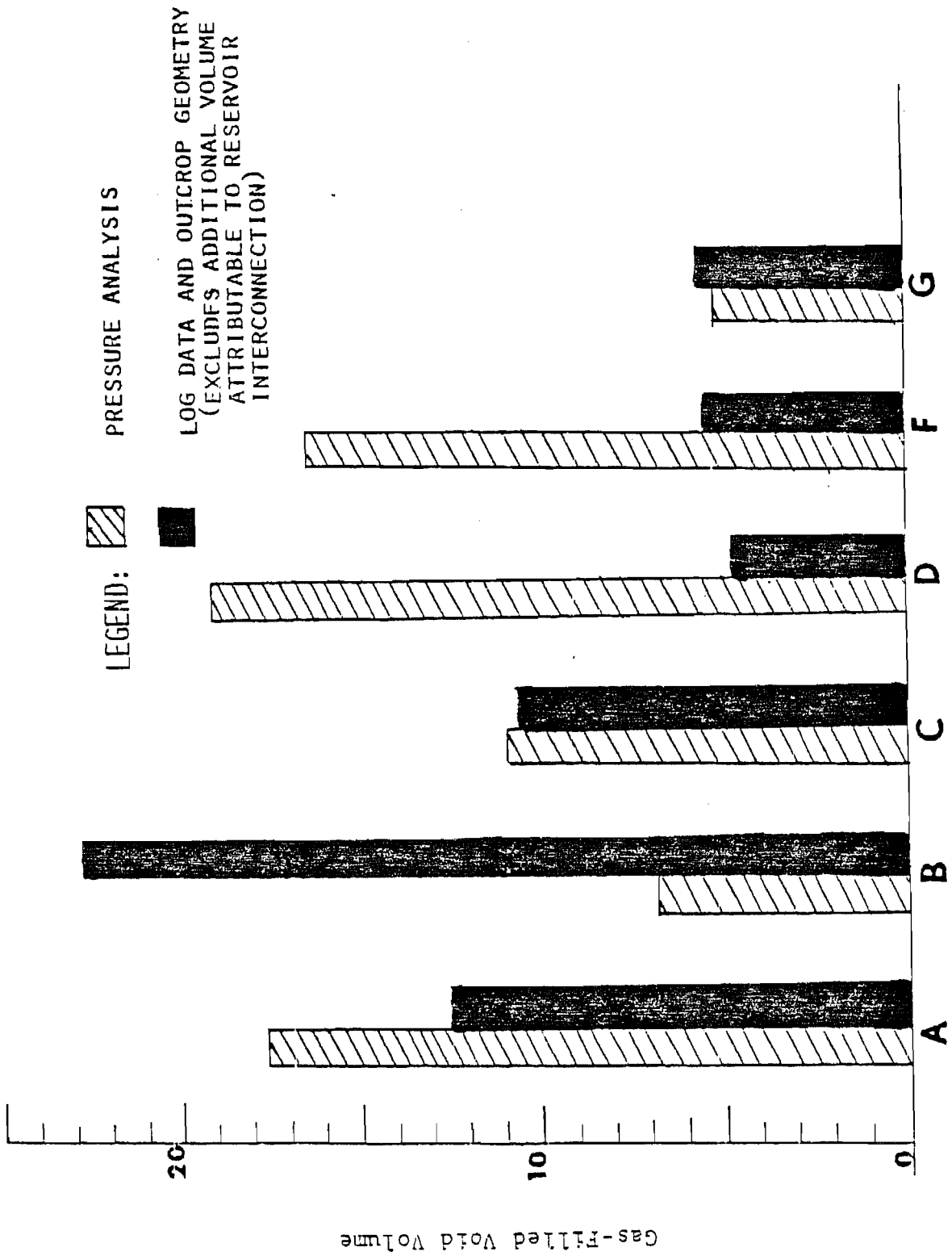


FIG. 16 Comparison of Gas-Filled Reservoir Volumes Determined by Two Methods.

WELL